PEPTIDE-TARGETED NITRIC OXIDE DELIVERY FOR THE TREATMENT OF GLIOBLASTOMA MULTIFORME

A Thesis
Presented to
The Academic Faculty

by

Shahana Safdar

In Partial Fulfillment
of the Requirements for the Degree
Doctor of Philosophy in the
School of Chemical & Biomolecular Engineering

Georgia Institute of Technology
DECEMBER 2012

PEPTIDE-TARGETED DELIVERY OF NITRIC OXIDE FOR THE TREATMENT OF GLIOBLASTOMA MULTIFORME

Approved by:

Dr. Lakeshia J. Taite, Advisor
School of Chemical & Biomolecular Engineering
Georgia Institute of Technology

Dr. Mark R. Prausnitz
School of Chemical & Biomolecular Engineering
Georgia Institute of Technology

Dr.Michelle R. Dawson
School of Chemical & Biomolecular Engineering
Georgia Institute of Technology

Dr. Ravi V. Bellamkonda
Department of Biomedical Engineering
Georgia Institute of Technology and Emory University

Dr. Hang Lu
School of Chemical & Biomolecular Engineering
Georgia Institute of Technology

Date Approved: August 9, 2012

- For my parents and grandparents -
- Who taught me the importance of education -

ACKNOWLEDGEMENTS

I would like to thank Lakeshia for being the most patient and supportive advisor that I could have ever hoped for. Thank you for challenging me, encouraging me to be confident and most of all thank you for convincing me to do a PhD. I would like to thank my committee members; Dr. Dawson, Dr. Lu, Dr. Prausnitz and Dr. Bellamkonda, for their advice and support.

I would like to thank Dhaval and Kai, for making the Taite Lab one of the most fun places to work in. Dhaval and Kai, thank you for your help and useful advice in troubleshooting the multiple problems I encountered in the last five years.

My work would not have been possible without the assistance of all my undergrads, especially Courtney, Nam and Rosine. Courtney, I have never had as much fun in lab as I did when we were working together, thank you. Nam, thank you for tirelessly counting endless cell samples and Rosine, thank you for quietly and efficiently helping me complete the last section of my project.

I would like to thank Jenny for teaching me how to culture cells; Swati for helping me study for the qualifying exams and Aparna for helping me in every crisis. I would like to thank Sana, without whom I would not have survived grad school. Most importantly, I would like to thank my family, especially my parents who have supported me in everything I have done and encouraged me to be the best I can possibly be.

TABLE OF CONTENTS

LIST OF FIGURES

LIST OF SYMBOLS AND ABBREVIATIONS

nM	nanomolar
μm	micron
μM	micromolar
BBB	Blood brain barrier
BCA	Bicinchoninic acid
BCNU	Carmustine, 1,3-bis(2-chloroethyl)-1-nitrosourea
BSA	Bovine serum albumin
BTB	Blood brain tumor barrier
cGMP	Cyclic guanosine monophoshate
cNOS	constitutive Nitric oxide synthase
CNS	Central nervous system
CTX	Chlorotoxin
CTX-FITC	CTX conjugated with fluorescein isothiocyanate
CTX-NO	CTX reacted with nitric oxide
DI	Nanopure water (18 mΩ resistance)
DQ collagen	Dye-Quenched collagen
ECM	Extracellular matrix
EDTA	Ethylenediaminetetraacetic acid
EGFR	Endothelial growth factor receptor
eNOS	endothelial Nitric oxide synthase
EPR	Enhanced permeability and retention

FBS	Fetal bovine serum
FITC	Fluorescein isothiocyanate
GBM	Glioblastoma multiforme
GPS	L-glutamine-penicillin-streptomycin
HB	Hemoglobin
HBMECs	Human brain microvascular endothelial cells
HRP	Horseradish peroxidase
IL-11RA	IL-11 receptor alpha chain
iNOS	inducible Nitric oxide synthase
L-NAME	N^G-nitro-L- arginine methyl ester
CBF	cerebral blood flow
SIN-1	3-morpholino-sydnonimine
MEM	Minimal essential media
MGMT	O^6-methylguanine-DNA methyltransferase
MMP-2	Matrix metalloproteinase-2
MMP-9	Matrix metalloproteinase-9
MTIC	5-(3-methyltriazen-1-yl)imidazole-4-carboxamide
NaOH	Sodium hydroxide
NHAs	Normal human astrocytes
nNOS	neural Nitric oxide synthase
NO	Nitric oxide
NOS	Nitric oxide synthase
O^6-G	O^6 position of guanine
PBS	Phosphate buffered saline

RNOS	Reactive nitrogen oxide species
sGC	Soluble-guanyl cyclase
SNAP	*S*-Nitroso-N-acetyl-DL-penicillamine
TMB	3,3',5,5'-tetramethylbenzidine
TMZ	Temozolomide
VEGF	Vascular endothelial growth factor
VTW	Glioma targeting peptide (VTWTPQAWFQWVGGGSKKKKK)
VTW-FITC	VTW conjugated with fluorescein isothiocyanate
VTW-NO	VTW reacted with nitric oxide

SUMMARY

Glioblastoma multiforme (GBM) is the most common malignant central nervous system tumor. The ability of glioma cells to rapidly disperse and invade healthy brain tissue, coupled with their high resistance to chemotherapy and radiation have resulted in extremely poor prognoses among patients. In recent years, nitric oxide (NO) has been discovered to play a ubiquitous of role in human physiology and studies have shown that, at sufficient concentrations, NO is able to induce apoptosis as well as chemosensitization in tumor cells. In this thesis the synthesis and characterization of targeted NO donors for the treatment of GBM is discussed.

Two glioma targeting biomolecules, Chlorotoxin (CTX) and VTWTPQAWFQWVGGGSKKKKK (VTW) were reacted with NO gas to synthesize NO donors. These NO donors, CTX-NO and VTW-NO, released NO for over 3 days and were able to induce cytotoxicity in a dose dependent manner in glioma cells. The biggest advantage, a result of the targeted delivery of NO, was that the NO donors did not have toxic effects on astrocytes and endothelial cells. To characterize the chemosensitizing effects of CTX-NO, cells were incubated with CTX-NO prior to exposure to temozolomide (TMZ) or carmustine (BCNU). These drugs are the most popular chemotherapeutics used in the treatment of GBM, but have only shown modest improvements in patient survival. Viability studies showed that CTX-NO selectively elicited chemosensitivity in glioma cells, whereas the chemosensitivty of astrocytes and endothelial cells remained unaffected. Further investigation showed that CTX-NO pretreatment decreased O^6-methylguanine DNA methyltransferase (MGMT) and p53

levels, suggesting that a decrease in DNA repair ability may be the mechanism by which chemosensitivity is induced.

Lastly, the effects of CTX-NO on glioma cell invasion and migration were studied using Boyden chamber and modified scratch assays. Non-toxic doses of CTX-NO decreased glioma cell invasion in a dose dependent manner. Studies quantifying matrix metalloproteinase-2 (MMP-2) and matrix metalloproteinase-9 (MMP-9) surface expression demonstrated that while MMP-2 expression was decreased by both CTX and CTX-NO, MMP-9 expression was decreased only by CTX-NO. Furthermore quantifying MMP-2 and MMP-9 activity levels showed that NO and CTX work synergistically to decrease the activity of the enzymes. These studies demonstrate that the decrease in glioma invasion resulting from CTX-NO treatment was partially a consequence of decreased levels of surface and activated MMP-2 and MMP-9. The work presented in this thesis describes a novel approach to treating GBM that can be modified to develop treatments for various other tumors. Furthermore this is the first study to develop glioma-targeting NO donors.

CHAPTER 1: INTRODUCTION

In this thesis, the development of novel, targeted nitric oxide donors for the treatment of glioblastoma multiforme, a Grade IV brain tumor, is discussed. The American Cancer Society estimates that 22,910 brain and spinal cord tumors will be diagnosed in the United States during 2012 [1]. Furthermore, they also estimate that in 2012, brain and spinal cord tumors will cause 2.4% of all deaths caused by cancer [1]. Glioblastoma multiforme is the most common central nervous system (CNS) tumor, accounting for over 50% of all CNS neoplasms in the United States [2-4]. It is also is the most aggressive brain cancer in adults [5]. Patients diagnosed with the disease have a median survival of only 14.6 months and the 5-year survival is less than 5% despite aggressive multimodal therapy [6-8]. The invasive nature of glioma cells allows the tumor to rapidly invade healthy brain tissue [8, 9]. This, coupled with their high resistance to chemotherapy and radiotherapy, has significantly hampered the success of various treatment options.

1.1 Classification of Brain Tumors

Brain tumors originating from glial cells, the supporting cells in the brain, are categorized as gliomas. There are three types of glial cells: astrocytes, oligodendrocytes, and ependymal cells [10]. Astrocytomas, which are gliomas developed from astrocytes, account for 80-85% of all gliomas [8]. The World Health Organization has classified astrocytomas into four grades according to histopathology. Grade I astrocytomas usually lack atypia, mitoses, endothelial proliferation, and necrosis, while Grade II only have

atypia [11]. Since these are the characteristics that reflect the malignant potential of the tumor, patients with Grade I or II actrocytomas, classified as low grade astrocytomas, have much better prognoses. Malignant astrocytomas are Grade III, anaplastic astrocytoma, and Grade IV, glioblastoma multiforme (GBM) [12].

1.2 Glioblastoma Multiforme

GBM is characterized by the presence of necrotic areas in the brain tissue surrounded by anaplastic and poorly differentiated cells and hyperplastic blood vessels [13]. Other histopathalogical features of the tumor include cellular polymorphism and brisk mitotic activity, resulting in tumor heterogeneity [14]. A defining feature of GBM tumors is rapid and highly invasive growth [9]. Among the most common symptoms in GBM patients are progressive headaches, along with vasogenic edema, a consequence of the rapidly growing nature of the tumor [15]. Other symptoms include vomiting and clouding of consciousness [16]. As the disease progresses, patients suffer from loss of neurological function [15]. The most devastating of GBM symptoms is cognitive dysfunction, with patients occasionally undergoing psychiatric evaluation because of changes in behavior and personality [15].

The invasive nature of GBM cells prevents complete tumor resection, as malignant glioma cells are able to spread and invade the brain parenchyma [17, 18]. This results in GBM reoccurrence within a median time of 7 months [6, 19]. Secondary GBM tumors, or lesions, usually occur within 2-3 cm from the border of the original tumor site, and are resistant to radiation and chemotherapy [12, 14, 20]. Secondary GBM lesions are

often irregularly shaped and include cystic areas, further complicating tumor resection [21]. There is no standard of care for recurrent GBM and treatment is case specific [22].

1.2.1 Glioma Invasion

The molecular mechanisms of glioma invasion are complex and not completely elucidated, but there is consensus that a critical step in tumor invasion is the degradation of the extracellular matrix (ECM) and penetration into adjacent brain structures [23-25]. Matrix metalloproteinases (MMPs) are a group of zinc dependent endopeptidases that play a key role in the degradation of the ECM [26-28]. There are over 20 different MMPs, all of which are expressed as inactive pro-enzymes, and activation requires proteolytic cleavage [29, 30]. MMPs are divided, based on their substrate specificities, into six major groups: collagenases, gelatinases, stromelysins, matrilysin, membrane-type matrix metalloproteinases (MT-MMPs), and others [29, 31]. MMP-1, MMP-8 and MMP-13 cleave triple helical collagen and are hence classified as collagenases [25]. MMP-2 and MMP-9, the gelatinases, degrade denatured collagen IV, while stromelysins and matrilysins degrade aggrecan, fibronectin, laminin and other molecules [25]. The MT-MMP subgroup differs from the other MMPs in that they are anchored to the plasma membrane [28]. MMP activity is controlled by gene transcription, zymogen activation by proteolysis, and inhibition by tissue inhibitors of metalloproteinases (TIMPs) [24]. In addition to MMPs, a variety of other chemokines, integrins and cell adhesion molecules play critical roles in modulating tumor cell invasion, and it is the cumulative effect of these mechanisms that dictates the rate of tumor cell invasion.

1.3 Glioblastoma Multiforme Treatment Options

Treatment of GBM is particularly challenging because of various reasons, which include localization in the brain, intrinsic resistance to chemotherapy, limited ability of the brain to repair itself, and the neurotoxicity of anti-tumor drugs [32]. Surgery, the earliest treatment option for GBM patients, remains the first step in patient care [16, 33-35]. Although significant improvements in surgical and imaging techniques have been made since the first reported GBM resection in 1904, the diffuse nature of these types of tumors makes complete tumor resection impossible [35-38]. Nonetheless, maximal tumor resection has been shown to enhance the efficacy of subsequent chemotherapy [35].

The first major advance in GBM treatment occurred in 1978 when Walker et al. showed that external beam radiation was able to increase median patient survival from 14 weeks to 35 weeks [39]. Between 1978 and 2003, no significant improvement in the prognoses of GBM patients was achieved, and overall patient survival remained in the range of 10-12 months [3, 12]. The current standard of care for GBM is multimodal treatment, involving surgical tumor resection followed by radiation and chemotherapy [51, 56, 57]. Figure 1.1 shows MRI scans of a patient who, despite undergoing surgical resection, radiation and chemotherapy, died 17 months after surgery [8]. Although numerous chemotherapeutics have been used to treat GBM in the last decade, two new therapies, Gliadel® wafers and temozolomide (TMZ), have been FDA approved for the treatment of GBM and have been incorporated into the standard GBM treatment regimen because of superior efficacy compared to other therapeutics.

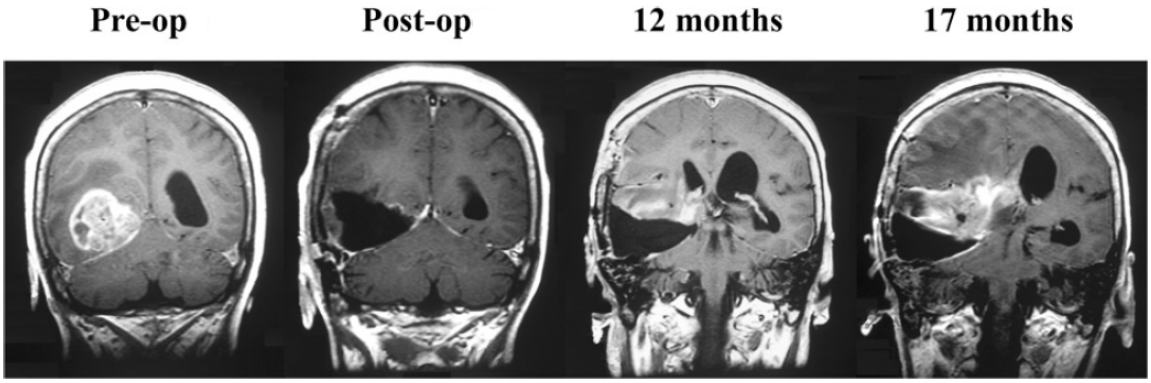

Figure 1.1. Local recurrence of glioblastoma. A right occipital glioblastoma (left) was operated upon, and a postoperative magnetic resonance imaging (MRI) scan confirmed complete removal (middle left). Chemotherapy and sixty-Gy radiation therapy were administered. Twelve months later, a routine MRI showed a recurrent tumor immediately adjacent to the resection cavity (middle right). Seventeen months after the operation, the patient succumbed to the tumor (right)[8].

Carmustine/BCNU

In 2003, carmustine (BCNU)-loaded wafers, Gliadel®, were FDA approved as adjuncts to surgery for first-line treatment of GBM [41]. BCNU, 1,3-Bis(2-chloroethyl)-1-nitrosourea, is a chemotherapeutic with alkylating and carbomylating effects that has been used for GBM treatment for more than 30 years [42]. Prior to the approval of Gliadel®, BCNU was administered intravenously [42]. In aqueous solution, BCNU decomposes to 2-chloroethyl diazohydroxide and 2-chloroethyl isocynate [43]. 2-chloroethyl diazohydroxide primarily has alkylating effects and inhibits DNA synthesis by adding alkyl groups to the O^6 position of guanine (O^6-G). Conversely, 2-chloroethyl isocynate has carbomylating effects, whereby enzymes involved in maintaining cellular redox homeostatis are inactivated, resulting in the accumulation of oxidized gluthatione and consequent tumor cell death [44].

BCNU has a small molecular weight, is highly lipophilic, and is able to cross the blood brain barrier rapidly [45]. Additionally, it is rapidly metabolized in brain fluid as

well as plasma, and has high urine clearance (60-70% of the dose is eliminated in urine) [46]. Thus, for therapeutic purposes high doses were necessary, resulting in severe side effects. Gliadel® wafers prevent the side effects associated with high systemic doses by providing continuous, intracranial delivery (Fig. 1.2) [47]. However, the wafer implant has been associated with cerebral edema, healing abnormalities, intracranial infections, seizures, and cyst formation [47, 48]. Furthermore, one-third of patients do not respond to BCNU treatment [49].

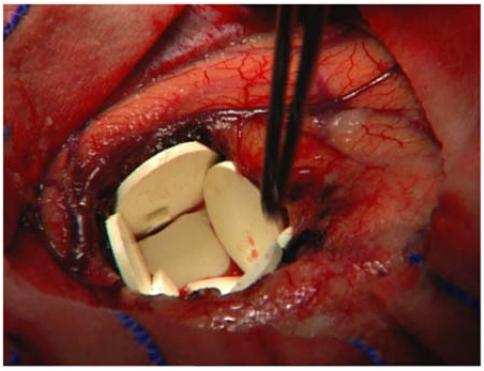

Figure 1.2. After glioma resection, eight Gliadel wafers were placed in the tumor cavity. Loading BCNU into the degradable polymer wafers allows controlled, localized delivery of the drug [50].

Temozolomide

In 2005, a new chemotherapeutic agent, TMZ, which had shown a modest increase in patient survival when administered with and after radiation (2 year survival 26% vs. 10%), was FDA approved for the treatment of GBM [41, 51]. TMZ is a second-generation imidazotetrazine prodrug, which acts as a methylating agent [2, 52, 53]. TMZ hydrolyzes at physiological pH into its active product, 5-(3-methyltriazen-1-yl)imidazole-4-carboxamide (MTIC) [53]. MTIC is able to methylate DNA at a variety of nucleophilic centers, including O^6-G, forming O^6-methylguanine [54]. O^6-methylguanine mispairs with thymine, and the failure of DNA mismatch repairs result in tumor cell death [54,

55]. TMZ has quickly been incorporated into the treatment regimen of GBM patients because it is taken orally, and has 100% bioavailability [53]. Furthermore, TMZ is able to cross the blood brain barrier, and over 30% of the drug enters the cerebrospinal fluid, which is a major reason for its efficacy [55].

Second line treatment options: Bevacizumab and the NovoTTF-100A System

For GBM patients who do not respond to surgery and radiation combined with TMZ or BCNU, two new therapeutic options, Bevacizumab and the NovoTTF-100A System, have recently received FDA approval as second-line treatment options. Bevacizumab (Avastin®) injection received FDA approval in May 2009 [41]. Bevacizumab is a recombinant humanized monoclonal IgG_1 antibody that selectively binds to vascular endothelial growth factor (VEGF) and subsequently neutralizes its activity [41]. Although Bevacizumab does not inhibit the growth of solid tumors, it is able to normalize tumor vasculature to a certain degree, reducing the incidence of tumor related edema [41].

The most recent treatment regiment to receive FDA approval for second-line glioma treatment is the NovoTTF-100A System, which was approved in April 2011 [58, 59]. The NovoTTF system emits an electromagnetic field that interferes with cell division, causing disruption of chromosome segregation, blebbing of the cytoplasmic membrane, and eventually, cell death [59]. This system, which is in clinical trials, has been shown to have equivalent efficacy to cytotoxic chemotherapies, but fewer side effects [60].

1.4 Experimental and Novel treatments

The poor prognoses of GBM patients, in spite of the administration of the best available therapy, has resulted in a variety of studies for the development of novel GBM therapies, some of which are discussed herein. Ascorbate, or vitamin C, is an essential micronutrient that has been shown to inhibit GBM growth and induce radiosenitivity in tumor cells; however, maintaining therapeutic plasma levels has been the main hindrance in the success of ascorbate as a GBM treatment [5, 61]. Curcumin is another biomolecule that is widely investigated as a potential GBM therapeutic because of its apoptosis-inducing and chemosensitization effects on glioma cells [62-64]. The main challenges in the use of curcumin are water insolubility, low bioavailability, and high rate of metabolism [65].

In addition to the use of naturally occurring molecules, gene therapy is another alternative for GBM treatment that is currently being researched. Gene therapy for GBM involves the delivery of suicide genes [66, 67], pro-apoptotic genes [68-71] or genes inhibiting invasion [72]. Some success has been achieved in preclinical trials of various gene therapies, but the main challenges in clinical trials have been the delivery of the genes specifically to tumor cells and minimizing the bystander effect to surrounding healthy tissues [73]

An indirect approach to treating GBM has been the development of anti-angiogenic therapy. Angiogenesis is a vital process for the growth of all tumors, and inhibiting this process decreases blood supply to the tumor, depriving tumor cells of vital nutrients and oxygen [74]. Numerous anti-angiogenic agents, such as cediranib [75], sorafenib [76], cilengitide [77], pazopanib [78] and sunitinib [79] have been developed

and are currently undergoing clinical trials. A major concern in anti-angiogenic therapy is the increased risk of intracranial hemorrhaging; however, the success of bevaciumab, an anti-angiogenic agent, in clinical trials and its consequent FDA approval has helped in affirming the safety of this approach to GBM treatment [6, 80]. Although various drugs have been developed, a major reason for the lack of GBM patient response to chemotherapy is the use of systemic delivery of chemotherapeutic drugs. The inability of chemotherapeutics to accumulate within the tumor because of hindrances caused by the blood brain barrier (BBB) and the blood brain tumor barrier (BTB) contributes significantly to the failure of a variety of drugs in treating GBM [81, 82].

1.5 The Blood Brain Barrier: Obstacle for drug delivery

The BBB is composed of endothelial cells supported by tight junctions. These junctions maintain the brain homeostasis by controlling the exchange of soluble factors between the endothelial cells and the cerebrospinal fluid [83]. The BBB plays an essential role in preventing bacteria from reaching the brain. As a result, only small, lipophilic compounds that have a molecular mass of less than 400-500 Daltons are able to passively cross the BBB [84]. However, certain endogenous large molecules (e.g. insulin and transferrin) are able to cross the BBB via receptor-mediated transcytosis [85].

In patients with gliomas, a secondary barrier, the BTB, also develops. The BTB, which includes the microvessels supplying brain tumors, retains many characteristics of the normal BBB and restricts the paracellular diffusion of hydrophilic molecules [86, 87]. However, some transmembrane tight junction components are down-regulated in glioblastomas, resulting in the BTB having a higher permeability than the BBB [81, 88].

Despite this, the BTB still is a significant barrier, restricting the penetration of therapeutics into the glioma [86]. Furthermore, the permeability of the BBB is disrupted only in close proximity to the tumor, and thus delivering drugs to single cells in the infiltration zone still remains a challenge [81, 89]. In order to address this challenge a variety of drug delivery techniques have been developed, some of which are discussed in the subsequent section.

1.6 Novel drug delivery techniques for GBM treatment

1.6.1 Intracerebral delivery

Intracerebral delivery of therapeutics, in comparison to systemic delivery, minimizes systemic drug levels, prolongs drug elevation at the tumor site, and limits side effects of chemotherapeutic agents [90]. Additionally, in contrast to non-CNS tumors, GBM rarely spreads systemically, making intracerebral delivery of chemotherapeutics for GBM extremely suitable [42]. Intracerebral delivery can be administered by convection enhanced delivery (CED) techniques, biodegradable drug delivery carriers, subcutaneous reservoirs, or manual injection [91]. A number of clinical studies have used intratumoral delivery of various chemotherapeutics, including BCNU [90, 92], TMZ [93], bleomycin [94], doxorubicin [95, 96], carboplatin [97, 98], and cisplatin [99], and found it to be a safe and effective method of delivery.

1.6.2 Nanoparticles

A number of researchers have developed passive tumor-targeting nanoparticles and micelles by exploiting the enhanced permeability and retention (EPR) effect [100-

102]. The EPR effect describes the accumulation of drug/nanoparticles at the tumor site due to high vascular density coupled with the defective architecture of vascular endothelium within a tumor [103]. Furthermore, the lack of lymphatic drainage within a tumor contributes to the retention of nanoparticles, increasing their accumulation at the tumor site [103-105]. An added advantage of nanoparticles is that by encapsulating the drug within the nanoparticle, plasma levels of the free drug are decreased, ameliorating the toxic effects to healthy tissue [34].

Solid Lipid Nanoparticles (SLNs) are the best characterized nontoxic nanoparticles used for the treatment of brain tumors [102]. Drug loaded SLNs have been shown to have higher physical stability, tolerability, greater protection from degradation, and better release profiles of incorporated drugs in comparison to other vehicles [106-109]. Magnetic nanoparticles are also widely studied as potential GBM therapeutics, particularly because of their multifunctionality as magnetic resonance imaging (MRI) contrast agents as well as drug carriers [22, 110-113].

1.6.3 Targeted drug delivery

GBM tumor masses are often composed of 10^9 to 10^{12} competent cells, often extending beyond the tumor margins, and the doses required to treat a tumor of this size are severely toxic to healthy tissue [82]. Despite the success of the passive targeting mechanism resulting from the EPR effect, it has been shown that a more active form of targeting, such as ligand-mediated targeting, proves to be more effective in tumor cell recognition and internalization of drugs via endocytosis [114, 115]. Nanoparticles coated with ligands for receptors overexpressed in GBM cells, such as endothelial growth factor

receptor (EGFR) [111, 116], interleukin-4 receptor [117], MMP-2 [115] and low-density lipoprotein receptor-related protein receptor [118], have resulted in increased drug accumulation at the tumor site, as well as MRI contrast enhancement in comparison to uncoated nanoparticles. Therefore, by efficiently targeting tumor cells via ligand-receptor binding, increased bioavailiblity and a reduction in minimum effective dose and systemic toxicity can be achieved [100, 119]. Furthermore, targeted drug delivery also limits the development of multidrug resistance, which is often the cause of tumor reoccurrence [119, 120].

Additionally, numerous targeted chemotherapeutics such as inhibitors of EGFR [121, 122], VEGF [75], and $\alpha_v\beta_3$ and $\alpha_v\beta_5$ integrins [80, 123] have been developed for the treatment of glioblastoma. Despite the number of targeted agents that have been developed for GBM treatment, most of them have resulted in disappointing clinical results, which at best have shown only modest improvement in patient survival [2]. Presented herein is the development of an innovative cytotoxic drug that can target glioblastoma cells. The objective of this work was the development of nitric oxide (NO) donors, which would be delivered intracerebrally, and deliver NO specifically to the tumor mass and infiltrating tumor cells (Fig. 1.3).

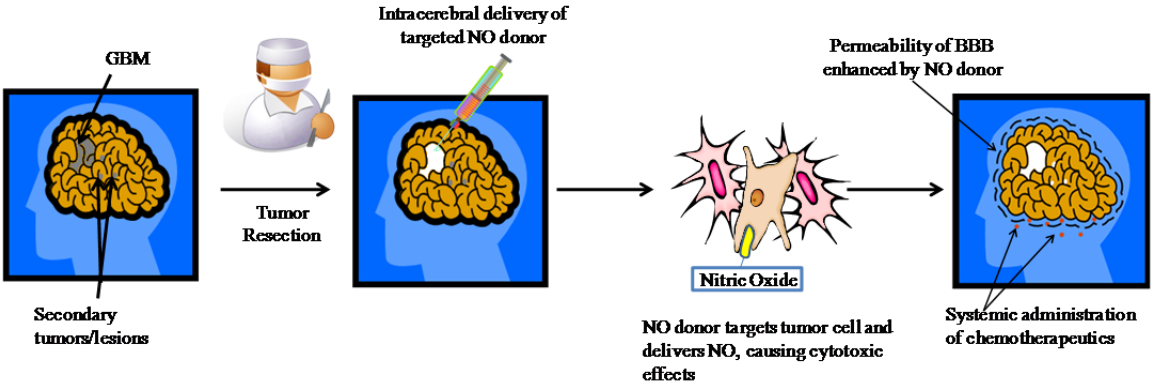

Figure 1.3. Proposed drug delivery scheme. GBM patient undergoes surgery for tumor resection; consequently the targeted nitric oxide drug is administered intracerebrally. The NO donor is able to deliver NO selectively to tumor cells, causing cytotoxic effects. A secondary benefit of NO is the enhanced permeability of the blood brain barrier which will result higher concentrations of chemotherapeutics at the tumor site.

1.7 Nitric Oxide

NO is a small, easily diffusible gaseous molecule that has been found to play numerous roles in human physiology. NO is soluble in water and lipids and its half-life *in situ* is a few seconds [124]. NO, as a result of its reactive nature, has a relatively small sphere of influence, extending approximately 100 µm from its origin [125]. NO acts as a signaling molecule in vascular, neurological and cytotoxic functions in the human body. Many of these functions, including smooth muscle relaxation, neurotransmission, and the inhibition of platelet aggregation, are mediated by the NO-cyclic guanosine monophosphate (cGMP) pathway [126]. Another mechanism of NO signaling is by the post-translational modification of proteins by the *S*-nitrosylation of cysteine thiol residues, resulting in protein activation or modulation of the protein's binding capability [127]. Alternatively *S*-nitrosylation can also cause the denaturation of proteins, resulting in a loss of catalytic functions [128, 129].

NO has both supportive and adverse effects to tissue function. NO transiently produced by inflammatory cells prevents invasion of tissue by microorganisms, whereas a sustained response would result in organ failure and septic shock [130]. NO can function as an antioxidant by removing the $O_2^{\bullet}$ radical; however, this reaction forms the cytotoxic peroxynitrite ($ONOO^-$) [130]. Conversely, by reacting with fatty alkoxyl or peroxyl radicals, NO effectively removes them from the system, where they would otherwise damage cell membranes [130]. In the presence of water and oxygen, NO can react with oxygen to form reactive nitrogen oxide species (RNOS) [131]. Some RNOS mimic the activity of NO, whereas others are toxic to the structure or function of proteins, lipids, carbohydrates, and nucleic acids [132]. Due to the important and double edged role NO plays in the body, its generation is enzymatically controlled by nitric oxide sythases [130].

Nitric oxide sythases (NOS)

Nitric oxide sythases (NOS) are a family of enzymes that catalyze the conversion of L-arginine to L-citrulline, a reaction that generates NO (Fig. 1.4) [133]. There are three isoforms of NOS; neuronal NOS (nNOS), inducible NOS (iNOS), and endothelial NOS (eNOS) [134]. eNOS and nNOS are constitutively expressed in neural and endothelial cells, and are hence referred to as constitutive NOS (cNOS). The activity of cNOS is dependent on cytosolic calcium concentration [135]. Various physiological stimuli can increase Ca^{2+} concentration, facilitating the binding of calmodulin to cNOS. The binding of calmodulin activates cNOS, consequently initiating the production of NO from L-arginine (Fig. 1.4) [136]. iNOS, conversely, is transcriptionally controlled, and its activity

is induced by inflammatory cytokines, endotoxins, hypoxia, and oxidative stress (Fig. 1.2) [137, 138]. The production of NO from iNOS, which may last up to a period of hours or even days, is independent of intracellular calcium levels and is much greater (micromolar) in comparison to that produced by cNOS (picomolar to nanomolar) [137, 139]. NO generated from eNOS and nNOS exerts its biological function via the cGMP pathway, whereas the effects of NO generated by iNOS are largely cGMP-independent [139].

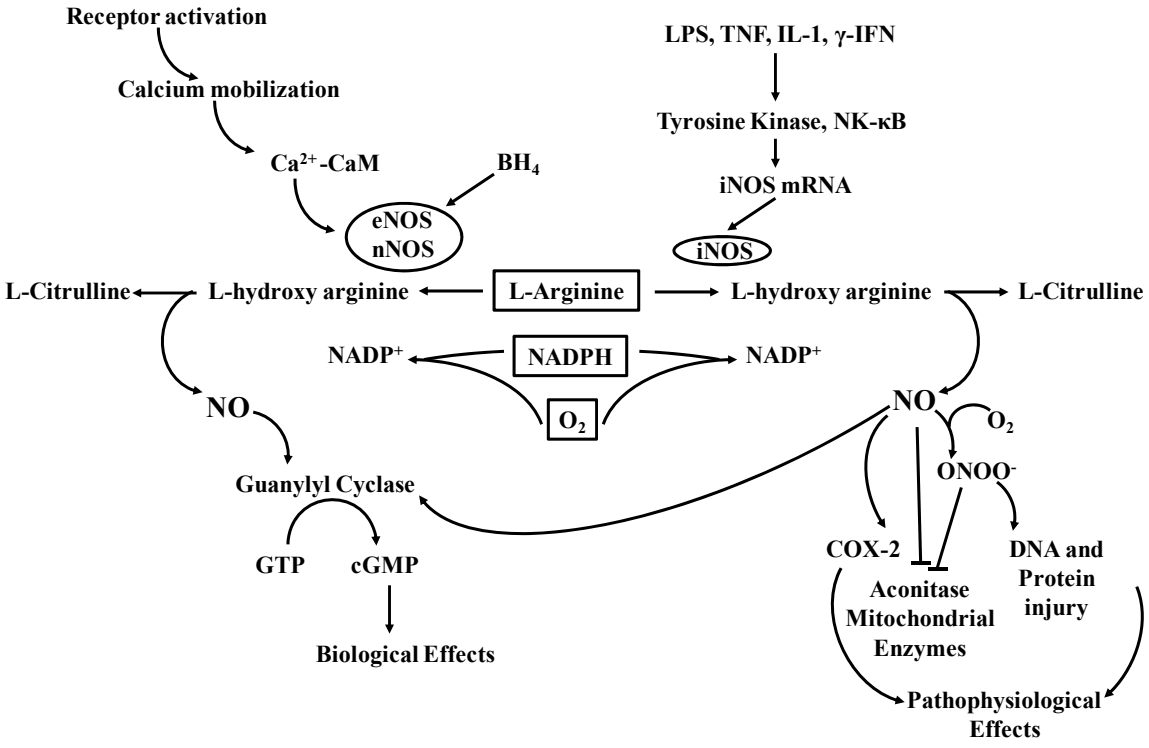

Figure 1.4. Schematic representation of the mechanisms of the different NOS isoforms Abbreviations BH_4: tetrahydrobiopterin, CaM: calmodulin, COX-2: cyclo-oxygenase type 2, γ-IFN: gamma interferon, IL-1: interleukin-1, LPS: lipopolysaccharide, NF-κB: nuclear factor-κB, TNF: tumor necrosis factor. Modified from [140].

1.7.1 Role of Nitric Oxide in Gliomas

Nitric oxide plays a ubiquitous role in malignant gliomas. Depending on the concentration and duration of exposure of NO to the glioma, it can induce or inhibit tumor progression and metastasis [126]. The effect of NO in gliomas is a culmination of: (1) the direct effect of NO on glioma cell proliferation and glioma cell invasion, (2) the effects of NO on chemotherapy and radiotherapy, (3) the indirect effect of NO on inflammatory and immune responses to gliomas, and (4) the vascular effects of NO in gliomas [141].

Effect of NO on glioma cell proliferation

In terms of cell viability, NO has been shown to have both pro and anti-tumor activity. A number of studies have shown that at micromolar concentrations of NO released from exogenous donors, glioma growth is inhibited [19, 142-146]. Exposure to NO, both directly and indirectly, has cytotoxic effects on glioma cells. NO can directly inhibit mitochondrial aconitase, thereby hindering cellular respiration [124]. NO can also inhibit the activity of ribonucleotide reductase and iron-responsive binding protein, which is essential in the regulation of the transcription of iron responsive elements [124]. Moreover, NO inhibits the activity of T4 DNA ligases, which repair DNA strands [131]. NO-damaged DNA repair enzymes induce delayed apoptosis, or alternatively, NO can increase levels of caspase-8 in glioma cells, triggering caspase-dependent apoptosis [146]. NO metabolites, nitrosothiols, nitrosamines, peroxynitrates, and RNOS also play a role in regulating the cytotoxic effects of NO, including DNA damage, lipid oxidation, protein modification, and alterations in enzyme activity, resulting in apoptosis and

necrosis [147, 148]. Thus, NO induces cytotoxicity via a number of different mechanisms.

Alternatively, *S*-nitrosylation of caspases, a family of cysteine proteases, by NO and its metabolites results in apoptosis-resistant cells, which in turn causes further accumulation of mutations and subsequent clonal selection [148]. Nitrosamines can be potentially carcinogenic and can also cause the deamination of nucleotides, leading to mutation and inhibition of DNA synthesis [124]. Studies have shown increased levels of cNOS and iNOS mRNA in gliomas in comparison to normal brain tissue [149, 150]. It has been reported that tumor-derived endogenous NO, usually in the pico- to nanomolar range, can enhance tumor growth [151]. Eyler et al. demonstrated that glioma stem cells (GSCs) have elevated iNOS levels and inhibition of iNOS resulted in decreased GSC growth and tumorgenicity, suggesting that NO has a cytoprotective role in GSCs [152]. Additionally the genetoxic properties of NO described previously can also be used by tumor cells to cause damage in surrounding healthy tissues. In order to explain these contradictory effects of NO on gliomas, it has been suggested that whereas endogenous NO is generally cytoprotective, the effects of exogenous NO, although dependent on the concentration and type of NO releasing compound, are by and large cytotoxic in gliomas.

Effect of NO on glioma cell invasion

The role of NO in glioma cell invasion, as its role in glioma cell proliferation, is ambiguous. The effect of NO on the proteolytic enzymes involved in invasion plays a critical role in determining whether invasion is enhanced or inhibited. Pullen et al. showed treatment of glioma cells with an NO donor resulted in increased MMP-1

secretion and glioma motility [153]. Another study showed increased MMP-2 expression in glioma cells after NO treatment [154]. On the other hand, it has been shown that treatment with NO releasing compound decreases MMP-9 activity [155, 156]. Additionally, NO treatment has been shown to inhibit hypoxia-induced tumor cell invasion by down-regulating hypoxia inducible factor-1 (HIF-1) and impairing mitochondria function [157]. Thus although there is contradictory evidence as to the effects of NO on glioma invasion, it is recognized that NO plays an important role in modulating invasion.

NO and GBM chemosensitivity and radiosensitivity

Similar to the effect of NO on glioma viability and invasion, the effect of NO on glioma chemosensitivity and radiosensitivity has been debated. Kurimoto et al. showed that when glioma cells were exposed to radiation in the presence of exogenous NO donors at a concentration of 100 μM, radiosensitivity was enhanced up to 1.9 times [143]. However, it is not completely understood as to how NO induces radiosensitization. Potential mechanisms include direct DNA damage, lipid peroxidation, mitochondrial damage, and intracellular reduction of glutathione [143]. Additionally, studies have used a variety of NO donors to induce chemosensitivity of glioma cells towards BCNU [158], TMZ [146], and carboplatin [19]. It is most likely that a variety of mechanisms, including inhibition of DNA synthesis, generation of toxic ROS, and inhibition of DNA repair by NO-induced interaction with DNA repair enzymes, result in the enhancement of chemosensitivity [146, 159, 160]. Deactivation of proteins involved with chemoresistance, for example, the arylation of glutathione (GSH) and the *S*-nitrosolyation

of glutathione-*S* transferases (GST) by NO and RNOS, has also been shown to contribute to the enhancement of chemosensitivity resulting from NO exposure [146]. On the other hand, studies have shown that overexpression of iNOS in glioma cells results in chemoresistance against the carbomylating action of BCNU [161]. Hence, NO plays a complicated role in glioma physiology, and the effects of NO vary greatly depending on the concentration as well as the NO releasing compound

Vascular effects of NO in gliomas

NO plays an important role in the glioma vasculature. One of the roles of NO in vasculature is the stimulation of VEGF production, the primary mediator of angiogenesis. An overstimulation of VEGF within the tumor tissue results in hyper-vasculature, which displays irregular morphology, defective architecture, and enhanced permeability [162]. This, coupled with the ability of NO to induce vasodilation via the NO-cGMP pathway, suggests that NO is at least partially responsible for the "leaky" vasculature of solid tumors [162]. Studies have shown that inhibiting NOS reduces the cerebral blood flow (CBF) by approximately 15%, whereas administration of an NO-donor increases the CBF by 33% [163]. In another study, oral administration of hydroxyurea and L-arginine enhanced levels of NO in the tumor tissue and increased uptake of a radio-labeled tracer [87]. Together, these studies suggest that increased levels of NO increase the permeability of both the BBB and the BTB. However, the ability to stimulate angiogenesis also means that NO can stimulate neovascularization, promoting tumor growth and invasion [135, 164, 165].

Effect of NO on inflammatory and immune responses to gliomas

In addition to its role in glioma proliferation, NO plays a significant role in the modulation of inflammatory and immune responses to glioma cells. Host cells, including macrophages, dendritic cells and natural killer cells, produce NO in response to the secretion of interferon gamma (INF-γ) [141]. These cells produce large amounts of NO via iNOS and cause glioma cell apoptosis by synergy with cytokines that are part of the tumor necrosis factor (TNF) family [124, 139]. In contrast to its effector role in the immune system, NO has been shown to have immunosuppressive effects as well. Studies have also shown that NO can limit T-cell proliferation and hence limit the antitumor response by these cells [166]. Additionally, NO can prevent the adhesion of leukocytes to tumor vasculature [166]. Furthermore, Badn et al. showed that the efficacy of immunotherapy for gliomas was significantly improved when iNOS activity in glioma bearing rats was inhibited [167].

1.8. Nitric Oxide Donors

The various physiological roles of NO have resulted in its use for the treatment of numerous diseases. Since NO gas itself has a short half-life and therefore limited utility as a therapeutic agent, a variety of NO donors have been developed [125, 168, 169]. NO donors are characterized in the following categories: 1) organic nitrates and nitrite esters, 2) iron-nitrosyl complexes, 3) *S*-nitrosothiols 4) hybrid NO donors, and 5) diazeniumdiolates [170].

The conventionally used cardiovascular drugs nitroglycerin, isosorbide dinitrite, and nicorandil are classified as organic nitrates and esters [170]. These drugs release NO by metabolism with the help of various enzymes. The major problem in using organic nitrates and esters for NO therapy is the development of drug tolerance after long term use [170]. The most commonly used NO donor from the second category, iron nitrosyl complexes, is sodium nitroprusside (SNP), which has a complex structure in which a nitrosyl group is bound to iron [170]. SNP has been used clinically as a vasodilator but its use is limited due to the potential for the induction of thiocynate toxicity as well as an increased potential for the formation of the cytotoxic peroxynitrite [140, 170].

S-nitrosothiols, the third category of NO donors, are formed by the *S*-nitrosation of thiols. Some *S*-nitrosothiols occur naturally *in vivo*, for example, *S*-nitrocysteine, *S*-nitroglutathione, and *S*-nitrosoalbumin [140]. Some common chemically synthesized *S*-nitrothiols are *S*-nitroso-N-acetylpenicillamine (SNAP) and *S*-nitrosocaptopril. *S*-nitrosothiols can release NO via a number of mechanisms including catalysis by Cu^{2+} ions, reaction with ascorbate, or enzymatic, photochemical or thermal decomposition [125, 140]. The fourth category of NO donors, hybrid NO donors, are synthesized by adding an NO-releasing moiety to a drug, to increase its effectiveness [125]. Various non-steroidal anti-inflammatory drugs (NSAIDs) including aspirin, ibuprofen and diclofenac have been modified to incorporate a NO-releasing molecule [125].

Diazeniumdiolates

Diazeniumdiolates, also called NONOates, are a class of NO donors that have a diolate group [N(O-)N=O] bound to an amine group [125]. These compounds decompose

to release NO in acidic or neutral solutions. Under basic, freeze-dried or frozen states diazeniumdiolates are stable. Release rates vary with temperature, pH, and the molecular structure of the donor. Increasing the pH of the solution increases the rate of NO release [171]. The by-product of the reaction is the original amine compound [172]; this is of great importance as many NO donors, such as SNP, produce toxic by-products after releasing NO. Diazeniumdiolates, on the other hand, if synthesized from innocuous peptides or proteins, can be tailored to release only non-toxic by-products [173].

Proteins and peptides have a high number of surface amines which, when exposed to NO gas, form diazeniumdiolates [174]. The reaction of amines with NO to form diazeniumdiolates is an exothermic reaction which can proceed via two different mechanisms (Fig. 1.5) [171]. The NO can either react with the amine to form a radical or with another NO molecule to form a dimer, which consequently reacts with the amine. However, if it is assumed that there is no significant difference in the dissociation of NO from either diazeniumdiolate, it is likely that the formation of the radical is the more favorable mechanism [171].

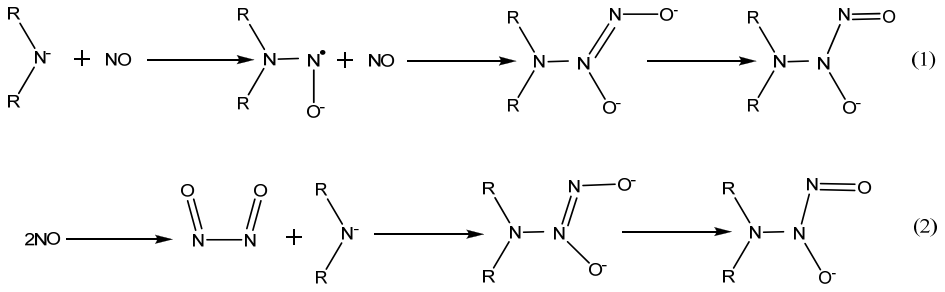

Figure 1.5. Reaction of free amines with NO gas to form NO-releasing diazeniumdiolates. There are two possible ways that the reaction of amines with NO can proceed. The NO can react with the amine to form a radical (mechanism 1) or two moles of NO can reaction to form a dimer, which then reacts with the amine to form a diazeniumdiolate (mechanism 2). Assuming that there are no significant differences in the association of NO from either diazeniumdiolate, it is likely that mechanism 1 is more favorable [171].

In the work discussed in this thesis, the aforementioned reaction of NO with amines to form diazeniumdiolate NO donors was utilized. Taylor et al. proposed the mechanism of NO release from diazeniumdiolates begins with the protonation of the compound to form a thermodynamically unstable moiety (Fig.1.6) [171]. This is followed by a second protonation step, in which the protonated NO dimer is released along with the original amine compound. Two moles of NO are released after protonation and homolytic cleavage of the NO dimer [171].

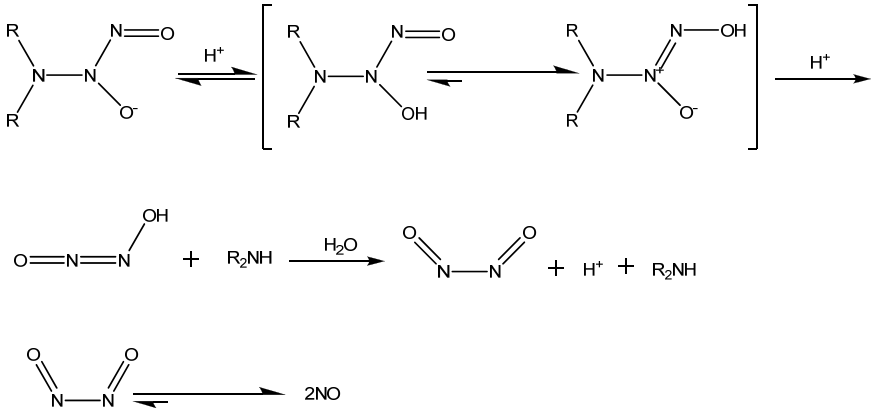

Figure 1.6. The mechanism of NO release from the decomposition of diazeniumdiolates. Release of NO is triggered by a protonation step which forms a thermodynamically unstable moiety. In a second protonation step the protonated NO dimer is released along with the original amine compound. Homolytic cleavage of the NO dimer results is the release of two moles of NO [171].

1.8.1 Nitric Oxide donors used in GBM treatment

A variety of exogenous NO donors have been investigated for their anti-glioma properties. Kurimoto et al. studied the glioma cell growth inhibition and radiosenitization effects of SNP and SNAP [143]. (*S,R*)-3-phenyl-4,5-dihydro-5-isoxazole acetic acid-nitric oxide (GIT-27NO) is a hybrid NO donor, developed by adding a NO releasing moiety to the immunodulatory drug VGX-1027, which has been shown to trigger glioma cell death [175]. However, controlled NO release from diazeniumdiolates has made this

group of NO donors more popular as potential anti-tumor agents. Weyerbrock et al. tested the effect of three diaziumdiolates, proline NONOate (PROLI/NO), diethlyamine NONOate (DETA/NO), and spermine NONOate (SPER/NO) and found that both DETA/NO and SPER/NO inhibited tumor cell growth at concentrations of 10 mM [19]. Additionally O^2-[2,4-dinitro-5-(*N*-methyl-*N*-4carboxyphenylamino) phenyl] (1-*N*,*N*-dimethylamino)diazen-1-ium-1,2-diolate) (PABA/NO), β-galactosyl-pyrrolidinyl diazeniumdiolate (β-Gal-NONOate), and O^2-(2,4-Dinitrophenyl) 1-[(4-ethoxycarbonyl)piperazin-1-yl]diazen-1-ium-1,2-diolate (JS-K) have been used to inhibit glioma cell growth [145, 146, 176]. Although all of these studies have shown that NO can be used to inhibit glioma cell growth, it has been recognized that because of their non-specific nature these NO donors can result in neurotoxicity.

Although a dichotomy appears to exist in the various roles NO plays in GBM physiology, there is sufficient evidence that exogenous NO donors, in particular diazeniumdiolates, are able to inhibit glioma cell growth and increase chemosensitivity. However the non-selective nature of previously studied NO donors has the potential to cause neurotoxicity. Therefore, in this thesis, the synthesis and characterization of novel glioma targeting diazeniumdiolates as well as their effect on glioma cell viability, chemosensitivity and invasion is discussed.

CHAPTER 2: SYNTHESIS AND CHARACTERIZATION OF GLIOMA TARGETING NITRIC OXIDE DONORS

2.1 Summary

GBM is among the most aggressive tumors in the human body, and patient survival is often less than one year. Various cytotoxic chemotherapeutic drugs have been used to treat GBM, but the efficacy of these drugs is severely limited due to their non-specific nature, resulting in toxicity towards normal cells. The non-specific nature of chemotherapeutics results in most anti-cancer drugs administered at maximum tolerated dose, which in turn results in a variety of side effects in the patient. Therefore in order to increase patient survival and minimize the toxic side effects of chemotherapy, a number of studies have focused on developing effective anti-tumor drugs that are able to target tumor cells. Herein, the synthesis and characterization of two novel glioma-targeting NO donors is presented. NO is a small yet important biological messenger, which at sufficient concentrations has been shown to induce apoptosis as well as increase radiosensitization in tumor cells. VTWTPQAWFQWVGGGSKKKKK (VTW) and chlorotoxin (CTX), two glioma targeting biomolecules, were transformed into NO donating diazeniumdiolates, with half-lives of 24.3 hours and 19.2 hours, respectively. Furthermore, tumor cell viability was significantly decreased when cells were incubated with the NO donors while the control cell viability was not affected significantly. Fluorescence microscopy confirmed that the biomolecules retained their glioma-targeting ability after the transformation to NO donors. In addition, confocal microscopy also confirmed the endocytosis of both NO donors. The techniques discussed in this chapter can be easily

modified to synthesize targeted NO donors from various tumor-targeting peptides and proteins to develop disease specific therapeutics.

2.2 Introduction

The first step in developing glioma specific NO-releasing peptides was the identification of GBM targeting peptide sequences. From extensive research, two biomolecules that have high affinity for glioma cells were identified. The first, chlorotoxin (CTX), is a 36-amino acid protein isolated from the venom of the Deathstalker scorpion *(Leiurus quinquestriatus*) [177, 178]. This protein has four disulfide bonds, making the molecule very compact [177]. CTX has a high affinity for a lipid raft anchored complex that contains MMP-2 [179-182]. MMP-2 is overexpressed in gliomas, but is not expressed in normal glial cells and neurons, allowing highly efficient targeting of glioma cells [180, 183-185].

CTX has previously been conjugated with supermagnetic nanoprobes, and has been used effectively as a diagnostic tool to image gliomas [113, 186]. CTX conjugated nanoprobes have shown enhanced targeting specificity as well as benign biological response in comparison to current imaging systems that utilize passive targeting to image tumors [113, 182, 186, 187]. Furthermore, CTX-labeled nanoparticles have been used for targeted green fluorescence protein (GFP) gene delivery, resulting in enhanced GFP expression in the glioma cells [188]. In other studies, CTX bound nanoparticles have been used to efficiently deliver methotrexate [115], short interfering RNA (siRNA) [113, 189], and plasmid DNA [190] to glioma cells. These studies showed that not only does CTX target glioma, it is also efficiently endocytosed by the cancer cells.

The second biomolecule identified was the 12 amino acid peptide sequence VTWTPQAWFQWV (VTW-1). This peptide sequence was identified using a 12-mer phage display library [191]. Wu et al demonstrated that VTW-1 bound 700-fold more effectively to glioma cells in comparison to normal human astrocytes [191]. By conjugating a 119 kDa subunit of β-galactocidase, it was also demonstrated that VTW-1 could be used to deliver proteins into cells [191]. From Basic Local Alignment Search Tool (BLAST) analysis, it was found that the VTW-1 sequence was similar to a 7-residue fragment of the interleukin-11 receptor alpha chain (IL-11RA) [191, 192]. IL-11RA is a transmembrane glycoprotein that binds to gp130, a cell surface molecule that is overexpressed in glioma cells. The mechanism by which VTW targets glioma cells is most likely a result of an interaction with the gp130 receptor [191]. Since the VTW-1 sequence described above is highly hydrophobic and only has one free amine, a GGGS spacer sequence and five lysine residues were added to the sequence. Thus, the peptide used was VTWTPQAWFQWVGGGSKKKKK (VTW).

2.3 Objective

In this chapter, the synthesis and characterization of glioma-targeting NO donors developed from CTX and VTW is discussed. The NO donors were assessed for the following:

- NO release
- Ability to target GBM cells
- Effects on GBM and normal cell viability and
- Ability to be endocytosed by glioma cells

2.4 Materials and Methods

2.4.1 Chemicals

Minimum Essential Media (MEM), fetal bovine serum (FBS), L-glutamine-penicillin-streptomycin (GPS), non-essential amino acids and 0.21% trypsin containing 0.25% ethylenediaminetetraacetic acid (trypsin-EDTA) were obtained from Mediatech, Inc. (Manassas, VA). NO gas was obtained from Airgas (Atlanta, GA). Unless otherwise mentioned, all other chemicals were obtained from Sigma-Aldrich (St. Louis, MO).

2.4.2 Cell Maintenance

T98G and U-87MG human glioblastoma cells (American Type Cell Culture, Manassas, VA) were cultured in MEM with 10% FBS, 1% GPS and 1% non-essential amino acids at 37^{o}C and 5% CO_2. Normal human astrocytes (NHAs, Lonza Inc. Walkersville, MD) were cultured in astrocyte basal media (ABM) supplemented with astrocyte growth medium SingleQuots (Lonza Inc. Walkersville, MD) at 37^{o}C and 5% CO_2. Human brain microvascular endothelial cells (HBMECs; ScienCell Research Laboratories, Carlsbad, CA) were cultured in Endothelial Cell Medium (ECM) supplemented with endothelial cell growth supplement (ScienCell Research Laboratories, Carlsbad, CA) at 37^{o}C and 5% CO_2. For experiments, NHAs passages 3-5, HBMECs passages 3-6 and T98G and U-87MG passages 5-12 were used.

2.4.3 Synthesis and characterization of NO donors

Known amounts of CTX (Bachem Chemicals, Torrance, CA) and VTW (Genscript USA Inc., Piscataway, NJ) were dissolved in nanopure water (DI, 18 mΩ resistance) at room temperature and pH 7.4. The solution was placed in a round bottom flask, the atmosphere was evacuated using a vacuum pump, and then the flask was filled with NO gas (Fig. 2.1). Evacuating the atmosphere to create a hypoxic environment is a critical process for the formation of the diazeniumdiolate complex, as it prevents the premature conversion of NO to nitrite. After an hour, the pH of the solution was adjusted to 7.4 using 1M sodium hydroxide (NaOH), thereby preventing the decomposition of the newly formed diazeniumdiolates at low pH. Consequently, the atmosphere was evacuated again, and the solution was exposed to NO gas for 24 hours to ensure conversion of remaining amines to diazeniumdiolates [193-195]. After 24 hours, the pH of the samples was re-adjusted to 7.4 as before, and the samples were frozen, lyophilized and stored at -20^{o}C until use. These samples were designated as CTX-NO and VTW-NO.

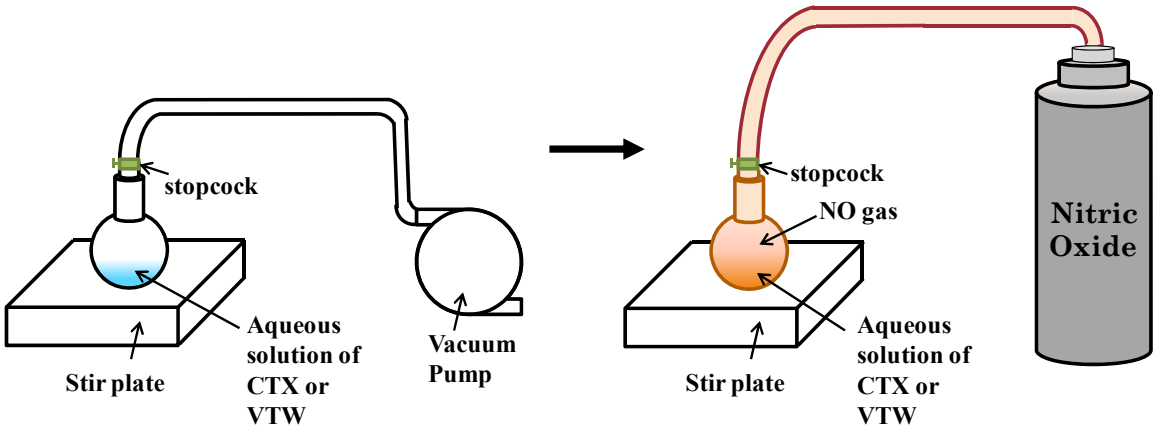

Figure 2.1. Reaction setup for synthesis of NO donors. An aqueous solution of the targeting biomolecules, CTX or VTW, was placed in a round bottom flask, and a vacuum pump was used to create a hypoxic environment. Subsequently, the flask was filled with NO gas and the biomolecules were allowed to react with the gas for 24 hours. At the end of the reaction, the samples were neutralized, frozen, lyophilized and stored until use.

In order to determine the percentage conversion of amines to diazeniumdiolates after the reaction of the biomolecules with NO gas, a colorimetric Ninhydrin assay was performed. Ninhydrin reacts with free amines to form a colored complex known as Ruhemann's purple which has an absorbance maxima at 570 nm [196, 197]. The assay was performed by adding Ninhydrin solution (Spectrum Chemicals, Gardena, CA) to aqueous solutions of CTX, CTX-NO, VTW, VTW-NO, as well as L-leucine solutions of known concentrations. These mixtures were then placed in a boiling water bath for 15 minutes and then allowed to cool for 30 minutes. Using a Beckman DTX 880 Multimode Plate Reader (Beckman Coulter, Drea, CA), sample absorbances were measured at a wavelength of 570 nm. Absorbance measurements from L-leucine samples were used to construct a standard curve which was used to determine the amount of amines in each sample.

2.4.4 Characterization of NO release

To measure NO release from the synthesized NO donors, lyophilized samples of CTX-NO or VTW-NO were dissolved in DI water and NO release at 37^{o}C from the NO donor was quantified using an ISO-NOPF nitric oxide sensor (World Precision Instruments Sarasota, FL) connected to an APOLLO 1000 Free Radical Detector (World Precision Instruments Sarasota, FL), as shown in Fig. 2.2. The ISO-NOPF sensor is a combination of an NO-sensing element and a reference electrode coated with an NO-selective membrane [198]. NO gas diffuses through the membrane and is oxidized at the surface of the working electrode generating, a redox current.

Prior to measurements with the NO donors, the ISO-NOPF sensor was calibrated as per manufacturer's instructions. In brief, nitrogen was bubbled first through 10% solution of potassium hydroxide (KOH) and then a glass vial containing 20 ml of DI water. After 30 minutes, nitrogen gas was substituted with NO gas. The NO gas was then bubbled through the aforementioned system for ten minutes, after which the glass vial was sealed. NO saturated de-oxygenated DI water has been reported to have an NO concentration of 1.91 mM [199]. Aliquots of this saturated NO solution were used to calibrate the probe.

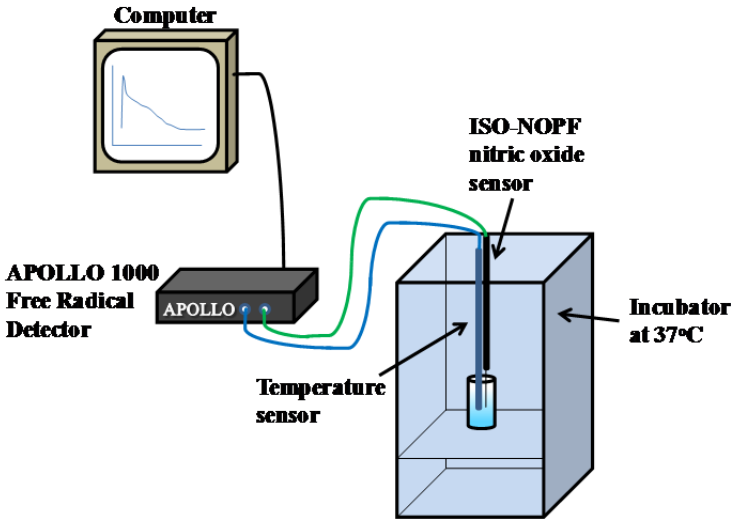

Figure 2.2. Experimental setup for measuring the release of NO from CTX-NO and VTW-NO. The NO donor was dissolved in DI water and placed in an incubator at 37°C. The ISO-NOPF nitric oxide probe and a temperature probe were placed in the sample. Readings were collected by the APOLLO 1000 free radical detector connected to the probes.

2.4.5 Verification of glioma targeting ability

In order to determine if VTW and CTX retained their tumor targeting abilities following the reaction of amines with NO gas, the biomolecules were first labeled with fluorescein isothiocyanate (FITC). In brief, the biomolecules were dissolved in DI water and reacted with a two-fold molar excess of a 0.1 mM solution of FITC in 0.1 M sodium

bicarbonate buffer (pH 9.0). The FITC solution was added dropwise to the solution of CTX or VTW and allowed to react for two hours in the dark. The FITC labeled biomolecules were then dialyzed for two hours against DI water and subsequently reacted with NO for 24 hours to neutralize the charge on any unreacted amines. The final products, designated as CTX-FITC and VTW-FITC, were frozen, lyophilized and stored at -20^{o}C until use.

T98Gs, U-87MGs, NHAs and HBMECs were seeded in black-walled 96-well plates at a density of 25,000 cells/cm^2. After allowing the cells to adhere for 24 hours, they were incubated for 30 minutes with FITC-labeled biomolecules. All cell types were exposed to 5 μM of FITC-reacted amines. This VTW/CTX concentration is equivalent to exposure of cells to 10 μM of NO. After 30 minutes, the media was removed and the cells were washed three times with phosphate buffered saline (PBS, pH 7.4) before fresh media was added. The ability of the fluorescently labeled biomolecules to adhere to the different cell types was visualized using a Leica DMI 4000B fluorescent microscope equipped with a Hamamatsu ORCA-ER digital camera (Leica Microsystems, Inc., Bannockburn, IL). A minimum of three pictures were taken per well. Furthermore, the fluorescence in each image was quantified using Image J software. In order to ensure changes in fluorescence were not due to changes in cell proliferation, a separate experiment was conducted in which cells were seeded at the aforementioned density and after 24 hours cells were trypsinized and counted using a Beckman z1 Particle Counter (Beckman Coulter, Drea CA).

2.4.6 Effect of NO on cell viability

T98Gs, U-87MGs, NHAs and HBMECs were seeded in 96-well plates at a density of 25,000 cells/cm^2. Cells were allowed to adhere for 24 hours, after which they were incubated with varying concentrations of CTX-NO or VTW-NO such that each cell type was exposed to 0, 10, 20 and 40 μM of NO. In control experiments, T98G and U-87MG cells were incubated with equivalent concentrations of VTW or CTX (not reacted with NO). After 48 hours, the media was aspirated and the cultures were rinsed with PBS to remove dead cells. The remaining cells were removed from the culture surface using trypsin-EDTA and counted using a Beckman z1 Particle Counter (Beckman Coulter, Drea, CA). Cell viability was calculated using the following formula:

$$\text{Cell viability} = \frac{\text{Cells counted after incubation with NO donor}}{\text{Cells counted after incubation with DI}} \times 100$$

Similar cell viability experiments were conducted with SNAP, which served as a non-targeting NO control. In brief, T98Gs and U-87MGs were seeded in 96-well plates at a density of 25,000 cells/cm^2. After 24 hours, cells were incubated for 48 hours with 0-200 μM solutions of SNAP in water. SNAP has been used in a variety of studies to inhibit glioma cell growth [19, 143, 158, 200-202]. It releases 1 mole of NO per mole of SNAP spontaneously under physiological conditions, with a reported half life of 4-5 hours [203, 204]. After 48 hours, as before, cells were removed from culture surface and counted.

In an alternate experiment to measure cell viability, after a 48 hour incubation with CTX-NO or VTW-NO, a Live/Dead assay (Invitrogen, Carlsbad, CA) was used to visualize viable cells. In brief, the cells were washed three times and then incubated with 2 μM calcein-AM and 4 μM ethidium homodimer-1. After 30 minutes of incubation, a

Leica DMI 4000B fluorescent microscope equipped with a Hamamatsu ORCA-ER digital camera (Leica Microsystems, Inc., Bannockburn, IL) was used to visualize green and red fluorescence emitted by the live and dead cells, respectively. A minimum of three pictures were taken per well. The number of cells stained red and green were counted to calculate the percentage of dead cells.

2.4.7 Effect of an NO scavenger on cytotoxicty of CTX-NO

T98Gs and U-87MGs were seeded in 96-well plates at a density of 25,000 cells/cm^2. After allowing cells to adhere for 24 hours, the cells were incubated with either MEM or MEM containing hemoglobin (HB), an NO scavenger. Immediately following the initial incubation, the cells were exposed to CTX-NO or VTW-NO such that cells were incubated with 0, 10 or 20 μM NO. After 48 hours, the cultures were rinsed to remove dead cells and the remaining cells were removed from the culture surface. Viability was measured as described in section 2.4.6.

2.4.8 Endocytosis of NO donors

Glass coverslips were coated with 0.5% gelatin for 2 hours, and T98G and U-87MG cells were seeded on the coverslips at a density of 25,000 cells/cm^2. After 24 hours, cells were incubated with CTX-FITC or VTW-FITC, as described in section 2.4.5. After the 30 minute incubation, cells were washed three times with PBS. The cells were then incubated with 5μg/ml of orange plasma membrane stain (Invitrogen, Carlsbad, CA) for 5 minutes at 37^{o}C. Subsequently, the cells were fixed with 4% formaldehyde for 10 minutes. Next, cells were incubated with 600 nM of 4',6-diamidino-2-phenylindole,

dihydrochloride (DAPI) stain for 5 minutes. The coverslips were then mounted on a glass slide and visualized using a Zeiss LSM 510 UV Confocal Microscope (Carl Zeiss Inc, Peasbody, MA) with the appropriate filters.

2.4.9 Statistical Analysis

All experiments were carried out minimally in triplicate. Different conditions were compared using an analysis of variance (ANOVA), with *p*-values less than 0.02 considered to be statistically significant.

2.5 Results

2.5.1 Characterization of NO donor

In order to measure the efficacy of the reaction with NO gas, the Ninhydrin assay was used to detect free amines on biomolecules in solutions, both before and after the hypoxic reaction with NO gas. Before the reaction with NO gas, 6.9 ± 0.26 amines/mole CTX (85.7 ± 3.31%) were detected, whereas after the 24 hour reaction with NO gas, 0.00 ± 0.00 amines/ mole CTX were detected. Similarly, 3.6 ± 0.07 amines/mole VTW (72.5 ± 1.42%) were detected before the reaction of VTW with NO gas, whereas after the reaction 0.05 ± 0.08 amines/mole VTW (0.91 ± 1.58%) were detected.

2.5.2 Characterization of NO release

As discussed in Chapter 1, diazeniumdiolates are able to dissociate in aqueous, acidic and neutral environments to release two moles of NO. Therefore, in order to

measure the decomposition of diazeniumdiolates, samples of CTX-NO and VTW-NO were dissolved in DI water and the NO release rates were measured using an NO probe. The NO probe is covered in an NO selective membrane and hence only detects NO and not the by-products of NO degradation that could be present in the solution.

The measurements from the NO-specific microsensor demonstrated that CTX-NO and VTW-NO had similar instantaneous NO release profiles. Peak NO release from CTX-NO was found to be after 3.93 hours of dissolution in DI water (Fig. 2.3A) whereas peak NO release from VTW-NO was after 4.45 hours (Fig. 2.3C). Cumulative release profiles for both NO donors, CTX-NO (Fig. 2.3B) and VTW-NO (Fig. 2.3D), were calculated using the results from the NO probe and the Ninhydrin assay. The cumulative release profiles showed that CTX-NO released 91.05% ± 1.30 of the expected NO in the first 72 hours (Fig. 2.3B), while VTW-NO released 87.9% ± 0.26 of the expected NO within the same time period (Fig. 2.3D). Further analysis also showed that CTX-NO and VTW-NO have a half life of 19.2 hours and 24.3 hours, respectively.

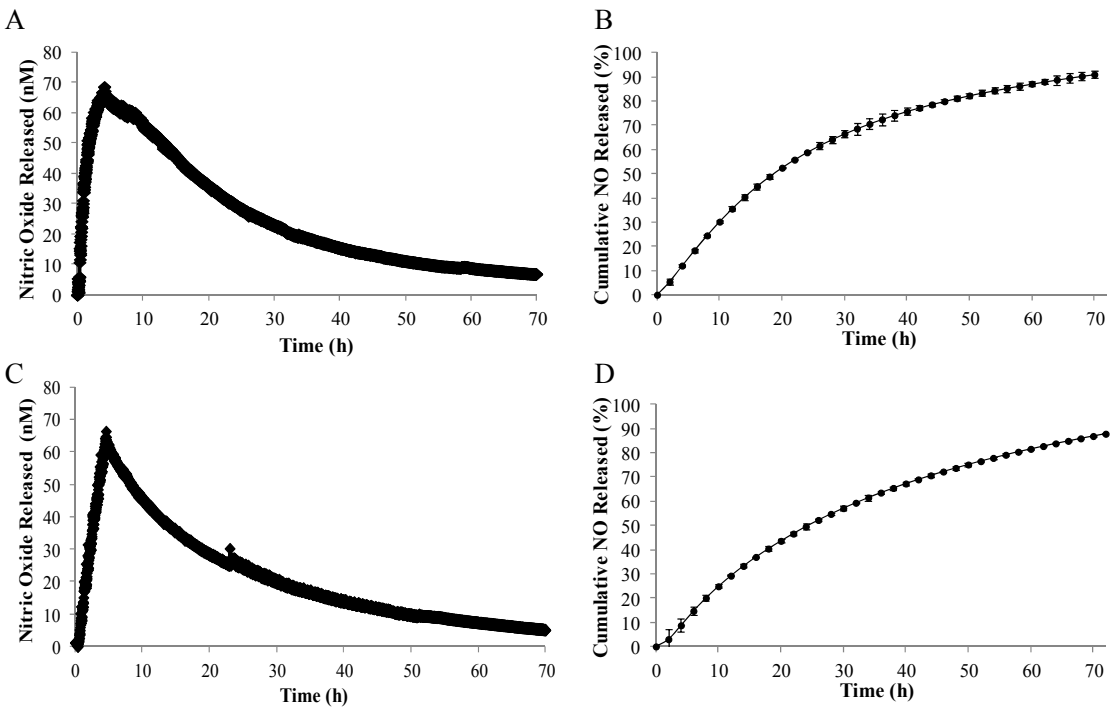

Figure 2.3. (A) Instantaneous NO release from CTX-NO at pH 7.4 in DI water at 37°C. Peak NO release was observed after 3.93 hours and NO release continued for at least 72 hours. (B) Cumulative release profile for CTX-NO based on results of Ninhydrin assay and instantaneous NO release profiles. Over 90% of the expected NO was released in the first 72 hours and CTX-NO has a half life of 19.2 hours. (C) Instantaneous NO release from VTW-NO at pH 7.4 in DI water at 37°C. Peak NO release was observed after 4.45 hours and NO release continued for at least 72 hours. (D) Cumulative release profiles for VTW-NO based on results of Ninhydrin assay and instantaneous NO release profiles. Over 85% of the expected NO was released in the first 72 hours and VTW-NO has a half life of 24.3 hours.

2.5.3 Verification of glioma targeting ability

In order to determine whether the biomolecules retained their targeting ability after the reaction of amines, the biomolecules were first tagged with FITC, incubated with cells and then visualized using fluorescence microscopy. It was visually determined that the FITC-labeled biomolecules, when incubated with T98G, U-87MG, NHA and HBMEC cells, bound preferentially to the glioma cell lines and only minimal binding to the NHAs and HBMECs was observed (Fig. 2.4A). This qualitative assessment suggested that the reaction of the amines with FITC did not hinder the ability of the biomolecules to

target glioma cells. Thus, it is inferred that the reaction with NO, which is a much smaller molecule than FITC, will not hinder the specificity of the biomolecules.

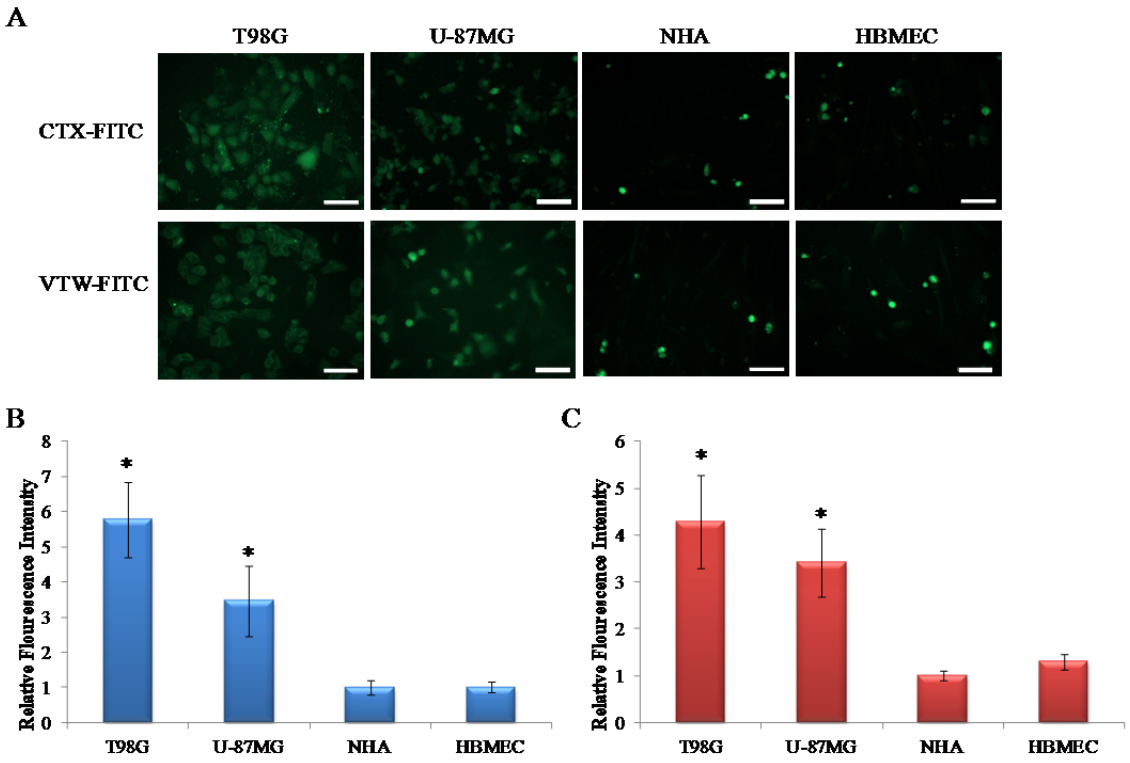

Figure 2.4. (A) Fluorescent images of cell cultures showing binding of FITC labeled CTX (top row) and VTW (bottom row) to different cell types after 30 minute incubation with the biomolecules Scale bar = 10 µM. Qualitative analysis shows that both biomolecules bind to glioma cells lines, T98G and U-87MG, very efficiently whereas non-tumor cell lines, NHAs and HBMECs, show only minimal binding. Relative fluorescence of cells incubated with fluorescently tagged with (B) CTX and (C) VTW, quantified using Image J. Both CTX and VTW show significantly higher binding to glioma cells in comparison to non-tumor cell lines, NHA and HBMEC. *$p < 0.02$ compared to NHA, n = 5.

In order to measure differences in the binding of FITC-labeled biomolecules to the different cell types, the relative fluorescence detected for each cell type was quantified using Image J software. From this quantitative analysis, it was determined that relative to the fluorescence detected in NHA cultures (normalized to 1.00 ± 0.21), labeled CTX bound to HBMECs had an intensity of 1.01 ± 0.15, while T98G and U-87MG cultures had fluorescence intensities of 5.78 ± 1.07 and 3.46 ± 0.99, respectively (Fig.

2.4B). Similarly, the differences in the binding of labeled VTW were quantified by showing that relative to fluorescence measured in NHAs (again normalized to 1.00 ± 0.11) and in HBMECs (1.30 ± 0.16), T98Gs (4.30 ± 0.99) and U-87MGs (3.42 ± 0.73) displayed significantly higher fluorescence, and hence binding, to VTW-FITC (Fig. 2.4C). Cell proliferation was also monitored during this experiment, and no significant increase in cell number was observed; the increased fluorescence is only due to the preferential binding of CTX-NO and VTW-NO to glioma cells.

2.5.4 Effect of NO on cell viability

Cells were incubated with either CTX-NO or VTW-NO for 48 hours, trypsinized, and counted to determine the effect of the NO donors on the viability of different cell types. In control experiments, the cytotoxicity of VTW and CTX was also investigated. No significant changes in glioma cell viability were observed after incubation with VTW or CTX that were not reacted with NO (Fig. 2.5).

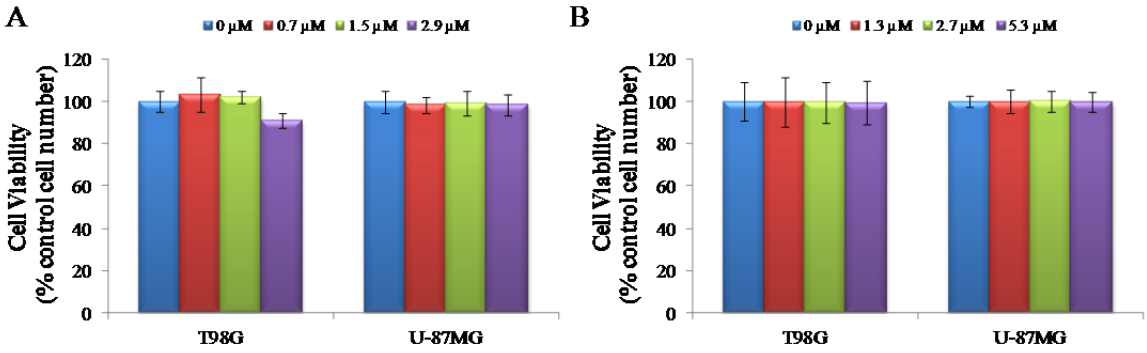

Figure 2.5. Effect of biomolecules, (A) CTX and (B) VTW on the cell viability of glioma cell lines, T98G and U-87MG. Legend refers to (A) CTX and (B) VTW concentrations. Data is presented as a percentage of the number of cells that were incubated with only media. Gioma cell viability is not significantly reduced by either biomolecules.*$p < 0.05$, n = 3-6

At an NO concentration of 10 µM, (the lowest concentration used for these experiments) CTX-NO was effective in reducing cell viability to 68.6 ± 14.4% and 72.7 ± 6.5% of the control cell number in T98G and U-87MG cells respectively (Fig. 2.6A). Conversely, NHA and HBMEC viability remained above 92.5 ± 3.0% at the same NO concentration.

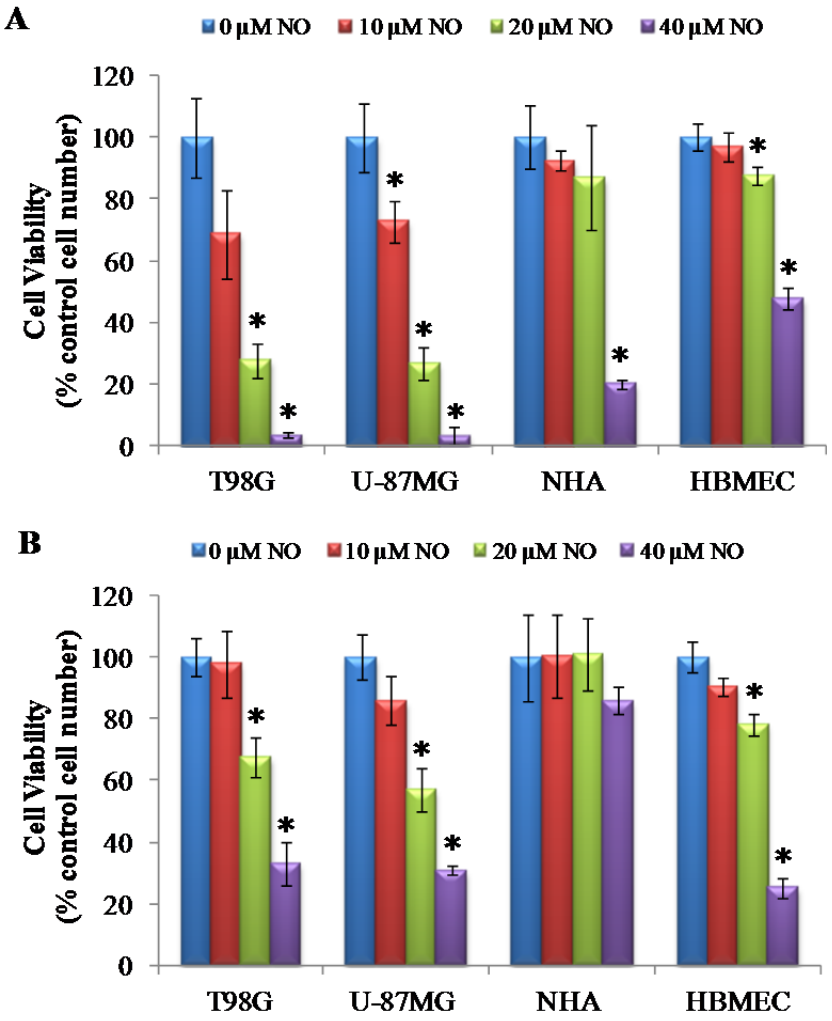

Figure 2.6. Effect of targeted NO donors, (A) CTX-NO and (B) VTW-NO, on the cell viability of glioma cell lines, T98G and U-87MG, and normal cell types, NHA and HBMEC. Data is presented as a percentage of the number of cells that were incubated with NO free media. The legend refers to NO concentrations corresponding to CTX concentrations of 0, 0.7, 1.5 and 2.9 µM and VTW concentrations of 0, 1.3, 2.7 and 5.3 µM. Both donors show a dose dependant effect on glioma cell viability and have no significant effect on the normal cell types at the lower NO concentrations. Comparing the effect of the two donors at a median concentration of 20 µM it is observed that CTX-NO is more efficient in reducing glioma cell viability in comparison to VTW-NO. *$p < 0.02$, n = 4.

At a higher NO concentration of 20 μM, CTX-NO reduced T98G and U-87MG cell viability to 27.4 ± 5.4% and 26.8 ± 5.1%, respectively. At this NO concentration NHA cells had a viability of 86.8 ± 16.9% and HBMECs had a viability of 87.5 ± 2.9% (Fig. 2.6A). At the highest NO concentration of 40 μM, released by CTX-NO, glioma cell viability was substantially reduced to 3.60 ± 0.9% and 3.1 ± 2.9% of the control cell number in T98G and U-87MG cells, respectively. However, at this high NO concentration NHA and HBMEC viability was also reduced to 20.1 ± 1.3% and 47.7 ± 3.5% respectively.

Although VTW-NO showed a similar effect on the viability of the different cell lines, it was not as efficient as CTX-NO in decreasing tumor cell viability. At the lowest concentration of NO, 10 μM, VTW-NO did not significantly change glioma cell viability which was measured to be 97.9 ± 10.9% and 85.9 ± 7.9% of the control cell number in T98G and U-87MG cells, respectively (Fig. 2.6B). At a higher NO concentration of 20μM, VTW-NO was able to reduce the cell viability of T98G cells and U-87MG cells to 67.4 ± 6.5% and 57.1 ± 7.2%, respectively (Fig. 2.6B). At this same concentration, NHA viability was not reduced and was measured to be 101 ± 11.9% of the control cell number. However, HBMEC viability was reduced to 78.0 ± 3.6% at the aforementioned concentration. At the highest NO concentration of 40 μM, the viability of the T98G cells was significantly reduced to 33.1 ± 6.9% and U-87MG viability was reduced to 30.8 ± 1.5%. As opposed to the lower concentrations, at an NO concentration of 40 μM donated by VTW-NO, the viability of the NHAs was also reduced to 86.0 ± 4.1% (Fig. 2.6B

In order to visualize the effect of NO on cell viability, following a 48 hour incubation with either VTW-NO or CTX-NO, cells were stained with a mixture of

calcein-AM and ethidium homodimer-1. Non-fluorescent calcein-AM is converted to green fluorescent calcein by viable cells, while ethidium homodimer-1, which is a fluorescent red DNA stain, is only able to permeate dead cells [205]. That is, the mixture stains live cells green and dead cells red.

For these experiments, cells were exposed to an NO concentration of 10 μM, since at higher concentration massive tumor cell death occurred, resulting in a majority of the cells detaching from the surface. Using fluorescence microscopy, cell viability was visualized and the percentage of cells stained red by the ethidium homodimer-1 (dead cells) was calculated for each cell type. Even at a low NO concentration, 13.3 ± 6.4% of the adherent T98G cells were stained red after the CTX-NO treatment, whereas without the CTX-NO treatment only 0.4 ± 0.5% of the adherent T98G cells were stained red (Fig. 2.7A). Similarly, when U-87MG cells were incubated with CTX-NO 27.8 ± 8.5 % of the adherent U-87MG cells stained red (Fig. 2.7B). NHA (Fig. 2.7C) and HBMECs (Fig. 2.7D) showed no significant changes in cell death when incubated with or without CTX-NO.

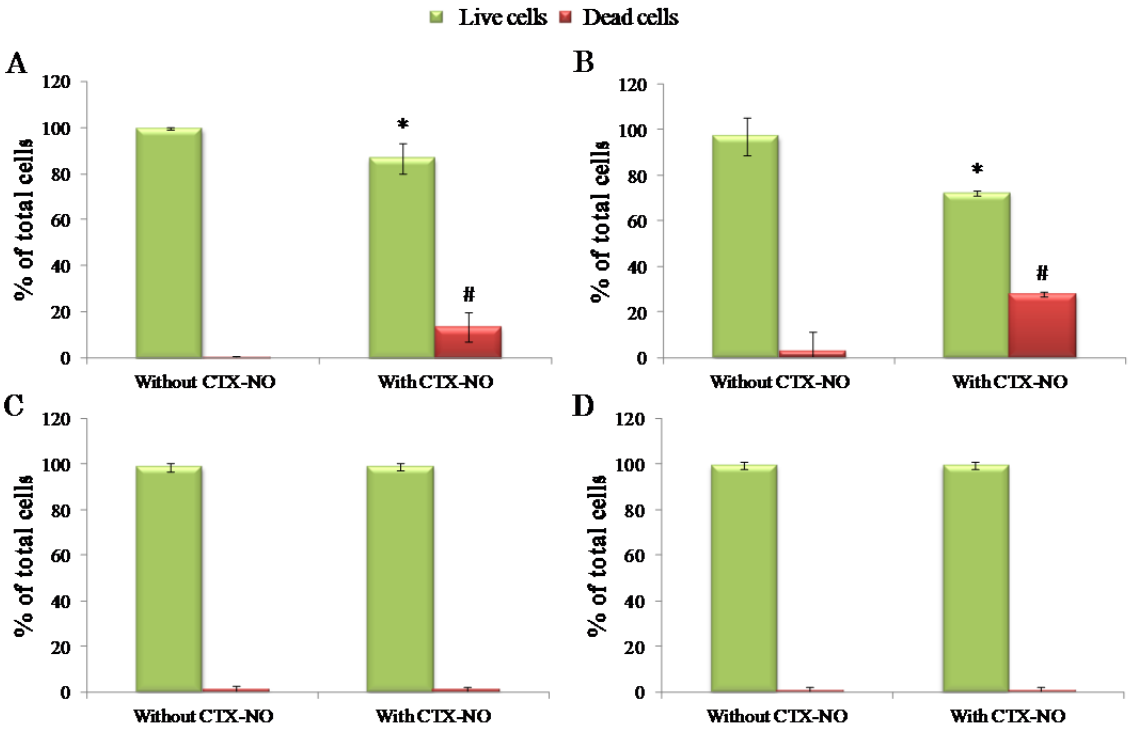

Figure 2.7. (A) T98Gs (B) U-87MGs (C) NHAs and (D) HBMECs incubated with 10 μM of NO donated by CTX-NO for 48 hours and then with a mixture of calcein-AM and ethidium homodimer-1. Non-fluorescent calcein-AM is converted to green fluorescent calcein by viable cells, whereas ethidium homodimer-1 is a fluorescent red DNA stain that is only able to permeate dead cells. T98G and U-87MG glioma cells, show significant increase in the proportion of cells that are non-viable after the CTX-NO treatment. NHAs and HBMECs show no significant changes with or without the CTX-NO treatment. *$p < 0.01$compared to cells stained green, #$p < 0.01$ compared to cells stained red, n = 5-9.

Similarly, cells were incubated with VTW-NO for 48 hours such that T98G, U-87MG, NHA and HBMECs were exposed to 10 μM of NO, and then stained with a mixture of calcein-AM and ethidium homodimer-1. After T98G cells were exposed to VTW-NO treatment, 17.0 ± 7.6% of the cell population stained red indicating cell death (Fig. 2.8A). In comparison, when cells were not exposed to VTW-NO only 0.6 ± 0.7% of the cell population were dead. Similarly, 6.7 ± 4.6% of the U-87MG cells exposed to VTW-NO were stained red, whereas only 1.4 ± 1.7% of the U-87MG cells not exposed

to VTW-NO were stained red (Fig. 2.8B). NHAs (Fig. 2.8C) and HBMECs (Fig. 2.8D) showed no significant changes in cell death when incubated with or without VTW-NO.

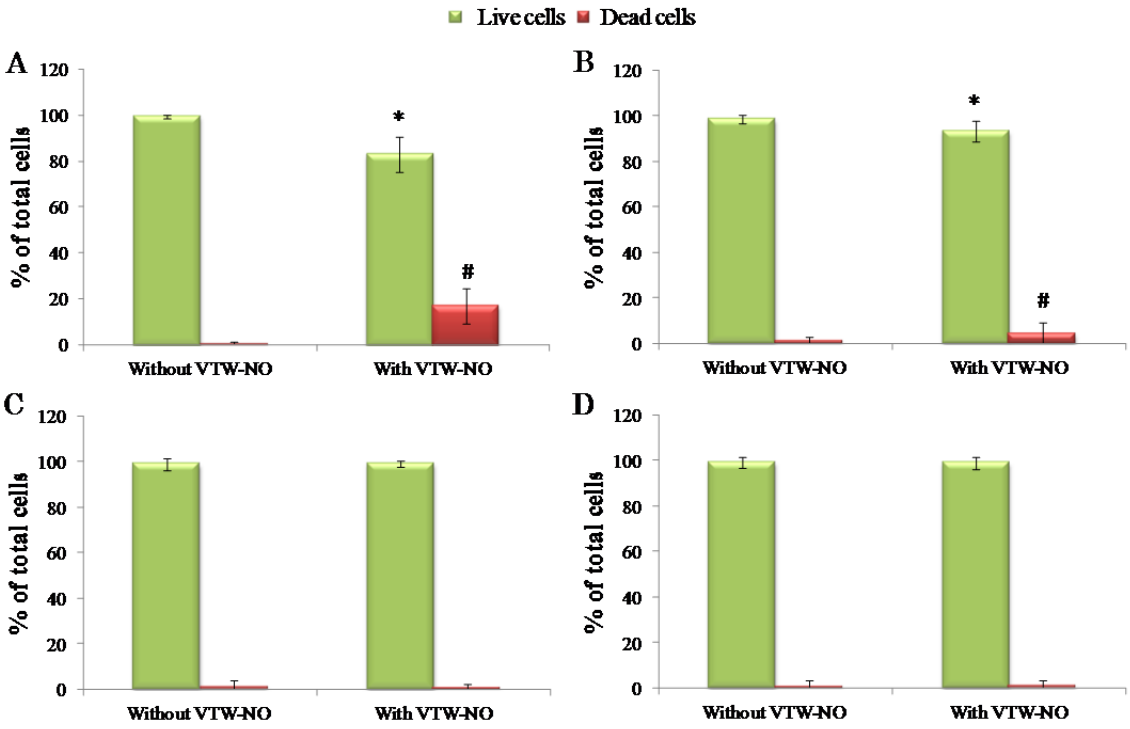

Figure 2.8. (A) T98Gs (B) U-87MGs (C) NHAs and (D) HBMECs incubated with 10 µM of NO donated by VTW-NO for 48 hours and then with a mixture of calcein-AM and ethidium homodimer-1. T98G and U-87MG, glioma cells, show significant increase in the proportion of cells that are non-viable after the CTX-NO treatment. Conversely NHAs and HBMECs show no significant changes with or without the CTX-NO treatment. *$p < 0.01$compared to cells stained green, #$p < 0.01$ compared to cells stained red, n = 5-9.

To compare the effects of a targeted NO donor and a non-targeting NO donor, glioma cells were incubated with various concentrations of SNAP for 48 hours. It was observed that U-87MG cells were more sensitive to the toxic effects of NO released by SNAP, with the cell viability decreasing to 60.0 ± 8.2% of the control cell number at an NO concentration of 50 µM (Fig. 2.9). T98G cell viability was not significantly reduced until the cells were exposed to a higher NO concentration of 100 µM. At 200 µM, the

highest NO concentration tested, T98G and U-87MG cell viability was reduced to 62.8 ± 22.0% and 30.1 ± 5.1% of the control cell number, respectively (Fig. 2.9).

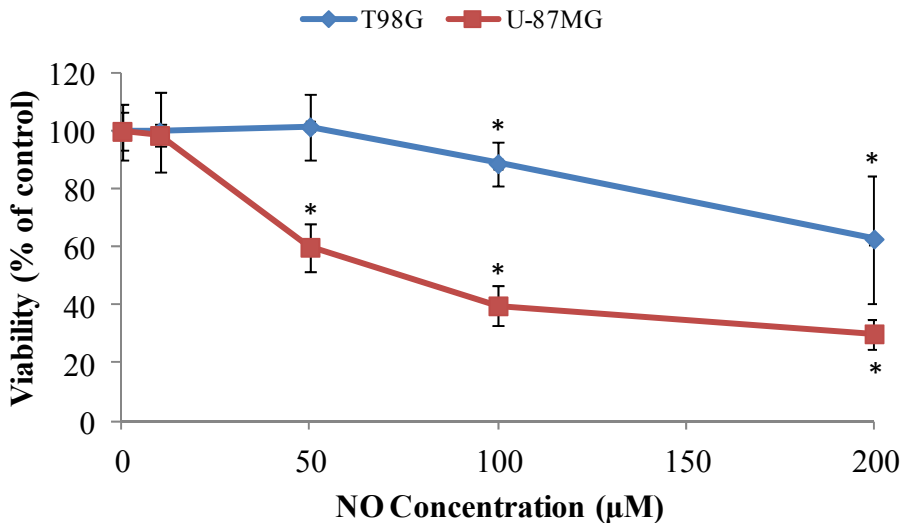

Figure 2.9. Glioma cell viability, T98G and U-87MG, after 48 hour incubation with different doses of non-targeting NO donor, SNAP. U-87MG cells begin to show significant decrease in cell death at NO concentrations of 50 µM and higher, whereas T98G cell viability decreases at concentrations of 100 µM and higher. Thus showing that much higher doses of NO are required in comparison to the doses required with targeted NO donors. *$p < 0.05$, n = 3-5

2.5.5 Effect of NO scavenger on cytotoxicty of NO donors

In order to determine whether the CTX-NO and VTW-NO released NO in the extra- or intracellular space, glioma cells were treated with NO donors in the presence of hemoglobin (HB), an extracellular NO scavenger. Adding HB prior to the CTX-NO treatment did not result in neutralization of the cytotoxic effects of the NO donor on T98G or U-87MG cells (Fig. 2.10). When HB was added to the glioma cells prior to the VTW-NO treatment, slight neutralization of the cytotoxic effects was observed in T98G cells (Fig. 2.11A), but no mitigation of toxic effects was seen in the U-87MG cells (Fig. 2.11B).

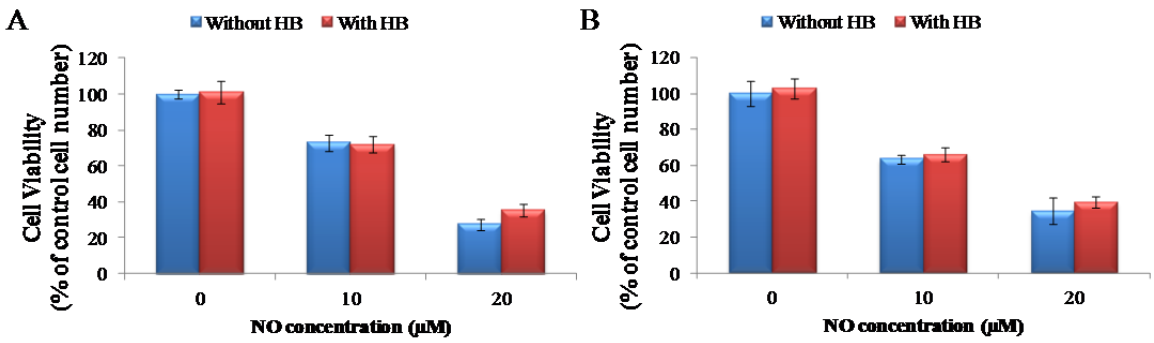

Figure 2.10. Cell viability of (A) T98G and (B) U-87MG after 48 hour incubation with CTX-NO in the presence of hemoglobin. The NO scavenger, hemoglobin did not mitigate the cytotoxic effects of CTX-NO, suggesting that the NO released is after the donor has been endocytosed. *$p < 0.02$, n = 3-5.

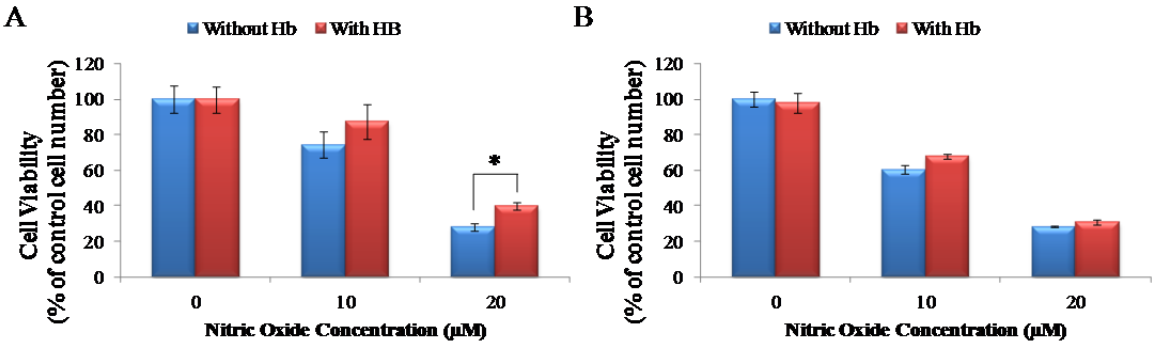

Figure 2.11. Cell viability of (A)T98G and (B)U-87MG after 48 hour incubation with VTW-NO in the presence of hemoglobin. Slight neutralization of the cytotoxic effects of VTW-NO was observed in T98G cells but no mitigation of toxic effects was seen in the U-87MG cells, suggesting that most of the NO donor is endocytosed. *$p < 0.02$, n = 3-5

2.4.6 Endocytosis of NO donors

Minimal attenuation of the cytotoxic effects of CTX-NO and VTW-NO by HB, indicated that only minimal amount of NO, from both of the NO donors, was released in the extracellular space. Thus it can be deduced that the NO donors were efficiently endocytosed by glioma cells. Nonetheless, a visual assessment of the endocytosis was also done using confocal microscopy. T98G and U-87MG cells were incubated with either CTX-FITC or VTW-FITC for 30 minutes, and afterwards the cell membranes and

nuclei were stained and images were taken using a confocal microscope. Incubation with CTX-FITC and VTW-FITC resulted in observations of green fluorescence in the intracellular space of T98Gs (Fig. 2.12) and U-87MGs (Fig. 2.13). Since NO is a much smaller molecule than FITC, it can be assumed that NO would not hinder the ability of the glioma cells to endocytose the biomolecules.

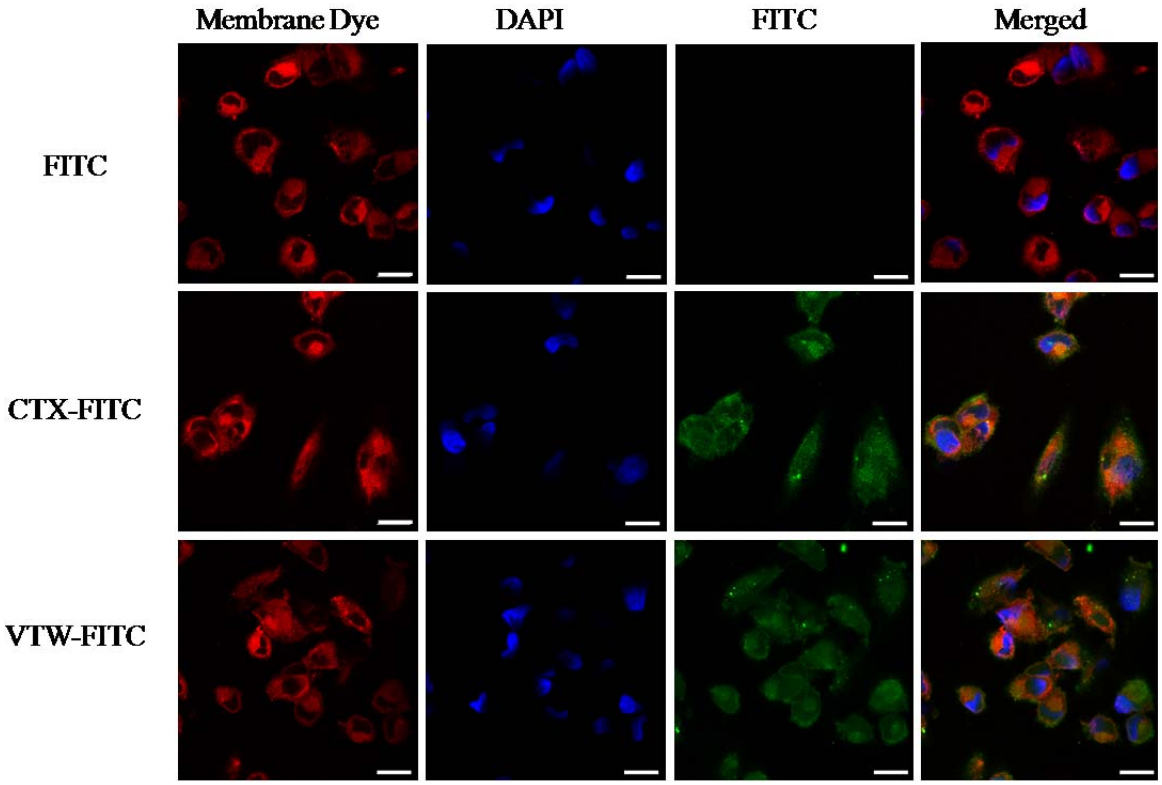

Figure 2.12. Confocal fluorescent images of T98G cells showing endocytosis of CTX-FITC (middle row) and VTW-FITC (bottom row) after a 30 minute incubation with biomolecules. The top row shows T98G cells incubated with FITC alone. Free FITC did not bind to T98G cells; it is only the conjugation of FITC with either CTX or VTW that results in the green fluorescence in the intracellular space. Red: dye stained membrane; Blue, DAPI-stained nuclei; Green: FITC. Scale bar = 20 μm

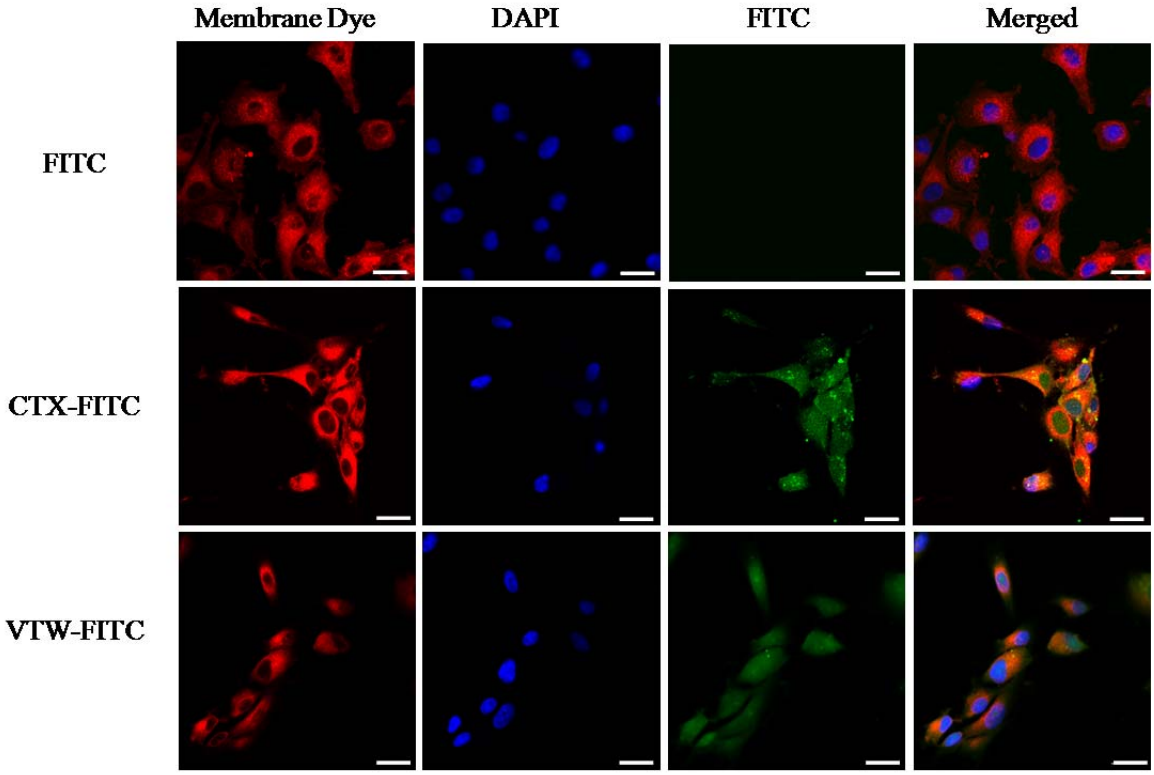

Figure 2.13. Confocal fluorescent images of U-87MG cells showing endocytosis of CTX-FITC (middle row) and VTW-FITC (bottom row) after a 30 minute incubation with biomolecules. The top row shows U-87MG cells incubated with FITC alone. Free FITC did not bind to U-87MG cells; it is only the conjugation of FITC with either CTX or VTW that results in the green fluorescence in the intracellular space. Red: dye stained membrane; Blue, DAPI-stained nuclei; Green: FITC. Scale bar = 20 μm

2.6 Discussion

As discussed in Chapter 1, although it is well established that NO plays a ubiquitous role in malignant gliomas, it is still debated whether NO promotes or inhibits tumor growth [126, 141, 152, 206, 207]. Using two glioma-targeting NO donors, it was demonstrated that NO can indeed inhibit glioma cell proliferation in two different brain tumor cell lines, T98G and U-87MG. *In vitro* studies demonstrated that when glioma cells were exposed for 48 hours to 20 μM of NO released from CTX-NO, glioma cell viability is reduced to less than 30% of the untreated control, whereas NHA and HBMEC

viability remained above 80%. At the same NO concentration, VTW-NO reduced glioma cell viability to 57% of the control, but NHA and HBMEC viability remained above 75%. The fact that HBMEC and NHA viability remained above 75% at an NO concentration of 20 μM (donated by either CTX-NO or VTW-NO), demonstrates that both donors are targeting glioma cells and the control cells are exposed to only minimal doses of NO. Furthermore control experiments in which cells were incubated with VTW or CTX demonstrated that the targeting sequences themselves are innocuous and thus the toxic effects are due to the conjugation of NO to the biomolecules.

Furthermore, in control experiments using SNAP, a non-targeting NO donor, it was shown that without targeting, NO doses upward of 50 μM are required to induce cytotoxic effects. This corroborates previous studies that have shown that non-targeted diazeniumdiolates such as SPER/NO are required at concentrations of 200 μM or higher to significantly decrease glioma cell viability [19]. Even higher concentrations, 20 mM and higher, of other non-targeted diazeniumdiolates (PROLI/NO and diethylamine NONOate (DEA/NO)), were required to significantly decrease glioma cell viability [19].

NO, as a result of its reactive nature, has a relatively small sphere of influence, extending approximately 100 μm from its origin [125]. Thus, the targeted NO donors are able to deliver NO within a closer proximity to the tumors cells, as well as intracellularly, and are more effective in utilizing the cytotoxic effects of NO in comparison to non-targeted NO donors. As a consequence, the amount of NO required to produce cytotoxic effects is decreased ten-fold. Importantly, the targeted delivery of NO dramatically reduces toxic effects to NHAs and HBMECs. At a median concentration of CTX-NO and VTW-NO, even though glioma cell viability is significantly reduced, NHA and HBMEC

cell viability is not significantly affected. By fluorescently tagging CTX and VTW, it was demonstrated that these biomolecules retain their tumor targeting abilities even after the reaction of amines with FITC. Thus, it stands to reason that the biomolecules retain their targeting ability even after the reaction of NO with amines. Furthermore, CTX-FITC and VTW-FITC are able to bind to cells within 30 minutes of exposure, well before the peak NO release of either of the donors, thereby ensuring that the majority of the NO is released after localization of the donors to glioma cells.

Uptake of the bound molecules by endocytosis is most certainly occurring early in the incubation period and perhaps enhancing the effects of the NO donors through intracellular delivery of NO to tumor cells. In order to assess the endocytosis of these biomolecules, two experiments were carried out. First, the NO donors CTX-NO and VTW-NO were incubated with cells in the presence HB. HB is a well documented NO-scavenger and has been shown to neutralize the cytotoxic effects of NO donors on glioma cells [175, 208]. HB is not endocytosed by glioma cells; therefore, it acts as an NO scavenger only in the extracellular space and is unable to scavenge NO that is released inside the cells [209]. It was found that the addition of HB did not mitigate the cytotoxic effects of CTX-NO and only slightly mitigated the effects of VTW-NO. This suggests that most of the NO is being released within the cell. To further asses this phenomena, the uptake of CTX-FITC and VTW-FITC was visualized by confocal microscopy. It was found that both biomolecules are endocytosed by the glioma cells, as evidenced by fluorescence observed in the intracellular space of both T98G and U-87MG cells. This data is in agreement with previous studies that have shown the uptake of CTX-conjugated nanoparticles and VTW-conjugated β-galactosidase by glioma cells [115, 191].

In comparing the cytotoxic effects of the two NO donors, at an NO concentration of 40 μM, CTX-NO reduced the viability of GBM cells to less than 5% of the control, but with VTW-NO the GBM viability remained 30-35% of the control. Furthermore, when incubated with HB some neutralization of the cytotoxic effects of VTW-NO, albeit minor, was observed. Based on these observations, CTX-NO was found to be a more efficient GBM-targeting NO donor. Control studies showed that CTX alone does not induce toxic effects and therefore it is hypothesized that CTX-NO is able to deliver NO more efficiently to glioma cells, or acts synergistically with NO to decrease cell viability. Thus, further studies investigating the effects of targeted NO delivery on GBM chemosensitivity and invasion were carried out using only CTX-NO.

CHAPTER 3: EFFECT OF TARGETED NO DELIVERY ON THE CHEMOSENSITIVITY OF GLIOMA CELLS

3.1 Summary

GBM is among the most chemoresistant of human tumors, resulting in tumor reoccurrence despite surgery, radiation, and chemotherapy. TMZ and BCNU are the two most commonly used chemotherapeutics for the treatment of GBM. However, a significant percentage of patients do not respond to either chemotherapeutic, and therefore the mean survival of patients remains under two years. Herein, CTX-NO, one of the targeted NO donors characterized in Chapter 2, was used to deliver NO specifically to glioma cells and induce chemosensitivity. NO, when delivered via a targeted donor decreased levels of MGMT, a DNA repair enzyme, as well as levels of p53, a protein that can activate DNA repair. As a consequence, both T98Gs, the more chemoresistant glioma cell line, and U-87MGs are able to respond to lower doses of TMZ and BCNU. Although all of the effects of NO delivery and subsequent chemosensitivity are yet to be elucidated, this work suggests that the use of targeted NO to sensitize cells towards chemotherapeutics holds great potential as an adjuvant in the multimodal treatment of the numerous tumors that are normally unresponsive to chemotherapy.

3.2 Introduction

GBM is among the most difficult tumors to treat due to a lack of response to chemotherapeutics. For the past three decades, the standard of care for GBM patients has

been surgery followed by radiation and/or chemotherapy [211]. Chemotherapeutics are generally classified as either cytostatic or cytotoxic [42]. Cytostatic drugs inhibit cell growth, whereas cytotoxic agents cause cell death via a variety of pathyways, including DNA alkylation, DNA cross-linkage, DNA strand breaks, and mitotic spindle disruption [42, 212]. As mentioned in Chapter 1, GBM treatment plans involve orally administering temozolomide (TMZ) in conjugation with radiation therapy [3]. TMZ is a cytotoxic alkylating agent which spontaneously hydrolyzes at physiological pH into 3-methyl-(triazen-1-yl)imidazole-4-carboxamide (MTIC), the active degradation product, which in turn induces methylation of various locations on DNA (Fig. 3.1A) [55].

An alternative GBM treatment involves the use of BCNU-loaded Gliadel® wafers. In comparison to the oral administration of TMZ, this unique drug delivery system utilizes biodegradable wafers that are placed in the tumor cavity after resection; the drug is delivered intracranially as the polymer degrades. BCNU, prior to the approval of Gliadel® wafers in 2003, was administered intravenously. BCNU acts via multiple cytotoxic actions, including carbamoylation and alkylation of DNA to kill tumor cells [45]. Despite these advances in glioma therapy, only modest improvements in patient survival have been observed, and median patient survival remains less than 2 years [213-215]. Hence, there is a dire need for improvement in the efficacy of these chemotherapeutics and there is a critical need to better understand the mechanisms of chemoresistance.

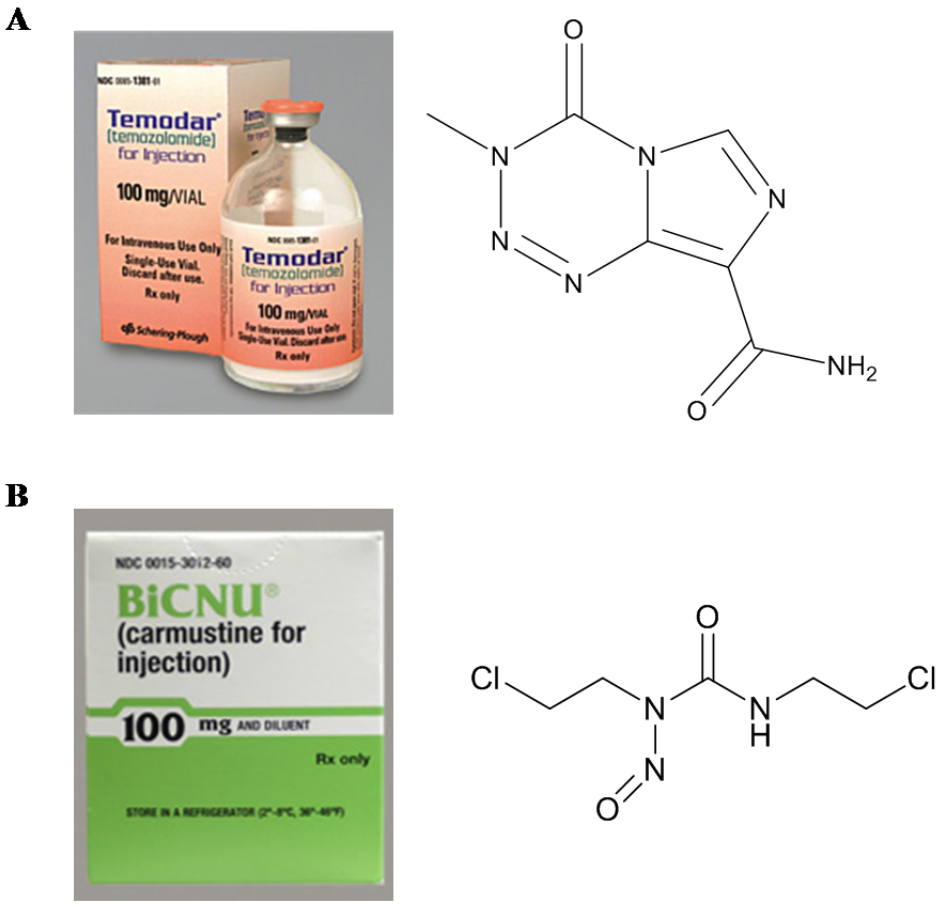

Figure 3.1. Commercially available (A) temozolomide (TMZ) and (B) carmustine (BCNU) are shown along with their chemical structures.

The resistance of tumor cells to the biological effects of alkylating and chloroethylating agents like TMZ and BCNU is partially due to the presence of the DNA repair protein O^6-methylguanine-DNA methyltransferase (MGMT) [216, 217]. MGMT is a 22 kDA protein that repairs alkylation of O^6–G on DNA strands by transferring the methyl group to an internal cysteine acceptor residue [2, 7, 216]. Alkylation, if left unrepaired, results in the induction of apoptosis; thus, MGMT serves as a defense mechanism against alkylating agents, including chemotherapeutics. The cytotoxicity of TMZ and BCNU has been correlated with intracellular levels of MGMT and high levels of MGMT are associated with chemoresistant gliomas [7, 218-221]. Furthermore,

inactivation of MGMT, via inhibitors of the enzyme, has been shown to increase tumor cell chemosentivity towards both BCNU and TMZ [222].

In addition to MGMT another biomolecule that plays an important role in determining chemosensitivity is the protein p53. The actions of p53 play a critical role in maintaining the integrity of the genome and determining cellular response, either activating DNA repair mechanisms or triggering apoptosis after exposure to damaging stimuli such as radiation or chemotherapy [223, 224]. However, more than half of all human cancers contain mutations of the p53 protein, which results in an increase of oncogenic functions, including decreased chemosensitivity [225, 226]. Despite the availability of a number of chemotherapeutics for GBM treatment, it is among the most chemoresistant tumors, and therefore it is of great interest to develop a therapeutic that in addition to having cytotoxic properties can enhance the chemosensitivity of glioma cells.

3.3 Objective

In this chapter, work on investigating the effects of a glioma-targeting NO donor on the chemosensitivity of glioma cells to TMZ and BCNU is discussed. Targeted NO pretreatment coupled with chemotherapy was assessed for effects on:

- Glioma and control cell viability
- MGMT expression in glioma cells
- p53 expression in glioma cells
- Glioma cell invasion

3.4 Methods and Materials

3.4.1 Chemicals

Minimum Essential Media (MEM), fetal bovine serum (FBS), L-glutamine-penicillin-streptomycin (GPS), trypsin-EDTA and non-essential amino acids were obtained from Mediatech, Inc. (Manassas, VA). NO gas was obtained from Airgas (Atlanta, GA), chlorotoxin (CTX, purity > 87%) was obtained from Bachem Chemicals (Torrance, CA). Unless otherwise mentioned, all other chemicals were obtained from Sigma-Aldrich (St. Louis, MO).

3.4.2 Cell Maintenance

T98G and U-87MG human glioblastoma cells (American Type Cell Culture, Manassas, VA), were cultured in MEM with 10% FBS, 1% GPS and 1% non-essential amino acids at 37^{o}C and 5% CO_2. Normal human astrocytes (NHAs; Lonza Inc. Walkersville, MD) were cultured in astrocyte basal media (ABM) supplemented with astrocyte growth medium SingleQuots (Lonza Inc. Walkersville, MD) at 37^{o}C and 5% CO_2. Human brain microvascular endothelial cells (HBMECs; ScienCell Research Laboratories, Carlsbad, CA) were cultured in Endothelial Cell Medium (ECM) supplemented with endothelial cell growth supplement (ScienCell Research Laboratories, Carlsbad, CA) at 37^{o}C and 5% CO_2. For experiments, NHAs passages 3-5, HBMECs passages 3-6 and T98G and U-87MG passages 5-12 were used.

3.4.3 NO donor synthesis

CTX-NO was synthesized as described in section 2.4.3. As before, reacted samples were freeze dried and stored at -20^{o}C until use. At the time of experiments, these samples, designated CTX-NO, were dissolved in DI to form solutions such that cells were exposed to the desired concentration of NO.

3.4.4 Chemosensitivity and Viability studies

T98G and U-87MG cells were seeded in 96-well plates at a density of 25,000 cells/cm^2. After allowing cells to adhere for 24 hours, the cells were incubated for 2 hours with CTX-NO, to allow the NO donor to bind to the glioma cells. The concentration of CTX-NO was adjusted such that each cell type was exposed to 0-5 μM of NO. After 2 hours, the cells were washed with PBS and treated with either BCNU (0-600 μM) or TMZ (0-800 μM) for 48 hours. Under control conditions, cells were pretreated with CTX (not reacted with NO gas) or left untreated. After 48 hours, the cultures were rinsed thoroughly to remove dead cells; the remaining adherent cells were removed from the culture surface using trypsin-EDTA and counted using a Beckman z1 Particle Counter (Beckman Coulter, Drea, CA). Viability was calculated as described in section 2.4.6.

Based on the results from these studies, a BCNU concentration of 75 μM and a TMZ concentration of 50 μM were chosen for further analysis. The NO range was also reduced to 0-2 μM. In order to study the differences in the CTX-NO pretreatment on glioma and control cells, further viability studies were performed. T98G, U-87MG, NHAs and HBMECs were seeded in 96-well plates at a density of 25,000 cells/cm^2. After allowing cells to adhere for 24 hours, the cells were incubated for 2 hours with CTX-NO

to allow the NO donor to bind to the glioma cells. The cells were then washed with PBS and treated with either BCNU (75 μM) or TMZ (50 μM) for 48 hours. After 48 hours viability was measured as described previously.

3.4.5 Analysis of active MGMT Levels

T98G cells were seeded in 24-well plates at a density of 25,000 cells/cm^2. After 24 hours, the cells were treated with CTX-NO for 2 hours, washed and then incubated with BCNU or TMZ for 48 hours. At the end of the incubation period, the cells were washed and removed from the well plate using trypsin-EDTA. After which, the cells were centrifuged at 1700 rpm for 4 minutes, the media was removed, and the cells were resuspended in sterile DI water. Subsequently, the cells were lysed in three freeze-thaw cycles.

Cell debris was removed by centrifugation and the resulting supernatant was used to quantify MGMT using an enzyme-linked immunosorbent assay kit (ELISA; USCN Life Sciences, Inc Wuhan, China) according to the manufacturer's instructions. In brief, samples were added to a 96-well plate, pre-coated by the manufacturer with a monoclonal antibody specific to MGMT, for 2 hours. Next, a biotin-conjugated polyclonal antibody specific for MGMT was added to the wells for 1 hour. After several washes, avidin-conjugated horseradish peroxidase (HRP) was added to the wells. Finally, the chromogenic HRP substrate, 3,3',5,5'-tetramethylbenzidine (TMB), was added to detect HRP. The sample absorbances were measured at a wavelength of 450 nm using a DTX 880 Multimode Detector (Beckman Coulter, Drea, CA) and compared to a set of standards of known concentration to determine MGMT levels in each sample.

In addition, the total protein content of each sample was measured using a bicinchoninic acid (BCA) protein assay as per manufacturer's instructions (Thermo Scientific Pierce, Rockford, IL). In brief, reagent A, containing sodium carbonate, sodium bicarbonate, bicinchoninic acid and sodium tartrate in 0.1M NaOH, was mixed in a ratio of 50:1 with 4% cupric sulfate to prepare the working reagent. 25μL of the cellular extracts were mixed with 200 μL of the working reagent and incubated at 37°C for 30 minutes. Standards containing known concentrations of bovine serum albumin (BSA) were also reacted with the working reagent. After allowing the samples to cool to room temperature, absorbances were measured at a wavelength of 560 nm using a DTX 880 Multimode Detector (Beckman Coulter, Drea, CA). Absorbance measurements from BSA samples were used to construct a standard curve, from which the concentrations of the samples were detected.

3.4.6 Assessment of p53 Levels

T98G and U-87MG cells were seeded in black walled 96-well plates at a density of 25,000 cells/cm2. As before, after 24 hours the cells were treated with CTX-NO for 2 hours, washed and then incubated with BCNU or TMZ. After 48 hours, the cells were fixed with 4% formaldehyde and intracellular p53 levels were measured using an In-Cell ELISA Colorimetric Detection Kit (Thermo Scientific Pierce, Rockford, IL), performed per manufacturer's instructions (Fig. 3.3). In brief, cells were permeabilized using Surfact-Amps X-100 detergent, which was then quenched using a 1% hydrogen peroxide solution. Nonspecific protein adsorption was prevented through incubation with a blocking buffer. Samples were then incubated with a p53-specific primary antibody

followed by incubation with a HRP-conjugated secondary antibody. In order to quantify the bound antibodies, TMB, a HRP substrate, was added to each well and sample absorbances were measured at a wavelength of 450 nm using a DTX 880 Multimode Detector (Beckman Coulter, Drea, CA). Additionally, cells were stained with Janus Green Whole-Cell Stain to determine cell number and sample absorbances were measured at a wavelength of 615 nm. p53 content per cell was calculated by dividing the absorbance measured at 450 nm with the absorbance measured at 615 nm.

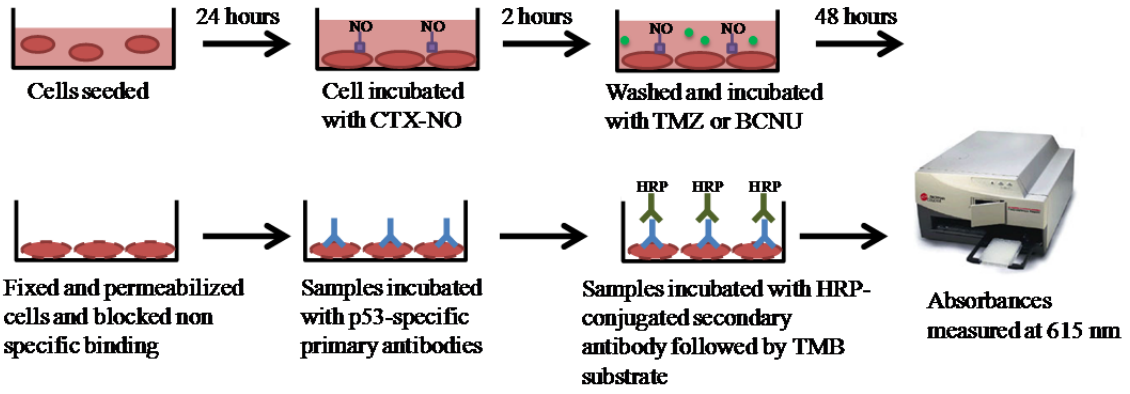

Figure 3.2. Schematic showing p53 assay protocol. Cells were treated with CTX-NO for 2 hours and then with TMZ or BCNU for 48 hours. After 48 hours, the cells were fixed and permeabilized. Samples were then incubated with p53-specific primary antibodies followed by HRP-conjugated secondary antibody. Next, TMB, an HRP substrate, was added to each well and sample absorbances were measured.

3.2.7 Invasion Assay

An invasion assay was performed with T98G and U-87MG glioma cells using a Boyden chamber system consisting of a 6-well culture plate and 8-µm pore polyethylene terephthalate (PET) membrane inserts [9, 227]. The inserts were coated with type IV rat tail collagen (Olaf Pharmaceutical Inc, Worcester, MA), after which cells were seeded on the inserts at a density of 25,000 cells/cm^2. After 24 hours, cells were exposed to CTX-

NO (2 μM of NO) or the equivalent concentration of CTX. After 2 hours, the inserts were washed and serum-free media containing either TMZ or BCNU was added to the inserts. The inserts were then moved to a new 6-well culture plate containing fresh media. After 48 hours of culture on the membranes, the cells were fixed in 4% formaldehyde and stained with 1% crystal violet in DI water (Fig. 3.3) [227, 228]. Cells on the upper side of the inserts were scraped off, and pictures of the cells on the underside of the filters were taken using a Nikon D90 digital camera attached to a Leica DM IL inverted contrasting microscope (Leica Microsystems, Inc., Bannockburn, IL). A minimum of three pictures were taken per insert.

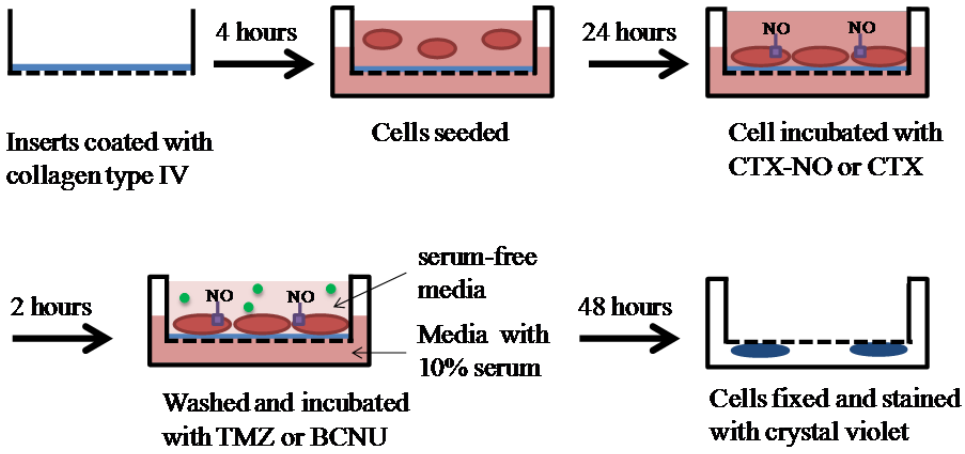

Figure 3.3. Schematic showing invasion assay protocol. 8-μm pore PET inserts were coated with collagen for 4 hours. T98G cells were then seeded on top chamber of the inserts. After 24 hours, cells were treated with CTX-NO for 2 hours and then with TMZ or BCNU for 48 hours. After 48 hours, the cells were fixed and stained with 1% w/v crystal violet. Cells on the upper side of the inserts were scraped off and pictures of the cells on the underside of the filters were taken

3.4.8 Statistical Analysis

All experiments were carried out minimally in triplicate. Statistical comparisons were conducted using an ANOVA, with *p*-values less than 0.05 considered statistically significant.

3.5 Results

3.5.1 CTX-NO pretreatment enhances the chemosensitivity of glioma cells

Before quantifying the chemosensitizing effects of CTX-NO, control experiments were done to determine whether CTX (not reacted with NO) had any chemosensitizing effects. A two-hour pretreatment of glioma cells with CTX, resulted in no significant decrease in T98G or U-87MG chemoresistance (Fig 3.4). After establishing that CTX had no chemosensitizing effects, non-toxic concentrations of CTX-NO, BCNU and TMZ were identified, to test the ability of CTX-NO to induce chemosensitivity. Using non-toxic doses of the therapeutics allowed any synergistic effects of the combined therapy to be easily observed.

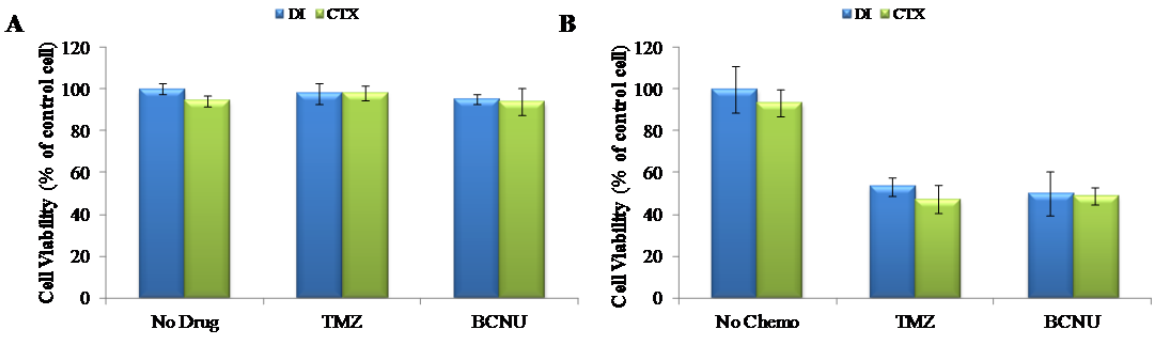

Figure 3.4. CTX (without reaction with NO) pretreatment does not affect the chemosensitivity of (A) T98G or (B) U-87MG cells. *$p < 0.05$, $n = 3$-5 for each experiment.

Preliminary studies showed that BCNU concentrations as low as 75 µM and TMZ concentrations as low as 50 µM significantly decreased U-87MG cell viability, verifying that the U-87MG cell line (Fig. 3.5C and D) is significantly more chemosensitive than the T98G cell line (Fig. 3.5A and B) [229, 230]. Therefore, preliminary results from the cell viability studies of T98G cells, the more chemoresistant cell line, were used to determine non-toxic dosages. A range of 0-600 µM of BCNU was tested and no significant changes

in cell viability were measured at concentrations of 75 µM and 150 µM (Fig. 3.5A). Furthermore, 1-5 µM of NO added for 2 hours prior to addition of the chemotherapeutics resulted in an increase in BCNU efficacy. Similarly, when 0-800 µM of TMZ were tested for effects on cell viability, decreased T98G cell viability was measured at concentrations higher than 50 µM of TMZ (Fig. 3.5B). Based on these preliminary studies all further experiments were performed using a BCNU concentration of 75 µM, a TMZ concentration of 50 µM and NO concentration of 0-2 µM.

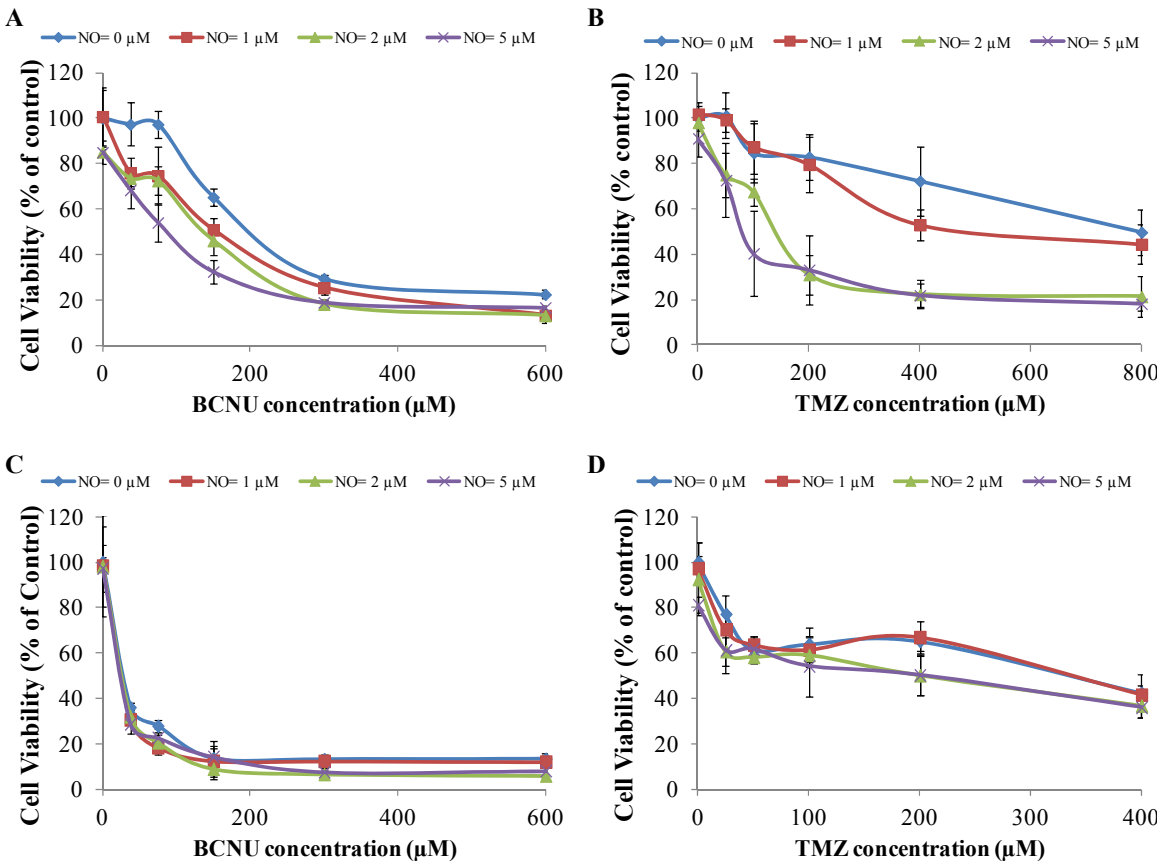

Figure 3.5. CTX-NO pretreatment is able to increase the efficacy of both (A) BCNU and (B) TMZ in a dose dependent manner in T98G cells. Conversely U-87MG cell lines are significantly more chemosensitive and (C) BCNU and (D)TMZ significantly decrease cell viability at all tested concentrations. BCNU concentration of 75 µM, TMZ concentration of 50 µM and NO concentrations of 0-2 µM were chosen for further analysis based on results from T98G dosage curves. At these concentrations, the chemotherapeutics alone were not able to significantly reduce T98G cell viability.

Once concentrations of NO and the chemotherapeutics were identified, further experiments to determine the effects of the combined therapy on glioma and control cells were carried out. Upon exposure to chemotherapeutics, the viability of T98G cells remained mostly unchanged; remaining at 96.4 ± 5.0% and 101.1 ± 4.8% of the control following TMZ and BCNU treatment, respectively (Fig. 3.6A). NO treatment alone at these low concentrations also failed to significantly change T98G cell viability, with 1 μM NO decreasing viability by less than 1% of the control and 2 μM NO decreasing cell survival to 94.9 ± 3.7% of the untreated control. NO pretreatment impacted T98G cell chemosensitivity towards TMZ and BCNU in a dose dependent manner. While exposure to 1 μM of NO released by CTX-NO for 2 hours prior to the TMZ treatment did not significantly reduce T98G cell viability (87.5 ± 7.2% of the control), doubling the NO dose to 2 μM of NO significantly decreased T98G cell viability to 76.8 ± 8.5% of the untreated control. BCNU treatment after NO delivery had an even more pronounced effect on cell viability. T98G cells exposed to 1 μM of NO had a cell viability of 82.9 ± 7.8% of the control, and doubling the NO dose further decreased T98G cell viability to 67.1 ±1.8% of the control (Fig. 3.6A).

As expected, U-87MG cells were significantly more sensitive than T98Gs to the cytotoxic effects of both therapeutics, with viability reduced to 60.3 ± 2.4% and 39.8 ± 1.9% of the control by TMZ and BCNU treatment, respectively (Fig. 3.6B). U-87MGs also displayed a higher sensitivity to NO; viability was reduced to 76.7 ± 3.2% and 63.0 ± 5.9% of the control by 1μM and 2 μM NO treatment, respectively. Cell viability levels of U-87MGs exposed to TMZ after the NO pretreatment were lowered to 45.1 ± 2.3% (1 μM NO) and 34.8 ± 2.5% (2 μM NO) of the control; treatment with 1 μM NO and BCNU

also led to reduced viability (31.8 ± 0.5% of the control). However, the greatest reduction in glioma cell viability was observed when U-87MGs were exposed to 2 µM NO pretreatment followed by BCNU, resulting in a cell viability of 22.4 ± 1.8% of the untreated control. The targeted delivery of NO by CTX-NO resulted in no significant changes in the chemosensitivity of non-tumor control cells (NHAs shown in Fig. 3.6C and HBMECs shown in Fig. 3.6D).

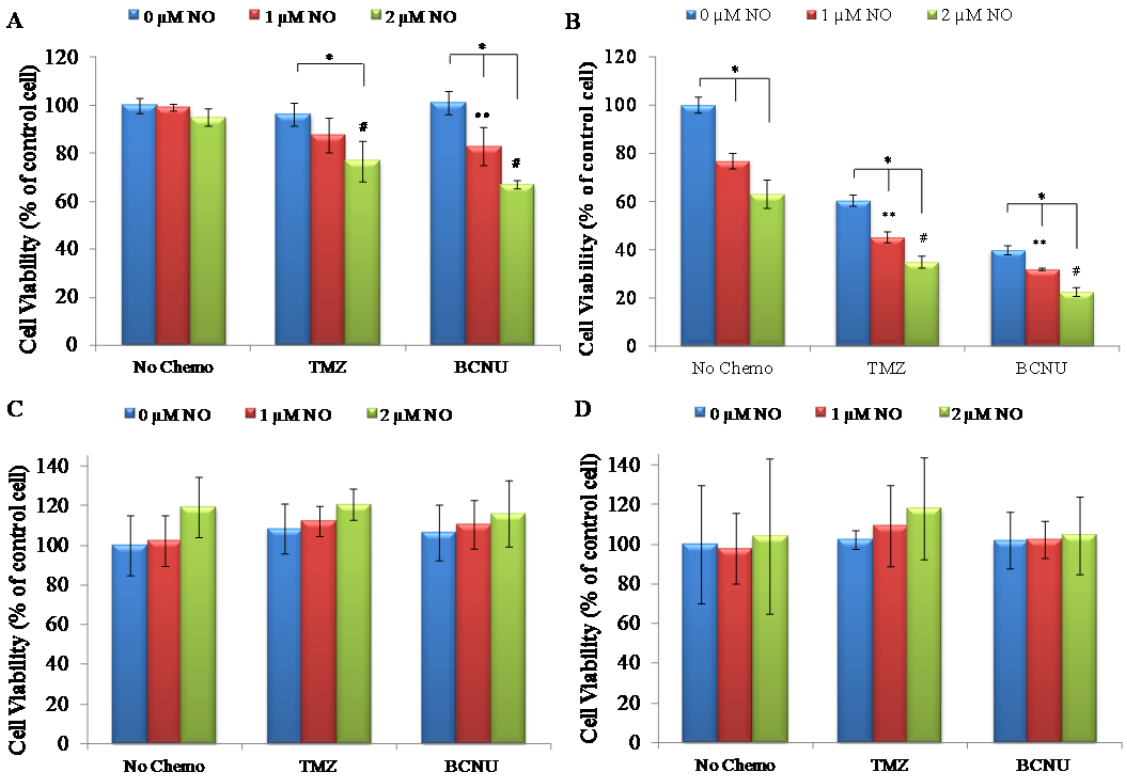

Figure 3.6. CTX-NO pretreatment is able to increase the efficacy of both chemotherapeutics on T98Gs (A) and of U-87MGs (B) cells without affecting NHA (C) and HBMEC (D) chemosensitivity. Glioma cell viability decreases in a dose dependant manner upon exposure to NO and U-87MG is more chemosensitive. Cells counted are presented as a percentage of the number of cells that received no treatment. *compared to no CTX-NO treatment (chemotherapeutic only), **$p < 0.05$ compared to treatment with only CTX-NO (1 µM), #$p < 0.05$ compared to treatment with only CTX-NO (2 µM), *$p < 0.05$, n = 3 for each experiment.

3.5.2 CTX-NO pretreatment significantly reduces MGMT expression in glioma cells

It has been widely reported that MGMT levels cannot be detected in U-87MG cells due to methylation of the enzyme and hence analysis of intracellular MGMT levels was assessed only in T98G glioma cells. The treatment of T98G cells with either TMZ or BCNU alone resulted in no significant changes in detected MGMT levels (Fig. 3.7). When T98G cells were treated with NO at concentrations of 1 µM or 2 µM, MGMT was decreased to 73.1 ± 5.9% and 60.1 ± 9.9% of the control, respectively. Equivalent concentrations of CTX (not reacted with NO gas) resulted no significant decrease in MGMT levels; however, the treatment of glioma cells with NO led to considerable decreases in detected MGMT. Exposure of T98Gs to both 1 µM NO and TMZ was able to decrease MGMT to 60.7 ± 15.2% of the untreated control, and increasing the NO to 2 µM further reduced MGMT levels to 43.4 ± 13.2%. While treatment with 1 µM NO and BCNU only reduced MGMT levels to 83.6 ± 6.3% of the control, 2 µM NO followed by BCNU treatment resulted in a drastic reduction of MGMT levels to 34.6 ± 8.0% of the control value (Fig. 3.7)

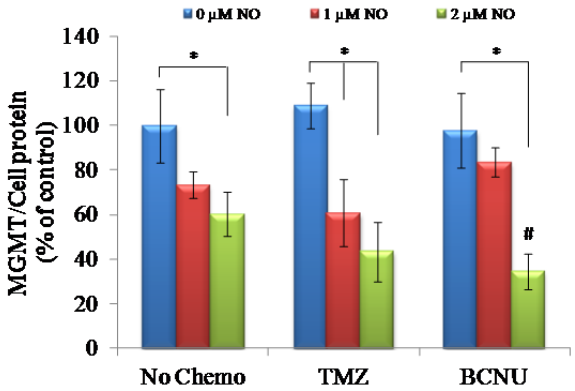

Figure 3.7. Levels of MGMT detected with treatment by CTX-NO alone and in conjugation with TMZ or BCNU treatment were significantly decreased in T98G cells. MGMT levels per total cell protein content are presented as a percentage of the untreated control (cell MGMT levels per cell protein content in cells receiving no treatment). #$p < 0.05$compared to treatment with only CTX-NO, *$p < 0.05$, n = 3-5.

3.5.3 Combination treatment significantly reduces p53 expression in glioma cells

Levels of intracellular p53 were also assessed, and neither chemotherapeutic had any effect on p53 levels in either cell type (Fig. 3.8). Though CTX-NO treatment was able to significantly decrease p53 expression in T98G cells in a dose dependent manner, with p53 levels decreased to 82.3 ± 11.4% and 79.8 ± 13.0% of the control at NO concentrations of 1 μM and 2 μM respectively (Fig. 3.8A), CTX-NO alone had no discernible effect on U-87MG glioma cells at either concentration of NO (Fig. 3.8B). The combination of TMZ and NO had little effect on p53 levels in T98G glioma cells, showing much the same trend as treatment with NO alone (81.5 ± 14.6% and 75.3 ± 12.9% of the control level at 1 and 2 μM NO, respectively). On the other hand, treatment of T98Gs with both NO and BCNU led to much more significant decreases in detected p53 levels. In conjunction with BCNU, the lower concentration of NO reduced p53 amounts to 73.1 ± 7.5% of the control, while 2 μM NO considerably decreased levels of p53 to 18.7 ± 7.0% of the untreated control. In U-87MGs the amounts of p53 did not vary significantly over most of the treatments, maintaining levels higher than 85% of the control, except at the combination of BCNU with 2 μM NO which reduced p53 levels to 46.3 ± 10.6% of the untreated control.

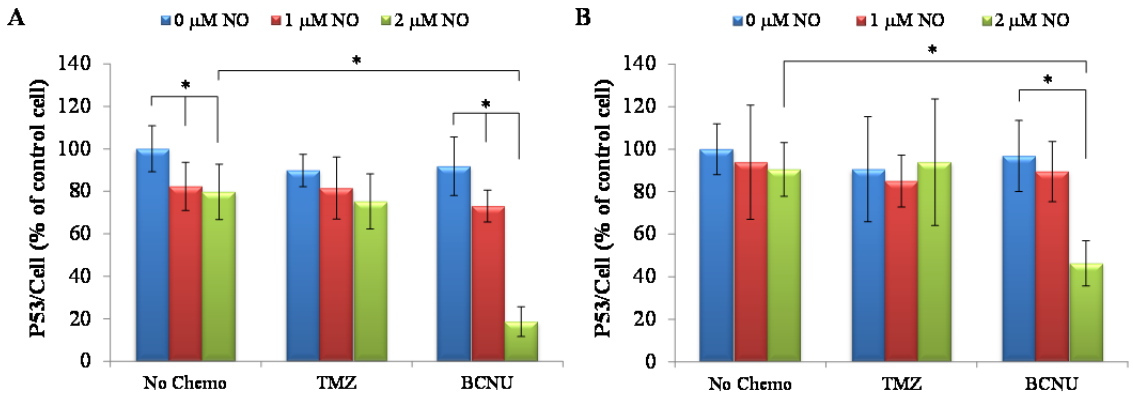

Figure 3.8. CTX-NO alone and in conjugation with TMZ or BCNU treatment stimulates a decrease in the p53 levels in T98G cells (A) in a dose dependant manner, while having little effect on U-87MG except with the combination of NO and BCNU (B). p53 expression per total cell number is presented as a percentage the untreated control value (p53 expression per total cells measured in cells receiving no treatment). *p <0.05, n = 3-5.

3.5.4 CTX-NO treatment with chemotherapy significantly reduces glioma cell invasion

Invasion assays were performed in transwell inserts coated with collagen to assess the effects of NO treatments on T98G human glioma cell invasion. After the 48 hour incubation period, cells which migrated through the collagen coating to the bottom of the insert were photographed (Fig. 3.9). As a result of significant decreases in cell death, effects of CTX-NO pretreatment on U-87MG could not be quantified. While it was visually observed that both the combination therapies, CTX-NO with BCNU and CTX-NO with TMZ, inhibited the invasion of the T98G cells, in order to quantitatively compare the effects of the individual treatments, cells were counted using ImageJ software and a percentage reduction in invasion was calculated (Fig. 3.10). CTX and CTX-NO were able to decrease T98G cell invasion by 26.9 ± 13.1% and 29.3 ± 9.5%, respectively; however, BCNU and TMZ individually were unable to significantly reduce cell invasion. When CTX-NO treatment was coupled with chemotherapy, significant reduction in cell invasion was observed; the combination of NO and BCNU decreased

invasion by 70.5 ± 8.6% while NO in conjunction with BCNU decreased invasion by 54.3 ± 6.1% (Fig. 3.10).

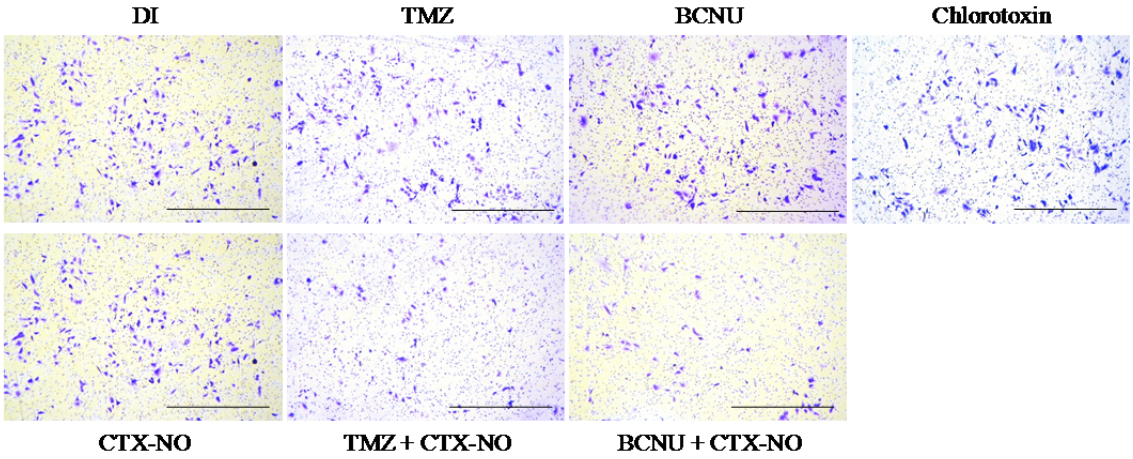

Figure 3.9. Inhibition of invasion of T98G cells through a collagen matrix was evident following the combination of NO pretreatment and chemotherapy. Photographs were taken of the bottom of collagen-coated transwell inserts showing invading T98G cells stained with crystal violet after the indicated treatment. Scale bar = 100 µm.

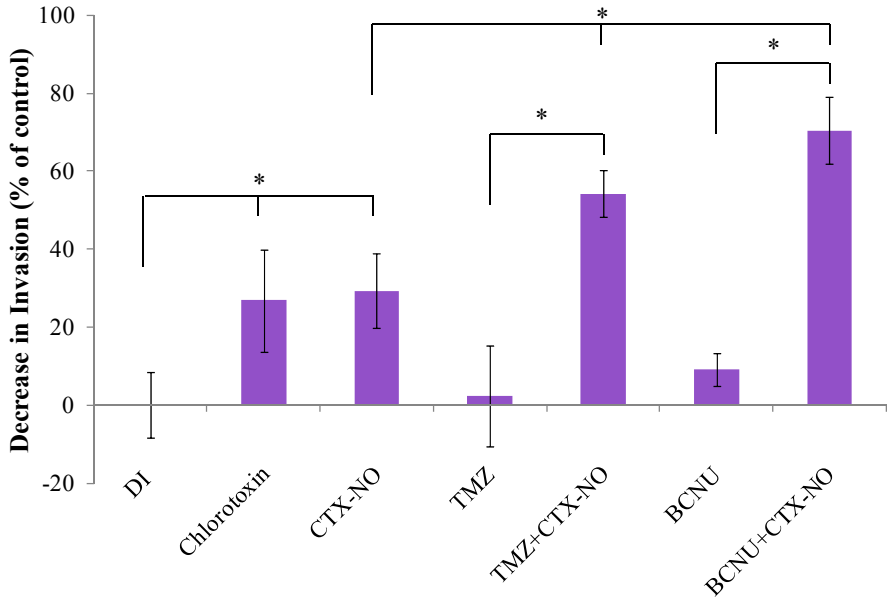

Figure 3.10. Percent decrease in transwell invasion of T98G cells resulting from the combination of NO treatment followed by TMZ or BCNU. The treatment of cells with CTX-NO combined with chemotherapeutics showed greater inhibition of glioma cell invasion than all other treatments. *$p < 0.05$, n = 3-5.

3.6 Discussion

NO has been shown to affect gliomas in a variety of ways, with research showing NO treatment results in the induction of apoptosis, radiosensatization and chemosensitization in tumor cells, and increased permeability of the BBB [143, 146, 231]. Previous studies have used non-specific NO donors, including SNAP, GSNO, PABA/NO, DEA/NO and SPER/NO, to stimulate chemosensitivity in glioma cells [19, 143, 146]. The non-specific nature of these NO donors requires that high doses of NO and thus, the donors themselves, be used for observable therapeutic benefit. This in turn may result in a variety of side effects. Herein, CTX-NO, a targeted NO donor, was studied for its ability to induce chemosensitivity selectively to glioma cells. A two hour incubation of glioma cells with CTX-NO prior to BCNU or TMZ treatment resulted in enhanced chemosensitivity in both T98G and U-87MG cell lines, whereas the chemosensitivity of the control cells, NHAs and HBMECs, was not affected. The selective effect of the NO pretreatment is a consequence of the targeted delivery of NO, as characterized in Chapter 2.

To understand the mechanism of chemosensitivity, not only must the chemoprotective mechanisms of the cells be understood, but also the effects of TMZ and BCNU on tumor cells. Both TMZ and BCNU are alkylating agents that cause DNA damage by the alkylation of guanine residues and inter-strand crosslinking of DNA [15, 161, 232]. MGMT restores DNA structure and function by transferring the methyl group from the oxygen in methylated guanine to a cysteine residue on MGMT [232]. Increased MGMT production in glioblastomas results in the heightened ability to repair the apoptosis-causing lesions and therefore, MGMT expression is often used as a predictor

for glioma response to chemotherapy [36, 233-235]. Studies have demonstrated the ability of MGMT inhibitors to induce chemosensitivity in tumor cells; however, their success in treating GBM has been limited because of systemic side effects and tumor cell resistance to the inhibitors [228].

To determine the mechanism by which CTX-NO was able to enhance chemosensitivity in glioma cells, the consequences of NO exposure on MGMT expression was examined. Methylation of MGMT in U-87MG glioma cells results in low levels of MGMT in these cells and is therefore undetectable by Western blot analysis [230, 236-238]. Consequently, MGMT analysis after CTX-NO pretreatment was carried out only using T98G cells. CTX-NO exposure resulted in decreased MGMT levels, and this reduction was further enhanced when CTX-NO treatment was coupled with chemotherapy. These results suggest that one of the mechanisms by which NO enhances chemosensitivity in T98Gs is by decreasing the amount of functional MGMT, thus enhancing the efficacy of DNA alkylation. It has been shown that *S*-nitrosylation of the cysteine residue in the active site of MGMT causes the irreversible loss of DNA repair activity [239]. Additionally, the *S*-nitrosylation of MGMT has also been shown to quickly target the protein for degradation [239]. It is hypothesized that the reduction in MGMT expression observed after CTX-NO treatment is a consequence of the *S*-nitrosylation of MGMT.

p53 has also been shown to play an integral role in numerous cytoprotective mechanisms. p53 not only limits the effect of chemotherapeutics, but also inhibits cytokine-induced NO production, thereby protecting glioma cells from the adverse effects of endogenously produced NO [124]. In fact, p53 is so effective in providing

glioma cells protection that studies have shown a positive correlation of p53 expression with glioma grade and proliferation indices [235, 240, 241]. Therefore, to further elucidate the mechanisms by which CTX-NO induced chemosensitivity in glioma cells, the effect of the targeted exogenous NO donor on p53 expression was examined.

CTX-NO was able to decrease p53 expression in T98G cells alone, as well as when combined with chemotherapy. In U-87MG cells, p53 expression was significantly decreased only when the highest concentration of CTX-NO was combined with BCNU treatment. This is particularly intriguing because T98G cells express mutated p53, whereas U-87MG cells express wild-type p53 [242-244]. Mutations of p53 occur in 10% of primary glioblastomas and 65% of secondary glioblastomas [230]. Cells with mutations of p53 often demonstrate diminished ability to trigger apoptosis and enhanced DNA repair ability [223]. Furthermore, it has been shown that p53 mutant cell lines retain MGMT expression, whereas wildtype p53 cells are able to suppress MGMT reporter gene activity [241]. Thus, it is likely that presence of mutated p53 and the resulting retention MGMT expression are the causes for the less dramatic changes in viability seen in T98G cultures in comparison to U-87MG cells.

Previous studies have also shown that NO can counter cytoplasmic sequestration of wild-type p53 and promote nuclear retention, leading to enhanced radiation-induced apoptosis in neuroblastoma [245]. Hence the results from the p53 assay suggest that wild-type p53 is retained in the nucleus by exposure to CTX-NO, leading to increased apoptosis and a more noticeable impact on cell viability upon exposure to chemotherapy. Treatment with 2 μM NO in conjunction with BCNU leads to a drastic decrease in detected p53 in both T98G and U-87MG glioma cells. Though studies have suggested

that NO release can lead to the formation of an *S*-nitrosyl p53 that has impaired DNA-binding ability and crosslinks upon NO release [246], this cannot explain the decrease in active p53 detected, especially since this phenomenon is observed only in the presence of BCNU and the highest concentration of NO. Further studies investigating the effect of NO on the p53-mediated apoptosis pathway are required to further understand the role of NO in inducing chemosensitivity.

Although CTX has been documented to inhibit glioma cell invasion [180, 210], the anti-invasive effect of CTX-NO, alone and in combination with chemotherapeutics is unknown, and hence was investigated. Using a Boyden chamber, T98G cells were seeded onto cell culture inserts coated with collagen IV and allowed to invade the matrix over 48 hours, as described by Kenig and colleagues [9]. It was not possible to adequately track U-87MG invasion due to the drastic decrease in U-87MG cell viability in response to the treatments. Therefore, the invasion of only T98G cells could be studied. It was observed that CTX-NO pretreatment combined with TMZ or BCNU resulted in significant decreases in cell invasion, which were not observed when the cells were treated with only one drug. Thus, it is suggested that the combination of CTX-NO and chemotherapeuctics have a synergistic effect on the inhibition of glioma cell invasion.

The studies discussed in this chapter demonstrate that CTX-NO is able to induce chemosensitivity in glioma cells by decreasing MGMT and mutant p53 expression. In addition to chemoresistance, another major hindrance to effective GBM treatment is the highly invasive nature of the glioma cells. This, combined with the anti-invasive effects observed in the Boyden chamber studies provided motivation to investigate, in an in-

depth manner, the effect of CTX-NO on the invasion and migration of glioma cells. The findings of this study are presented in the next chapter.

CHAPTER 4: EFFECT OF TARGETED NO DELIVERY ON THE INVASIVE PROPERTIES OF GLIOMA CELLS

4.1 Summary

The highly invasive nature of GBM cells has proven to be a great challenge in the treatment the disease. Glioma cells are able to readily invade healthy brain tissue, making complete tumor resection impossible. Herein, an investigation into the effects of CTX-NO, a targeted NO donor, on the invasive properties of glioma cells is presented. CTX has been reported to have significant anti-invasive effects in gliomas; however, the role of NO in tumor cell invasion is debated. The study presented herein sheds light on the role NO plays in the invasion of glioma cells and demonstrates that the anti-invasive properties of CTX are enhanced by conversion of CTX to CTX-NO. Using a Boyden chamber invasion assay and a modified scratch migration assay, it was observed that CTX-NO increased the ability of CTX to inhibit glioma cell invasion and migration. Further studies revealed that MMP-2 cell surface expression was reduced by both CTX-NO and CTX, but MMP-9 expression was reduced only by CTX-NO. Additionally, the activity of MMP-2 and MMP-9 was modestly decreased by CTX and drastically reduced by CTX-NO.

4.2 Introduction

A major obstacle to the successful treatment of GBM is the rapid and highly invasive growth of the tumor [9, 247-249]. The glioma microenvironment is characterized by one large localized aggregation of tumor cells and numerous smaller

populations distant from the main tumor mass [250]. Although systemic spread is rare, infiltration of the brain parenchyma by glioma cells results in the recurrence of the tumor [153, 190, 250, 251]. Invasion of normal tissue by tumor cells is a multi-step process but one major step in the process is the degradation of the ECM [26, 185].

MMP-2, also referred to as gelatinase A, a 72-kilodalton enzyme, has the ability to degrade collagen type IV, an important component of the brain ECM. Consequently, cells expressing MMP-2 are able to degrade ECM and invade surrounding tissue [8, 252]. As mentioned in Chapter 2, CTX is able to target glioma cells by binding to cell surface-bound MMP-2, which is overexpressed in glioma cells but is not expressed in normal glial cells and neurons. On binding to MMP-2, CTX has dual effects, not only inhibiting enzymatic activity, but also reducing MMP-2 surface expression [180]. As a consequence, the chloride channel that is part of the MMP-2 complex is also internalized [253]. This reduction in chloride channels decreases the outward directed chloride gradient, which in turn inhibits the cell volume shrinkage required for cell invasion [254]. These effects cumulatively result in an inhibition of glioma cell invasion as a result of CTX exposure.

In addition to MMP-2, MMP-9, referred to as gelatinase B, has been shown to also have a prominent role in glioma invasion [10, 255]. Expression of MMP-9, which is significantly higher in gliomas compared to normal brain tissue, directly correlates with the malignancy grade of the glioma [10, 256-258]. Furthermore, studies have shown that suppression of MMP-9 in mice not only results in an inhibition of glioma migration and invasion, but also in the prevention of intracranial tumor growth following tumor cell injection [259-261]. The role of NO in tumor invasion is ambiguous and therefore to

clarify the role of this biomolecules on glioma invasion, the anti-glioma effects of a targeted NO donor, CTX-NO, were investigated in this study.

4.3 Objective

In this chapter, a study of the differences in the effect of CTX and CTX-NO treatments on glioma cell invasion and migration is presented. CTX-NO and CTX were assessed for their effect on:

- Glioma cell invasion
- Glioma cell migration
- MMP-2 and MMP-9 surface expression
- MMP-2 and MMP-9 activity

4.4 Methods and Materials

4.4.1 Chemicals

Minimum Essential Media (MEM), fetal bovine serum (FBS), L-glutamine-penicillin-streptomycin (GPS), trypsin-EDTA and non-essential amino acids were obtained from Mediatech, Inc. (Manassas, VA). NO gas was obtained from Airgas (Atlanta, GA), chlorotoxin (CTX, purity > 87%) was obtained from Bachem Chemicals (Torrance, CA). Matrigel and transwell inserts was purchased from BD Biosciences (Bedford, MA). Unless otherwise mentioned, all other chemicals were obtained from Sigma-Aldrich (St. Louis, MO).

4.4.2 Cell maintenance

T98G and U-87MG human glioblastoma cells (American Type Cell Culture, Manassas, VA), were cultured in MEM with 10% FBS, 1% GPS and 1% non-essential amino acids at 37^{o}C and 5% CO_2. Cell passages 5-12 were used.

4.4.3 NO donor synthesis

CTX-NO was synthesized as described in section 2.4.3. As before reacted samples were freeze dried and stored at -20^{o}C until used. At the time of experiments CTX-NO samples were dissolved in DI to form solutions such that cells were exposed to the desired concentration of NO.

4.4.4 Viability studies

T98G and U-87MG cells were seeded in 96-well plates at a density of 25,000 cells/cm^2. After allowing cells to adhere for 24 hours, the cells were incubated for 48 hours with 0-145 nM of CTX-NO (0-2 μM of NO) or CTX. After 48 hours, the cultures were rinsed thoroughly to remove dead cells; the remaining adherent cells were removed from the culture surface using trypsin-EDTA and counted using a Beckman z1 Particle Counter (Beckman Coulter, Drea, CA). Viability was calculated as described in section 2.4.6

4.4.5 Invasion assay

An invasion assay was performed using a Boyden chamber system consisting of a 24-well culture plate and 8-μm pore polyethylene terephthalate (PET) membrane inserts

(Fig 4.1). The inserts were coated with Matrigel (0.25mg/ml) in 0.01 M Tris (pH 8.0) containing 0.7% sodium chloride and incubated at 37^{o}C for 4 hours, after which cells were seeded on the inserts at a density of 37,500 cells/cm^{2}. After 24 hours, cells were incubated with serum-free media containing 0-145 µM of CTX-NO or CTX. The lower portion of the boyden chamber was filled with media containing 10% FBS, thereby using serum as a chemotactic factor to induce cells to invade the Matrigel coating. After 48 hours of culture, the cells on the underside of the inserts were fixed in 4% formaldehyde and stained with 1% w/v crystal violet in DI. Cells on the upper side of the inserts were scraped off, and pictures of the cells on the underside of the filters were taken using a Nikon D90 digital camera attached to a Leica DM IL inverted contrasting microscope (Leica Microsystems, Inc., Bannockburn, IL). A minimum of three pictures were taken per insert. ImageJ software was used to quantify the number of cells in per field of view.

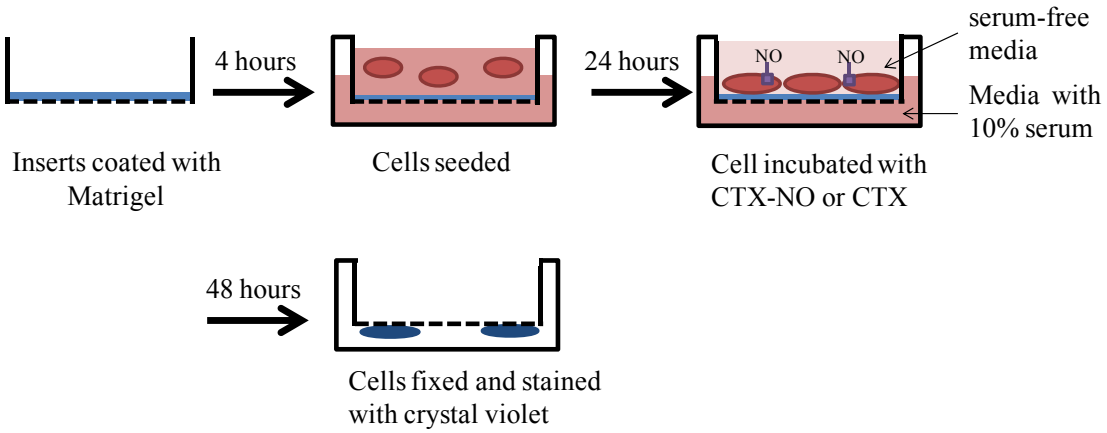

Figure 4.1. Schematic representation of the invasion assay**.** 24-well cell culture inserts with an 8 µm pore size PET membrane, were uniformly coated with Matrigel matrix for 4 hours. Glioma cells were seeded on the upper compartment, and after 24 hours incubated with CTX or CTX-NO in serum-free media. Media containing 10% FBS was placed in the lower chamber. After 48 hour of incubation cells which had invaded the matrigel, were fixed, stained and counted.

4.4.6 Migration assay

To assess the effect of CTX-NO on cell migration, the Oris™ 96-well cell migration assay kit (Platypus Technologies, Madison, WI) was used according to the manufacturer's instructions (Fig 4.2). In brief, 4×10^4 T98G cells were seeded in each well. After 24 hours, the stopper was removed and cells were incubated with media containing 0-145 nM CTX or CTX-NO. The cells were then allowed to migrate into the detection zone. After 48 hours the cells were fixed with 4% formaldehyde and stained with 1% w/v crystal violet in DI. Pictures of the cells invading the detection zone were taken using a Nikon D90 digital camera attached to a Leica DM IL inverted contrasting microscope (Leica Microsystems, Inc., Bannockburn, IL). Migration was calculated by quantifying the area of the detection zone covered by migrating T98G cells using ImageJ analysis software.

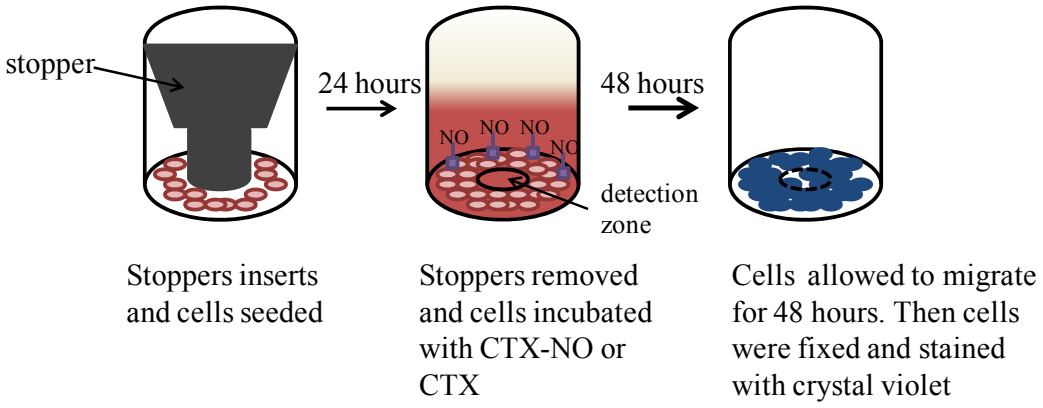

Figure 4.2. Schematic representation of the Oris™ migration assay. Stoppers were placed in the center of 96-well plates and glioma cells were seeded. After 24 hours the stoppers were removed to expose the detection zone. Cells were incubated with CTX or CTX-NO and allowed to migrate into the detection zone. After 48 hours the cells were fixed and stained.

U-87MG cell migration was quantified using the same assay, albeit some modifications were made to the protocol. In brief, 5×10^4 U-87MG cells were seeded in

each well. After 24 hours, the stopper was removed and cells were incubated with media containing 0-72 nM CTX or CTX-NO. Higher concentrations of CTX-NO resulted in significant cell death and that is why U-87MG migration assays were performed using the aforementioned CTX-NO concentration range. The cells were allowed to migrate into the detection zone and migration was quantified after 24 and 48 hours. At the end of the incubation period, the cells were fixed, stained and photographed as previously described.

4.4.7 MMP-2 and MMP-9 immunocytochemistry studies

T98G and U-87MG cells were seeded in black walled 96-well plates at a density of 25,000 cells/cm^2. As before, after 24 hours the cells were treated with CTX-NO or CTX for 48 hours. After 48 hours, the cells were fixed with 4% formaldehyde and stained for either MMP-2 or MMP-9 surface expression (Fig. 4.3). In brief, formaldehyde was removed from wells and cells were then washed with PBS and incubated at room temperature for 1 hour with 5% BSA in PBS, which served as a blocking agent for nonspecific binding. Antibodies to MMP-2 (Abcam, Cambridge, MA), or MMP-9 (Abcam, Cambridge, MA) at a dilution of 1:200 in 1% BSA solution, were incubated with glioma cells overnight at 4^{o}C. Cells were then washed and incubated in the dark for 2 hours with fluorescein-conjugated anti-rabbit IgG secondary antibody (Rockland Immunochemical, Gilbertsville, PA) at a dilution of 1:500 in 1% BSA solution. After 2 hours, the cells were washed with PBS and fluorescence was assessed using a Leica DMI 4000B fluorescent microscope equipped with a Hamamatsu ORCA-ER digital camera (Leica Microsystems, Inc., Bannockburn, IL). A minimum of three pictures were taken per well and the fluorescence in each image was quantified using Image J software.

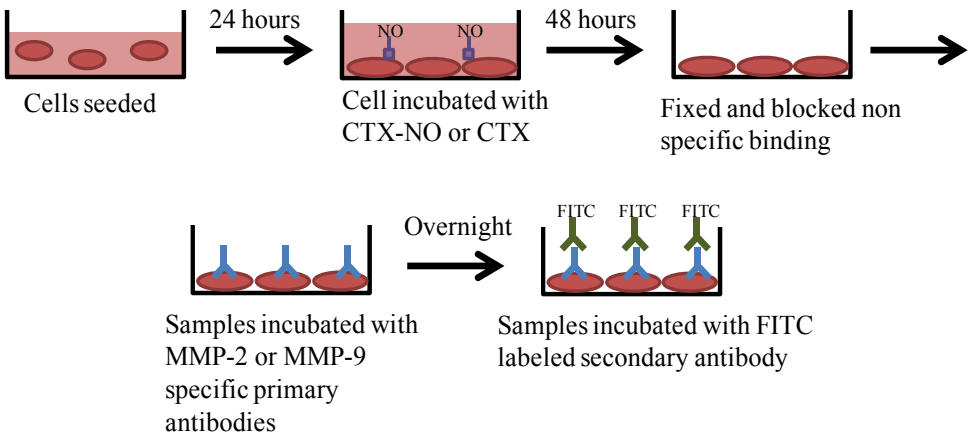

Figure 4.3. Schematic of the MMP surface expression assay**.** Cells were treated with CTX-NO or CTX for 48 hours. At the end of the incubation period were fixed with 4% formaldehyde and blocked with BSA. The cells were then incubated overnight with primary antibodies specific for MMP-2 or MMP-9. The next day, cells were incubated for 2 hours with FITC labeled secondary antibodies. Fluorescence microscopy was then used to assess the surface expression of the MMP-2 or MMP-9.

4.4.8 MMP-2 and MMP-9 activity assay

While the immunocytochemistry studies were able to quantify the surface expression of MMP-2 and MMP-9, it is the activated forms of the enzymes that are secreted and degrade the ECM. It was therefore necessary to quantify the effect of CTX and CTX-NO on secreted MMPs. T98G and U-87MG cells were seeded in 96-well plates at a density of 25,000 cells/cm^2. As before, after 24 hours the cells were treated with CTX or CTX-NO for 48 hours. At the end of the incubation period, the media was collected and centrifuged at 10,000 x *g* for 10 minutes. The supernatant was mixed 50:50 with 100 µM of a quenched fluorogenic substrate specific for MMP-2 and MMP-9 (DNP-Pro-Leu-Gly-Met-Trp-Ser-Arg-OH; EMD Millipore Billerica, MA) in black walled 96-well plates [262]. The mixtures were incubated for 20 minutes at room temperature with gentle agitation. The fluorescent signal at an excitation wavelength of 280 nm and an

emission wavelength of 360 nm was monitored at room temperature on a Synergy H4 Multi-Mode Plate Reader (Biotek, Winooski, VT) to measure enzymatic activity.

4.4.8 DQ-collagen assay

Glass coverslips were coated with Matrigel containing with 100 μg/ml DQ-collagen IV (Invitrogen, Carlsbad, CA) for 15 min at 37°C [263, 264]. T98G or U-87MG cells were plated at a density of 25,000 cells/cm^2. As in previous experiments, cells were allowed to adhere for 24 hours and then incubated with 36 nM of CTX or CTX-NO for 48 hours. At the end of 48 hours, cells were incubated with 5μg/ml of orange plasma membrane stain (Invitrogen, Carlsbad, CA) for 5 minutes at 37^{o}C. Fluorescent degradation products from the DQ-collagen were then imaged using a Zeiss LSM 510 UV Confocal Microscope (Carl Zeiss Inc, Peasbody, MA) with the appropriate filters.

4.5 Results

4.5.1 Viability studies

To ensure that changes in migration and invasion were not due to cell death, viability studies were performed in which T98G and U-87MG cells were exposed for 48 hours to 0-145 nM of CTX-NO (0-2 μM of NO) as well as 0-145 nM of CTX. T98G cell viability was not significantly affected at these concentrations, and three concentrations, 36, 72 and 145 nM, of CTX-NO were identified for further experiments. At these concentrations T98G viability was measured to be 100.0 ± 2.4%, 100.2 ± 6.6% and 93.4 ± 2.5% of the control (Fig 4.4A). T98G cell viability was not affected at any of the CTX concentrations (Fig 4.4A).

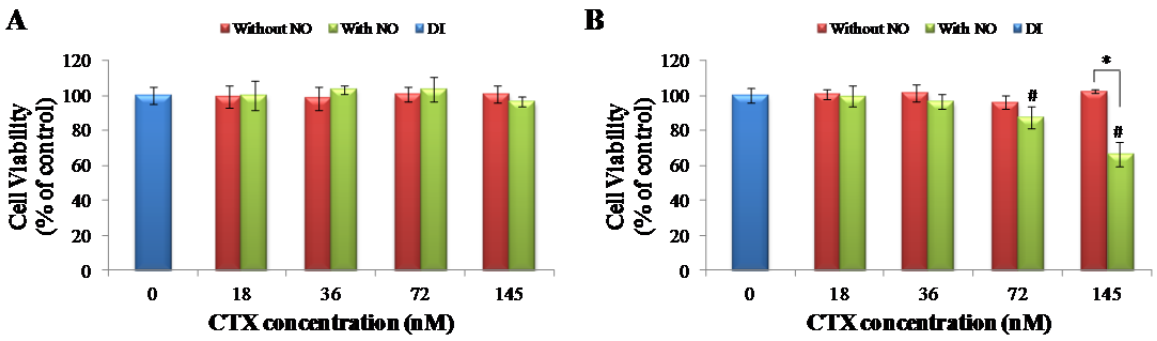

Figure 4.4. Effect of low doses of CTX and CTX-NO on the cell viability assay of (A) T98G and (B) U-87MG cells. The non-cytotoxic range for T98Gs was identified as 0-145 nM of CTX-NO; whereas the concentration range for further experiments with U-87MGs was identified as 0-72 nM of CTX-NO. *$p < 0.05$, #$p < 0.05$ compared to DI, n = 3-5.

As observed in earlier chapters, U-87MG cells were more sensitive to NO treatment. U-87MG cells incubated with 145 nM of CTX-NO had reduced cell viability of 66.4 ± 6.9%. Therefore the concentration range for further experiments with U-87MG cells was reduced to 0-72 nM of CTX-NO. U-87MG cell viability was measured as 99.7 ± 6.0% at a CTX-NO concentration of 18 nM; 96.4 ± 4.4% at a CTX-NO concentration of 36 nM and 87.6 ± 6.3% of the control at a CTX-NO concentration of 72 nM (Fig 4.4B). CTX, at all tested concentrations, was innocuous and did not affect U-87MG cell viability (Fig 4.4B)

4.5.2 CTX-NO enhances ability of CTX to inhibit glioma cell invasion

Invasion assays were performed in transwell inserts coated with Matrigel to assess the differences in the effects of CTX and CTX-NO treatments on glioma cell invasion. After the 48 hour incubation period, T98MG (Fig. 4.5A) and U-87MG (Fig. 4.6A) cells that were initially seeded on top of the insert and had migrated through the Matrigel coating to the bottom of the insert were photographed. In order to quantify the effects of

the individual treatments, cells were counted using ImageJ software and the percent of invading cells was calculated.

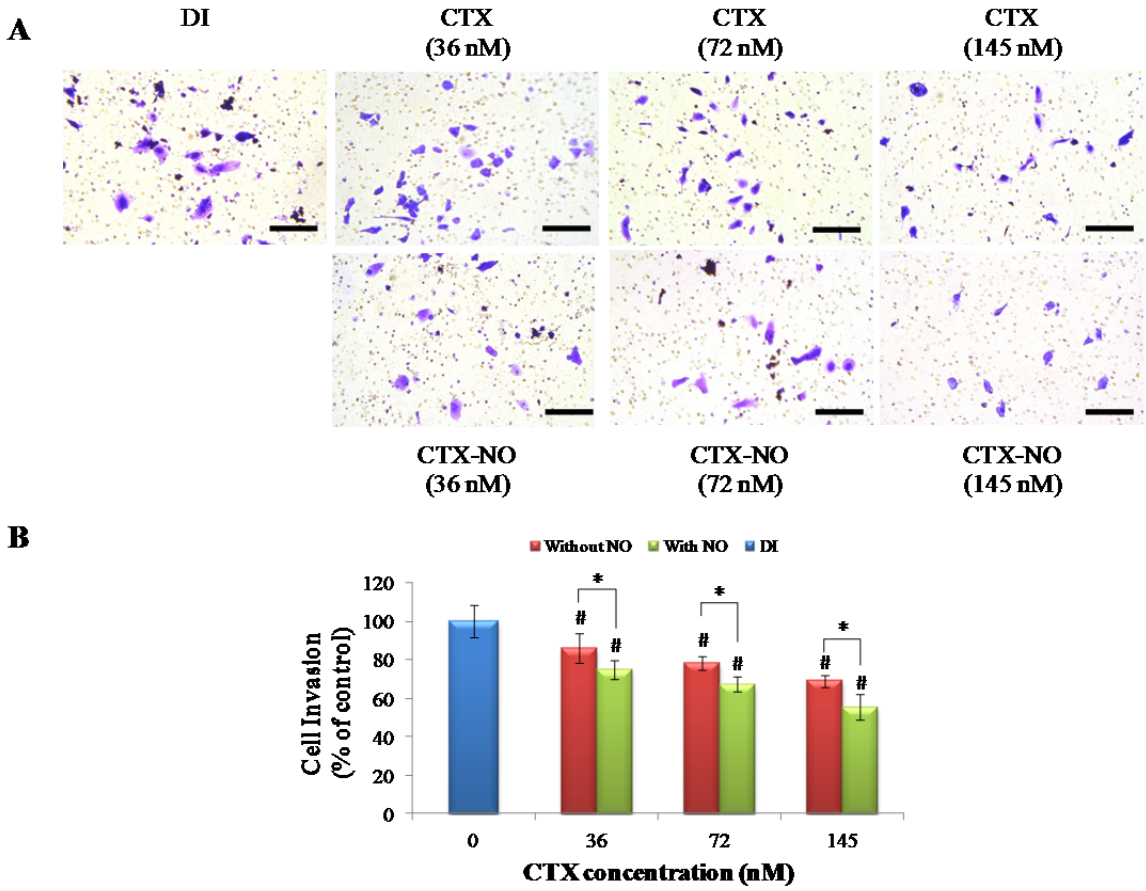

Figure 4.5. Invasion assay with T98G cells. (A) Pictures showing the invasion through a matrigel matrix of T98G cells incubated for 48 hours with 0-145 nM of CTX (upper row) or CTX-NO (lower row). Pictures were taken of the bottom of Matrigel-coated transwell inserts showing invading T98G cells stained with crystal violet after the indicated treatment. Scale bar = 20 µm. (B) Quantification of the cell invasion using ImageJ software shows that both CTX and CTX-NO inhibit T98G cell invasion and CTX-NO enhances the anti-invasive properties of CTX. *$p < 0.05$, #$p < 0.05$ compared to DI water, n = 7.

CTX was able to decrease T98G cell invasion in a dose dependent manner and CTX-NO enhanced this inhibition. At a concentration of 36 nM invasion was reduced to 85.9 ± 7.6% of the control by CTX, and CTX-NO at the same concentration reduced invasion to 74.8 ± 4.9% (Fig 4.5B). This same phenomenon was observed at higher concentrations, with CTX at a concentration of 72 nM reducing T98G cell invasion to

78.1 ± 3.6%, while CTX-NO at the same concentration reduced invasion to 67.1 ± 3.8% of the control. At the highest concentration tested, 145 nM, invasion was reduced to 69.1 ± 3.0% and 55.5 ± 6.5% of the control, by CTX and CTX-NO, respectively (Fig 4.5B).

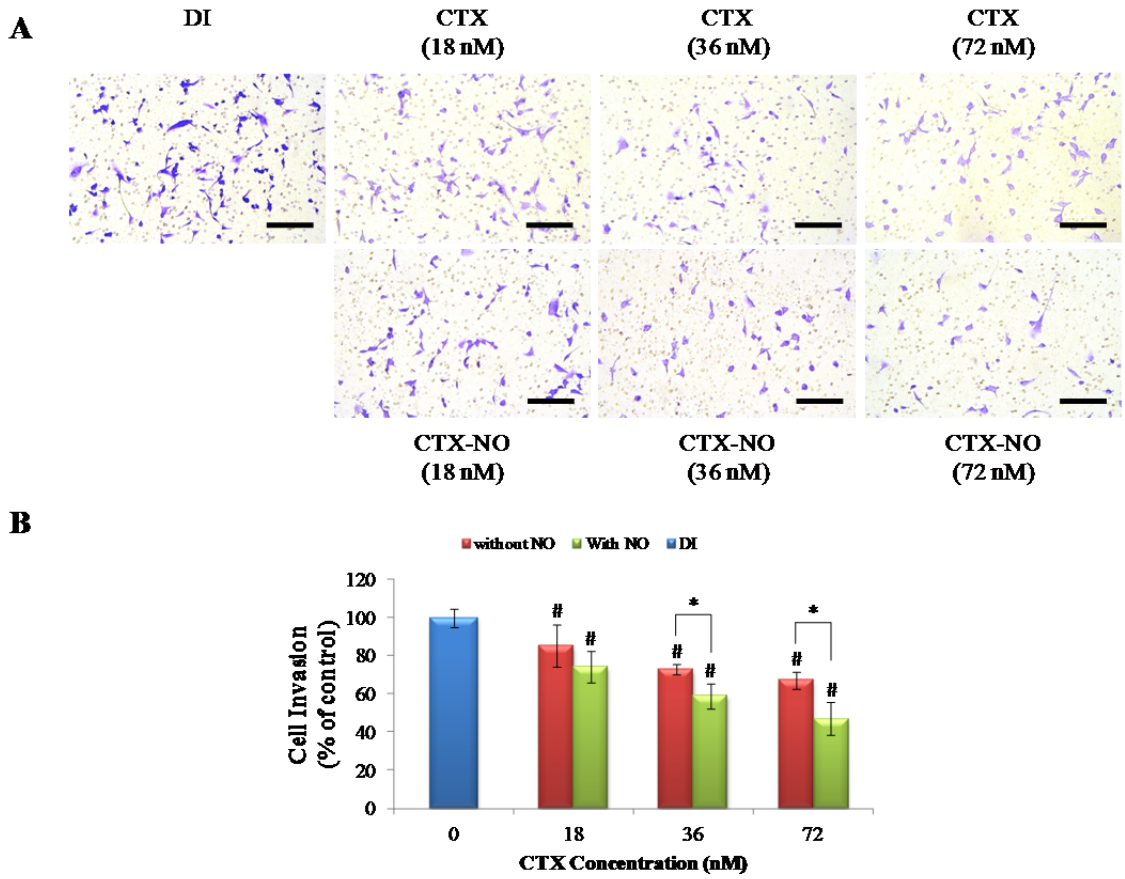

Figure 4.6. Invasion assay with U-87MG cells. (A) Pictures showing the invasion through a matrigel matrix of U-87MG cells incubated for 48 hours with 0-72 nM of CTX (upper row) or CTX-NO (lower row). Pictures were taken of the bottom of matrigel-coated transwell inserts showing invading U-87MG cells stained with crystal violet after the indicated treatment. Scale bar = 20 µm. (B) Quantification of the cell invasion using ImageJ software shows that, as observed in T98G cells, both CTX and CTX-NO inhibit U-87MG invasion in a dose dependent manner and CTX-NO enhances the anti-invasive properties of CTX. *$p < 0.05$, #$p < 0.05$ compared to DI water, n = 7.

Similar to the effects seen in T98G cells, CTX-NO enhanced the dose dependent attenuation of glioma cell invasion elicited by CTX. At the lowest concentration, 18 nM, U-87MG invasion was reduced to 85.2 ± 11.1% and 74.2 ± 8.5% of the control by CTX and CTX-NO, respectively (Fig. 4.6B). U-87MG invasion was reduced to 72.7 ± 2.9%

and 67.1 ± 4.7% by CTX at concentrations of 36 nM and 72 nM, respectively. At the same concentrations, CTX-NO reduced U-87MG invasion to 58.8 ± 6.5% and 47.0 ± 8.7% of the control (Fig. 4.6B).

4.5.3 CTX-NO enhances ability of CTX to inhibit glioma cell migration

In addition to the invasion assay, a modified scratch assay was performed to compare the effects of CTX and CTX-NO on glioma cell migration. In T98G cells exposed to 36 nM of CTX, migration was reduced to 88.9 ± 9.1% of the control, whereas the same concentration of CTX-NO reduced cell migration to 77.5 ± 7.8%. The enhanced effect of CTX-NO on T98G migration was more pronounced at higher concentrations. In T98G cells exposed to 72 nM of CTX-NO, migration was reduced to 72.6 ± 3.6% of the control, whereas the same concentration of CTX reduced cell migration to 86.9 ± 9.2%. The greatest difference in glioma cell migration was observed at a concentration of 145 nM, at which CTX was able to limit migration to 78.5 ± 7.2% and CTX-NO limited migration to 45.8 ± 7.4% of the control (Fig. 4.7).

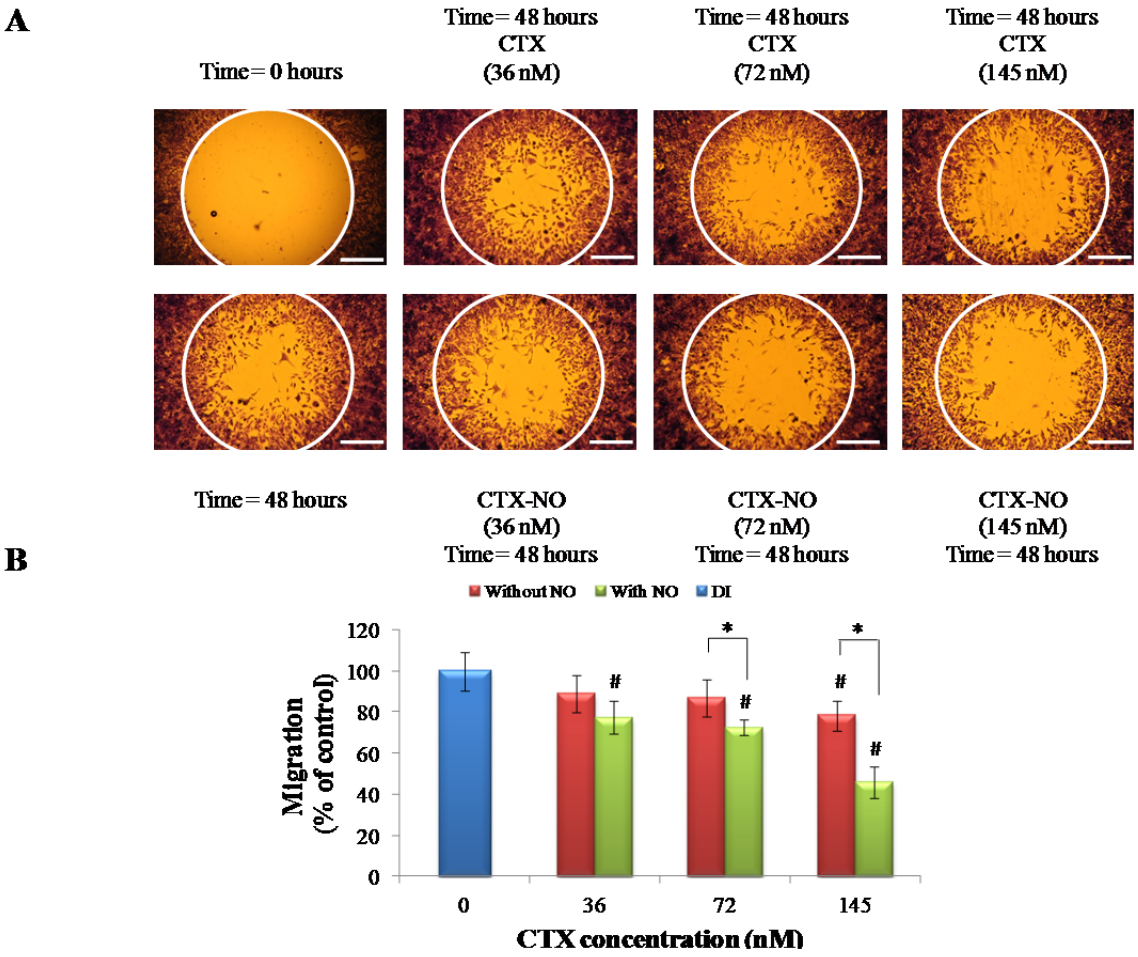

Figure 4.7. Oris™ Migration assay with T98G cells (A) Pictures showing the migration of T98G cells, incubated for 48 hours with 0-145 nM of CTX (upper row) or CTX-NO (lower row). Scale bar = 500 µm. (B) Quantification of cell migration using ImageJ software shows that both CTX and CTX-NO inhibit T98G cell migration in dose dependent manner. CTX-NO enhances the anti-migration effects of CTX. *$p < 0.05$, #$p < 0.05$ compared to DI water, n=4.

U-87MG cells have a different morphology than T98G cells and therefore did not form a uniform monolayer around the stopper. The morphology of these cells made quantifying cell migration challenging. When the migration assay was performed for 48 hours, as done with the T98G cells, the U-87MG cells migrated to cover the detection zone in all conditions (Fig. 4.8A). At the two lower concentrations of CTX, 18 nM and 36 nM, no significant decreases in U-87MG cell migration was observed. At 72 nM, the highest concentration of CTX, migration was reduced to 89.6 ± 2.3% of the control.

CTX-NO reduced migration to 90.7 ± 2.0% and 86.0 ± 9.9% of the control at concentrations of 36 nM and 72 nM, respectively (Fig. 4.8B). The reductions at both these concentrations, although statistically significant from the control, were not statistically different from the reductions observed after incubation with the same concentrations of CTX (Fig. 4.8B).

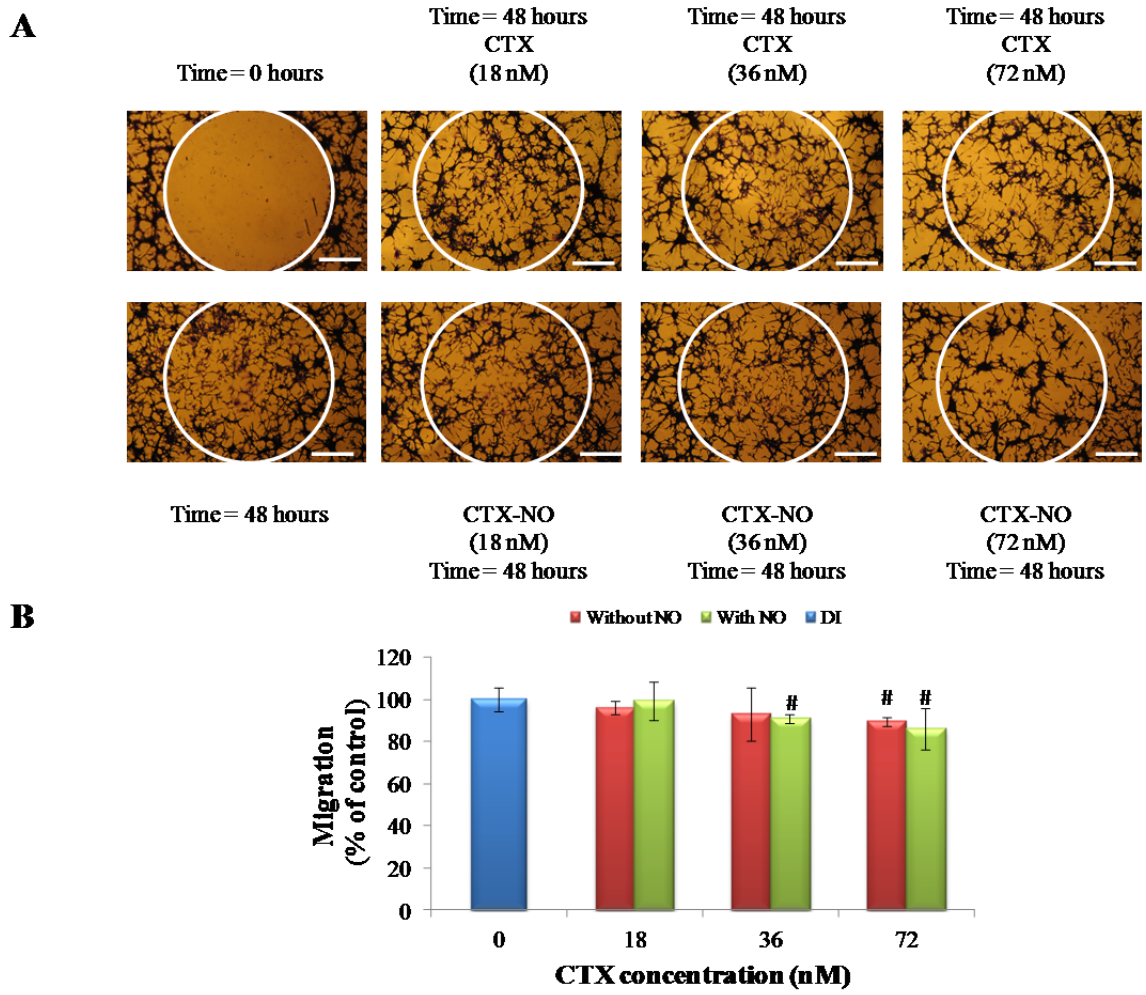

Figure 4.8. Oris™ Migration assay with U-87MG cells (A) Pictures showing the migration of U-87MG cells, incubated for 48 hours with 0-72 nM of CTX (upper row) or CTX-NO (lower row). Scale bar = 500 µm. (B) Quantification of the cell migration after 48 hours using ImageJ software. No differences between the effects of CTX and CTX-NO were observed. *$p < 0.05$, #$p < 0.05$ compared to DI water, n=4.

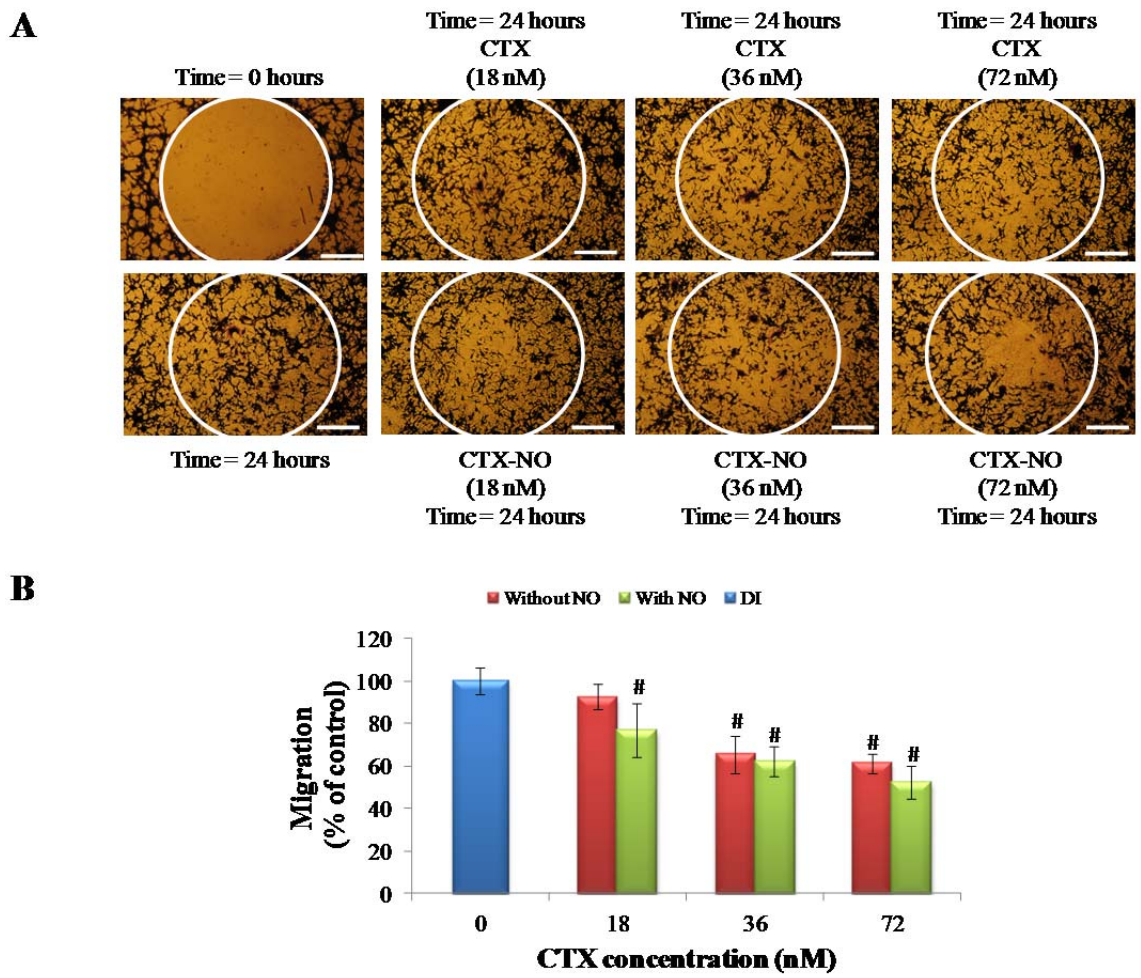

Figure 4.9. Oris™ Migration assay with U-87MG cells over 24 hours. (A) Pictures showing the migration of U-87MG cells, incubated for 24 hours with 0-72 nM of CTX (upper row) or CTX-NO (lower row). Scale bar = 500 µm. (B) Quantification of the cell migration after 48 hours using ImageJ software. CTX-NO attenuated U-87MG migration at all concentrations, whereas CTX decreased glioma cell migration only at the highest concentrations. *$p < 0.05$, #$p < 0.05$ compared to DI water, n=4.

In an alternate experiment with U-87MG cells the migration assay was performed only for 24 hours, instead of 48 hours. In this shortened incubation period, inhibition of U-87MG migration was observed after exposure to both CTX and CTX-NO (Fig 4.9A). After a 24 hour exposure to 18 nM of CTX, U-87MG migration was decreased to 92.6 ± 5.9% of the control, whereas at the same concentration of CTX-NO, U-87MG migration was decreased to 77.0 ±12.9% of the control (Fig. 4.9B). Similarly, migration of U-

87MG cells exposed to 72 nM of CTX was decreased to 61.4 ±4.5%, while migration of cells exposed to the same concentration of CTX-NO was reduced to 52.7 ± 7.6 % of the control (Fig. 4.9B).

4.5.4 CTX and CTX-NO decreased MMP-2 surface expression in a dose dependent manner

Although it is well documented that CTX binds to MMP-2 on glioma cell surfaces and consequently decreases MMP-2 surface expression, the effect of CTX-NO on MMP-2 surface expression also needed to be investigated. In T98G cells exposed to 36 nM of CTX, MMP-2 expression was decreased to 69.5 ± 7.5% of the control (Fig. 4.10A). MMP-2 expression in T98G cells was reduced to 56.2 ± 5.6% of the control after exposure to 145 nM of CTX, which was the highest concentration of CTX tested. At the two lower concentrations of CTX-NO, 36 nM and 72 nM, although MMP-2 was decreased to 62.5 ± 6.2% and 52.2 ± 5.6% of the control, respectively, these reductions were not significantly different from those observed at the corresponding concentrations of CTX. When T98G cells were exposed to 145 nM of CTX-NO, MMP-2 surface expression was measured to be 47.4 ± 0.9% of the control, which was significantly different to the decrease observed when T98G cells were exposed to the corresponding concentration of CTX (Fig. 4.10A).

As observed in T98G cells, when U-87MG cells were exposed to CTX or CTX-NO, MMP-2 surface expression was decreased in a dose dependent manner (Fig 4.10B). MMP-2 expression in U-87MG cells was decreased to 72.4 ± 9.6% and 69.8 ± 4.3% of the control after they were exposed to 18 nM of CTX and CTX-NO respectively. At

higher CTX and CTX-NO concentrations, more pronounced differences in the effects of the two biomolecules were observed. MMP-2 expression in U-87MG cells, after incubation with 36 nM of CTX, was decreased to 51.9 ± 2.6% of the control, whereas exposure to the corresponding CTX-NO concentration resulted in MMP-2 expression reduced to 35.3 ± 8.7% of the control. The lowest MMP-2 expression in U-87MG cells, 27.5 ± 8.7% of the control, was observed after the cells were exposed to 72 nM CTX-NO (Fig 4.10B). Exposure to the corresponding concentration of CTX decreased MMP-2 expression to 49.5 ± 6.4% of the control.

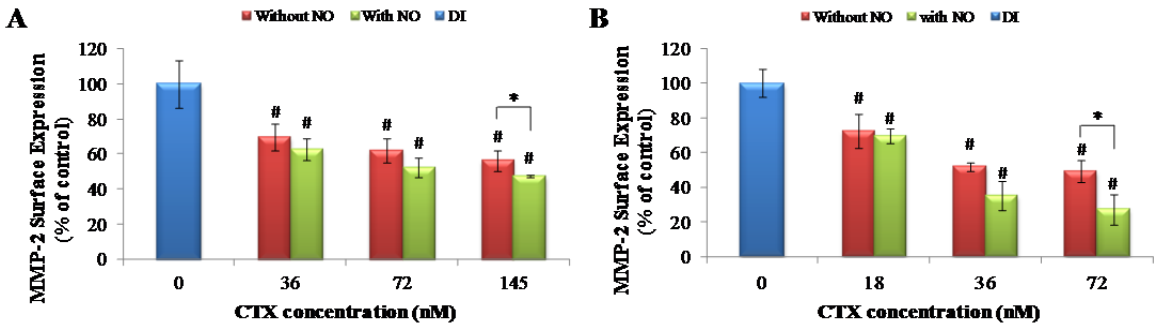

Figure 4.10. MMP-2 surface expression in (A) T98Gs and (B) U-87MGs after incubation with CTX or CTX-NO for 48 hours. Both CTX and CTX-NO decreased MMP-2 expression but it was only at the highest concentrations that CTX-NO enhanced the effect of CTX in decreasing MMP-2. *$p < 0.05$, #$p < 0.05$ compared to DI water, n = 3-5.

4.5.5 MMP-9 expression reduced only by CTX-NO

MMP-9 surface expression in T98G cells was not significantly reduced by CTX and was measured to be 98.0 ± 10.9% of the control after the cells were exposed to 145 nM of CTX, the highest concentration of CTX tested (Fig. 4.11A). At a concentration of 36 nM CTX-NO, MMP-9 surface expression in T98G cells was reduced to 89.9 ± 9.4% of the control. This decrease, however, was statistically insignificant from the control. At higher concentrations of CTX-NO, 72 nM and 145 nM, MMP-9 surface expression in

T98G cells was reduced to 85.8 ± 9.5% and 84.9 ± 6.0% of the control, respectively (Fig. 4.11A).

Similarly, no significant decreases in MMP-9 expression were observed when U-87MG cells were incubated with CTX. At the highest concentration of CTX tested, MMP-9 expression was 100.6 ± 10.8% (Fig. 4.11B). On the other hand, MMP-9 expression in U-87MG cells was reduced in a dose dependent manner by CTX-NO. At the lowest concentration of CTX-NO, 18 nM, MMP-9 expression was reduced to 80.6 ± 13.8% of the control. The most pronounced decrease in MMP-9 expression to 55.9 ± 15.6% was observed after U-87MG cells were exposed to 72 nM of CTX-NO (Fig. 4.11B).

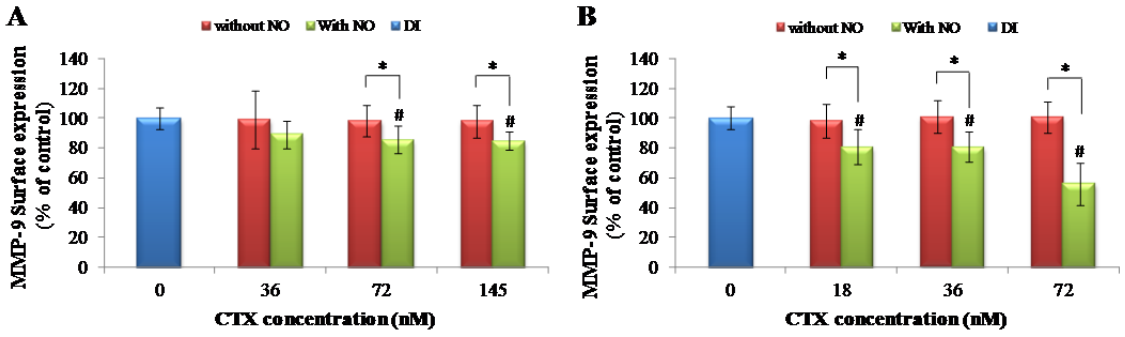

Figure 4.11. MMP-9 surface expression in (A) T98Gs and (B) U-87MGs after incubation with CTX or CTX-NO for 48 hours. CTX did not decrease MMP-9 expression at any of the tested concentrations, whereas CTX-NO decreased MMP-9 significantly. *$p < 0.05$, #$p < 0.05$ compared to DI water, n = 5-8.

4.5.6 CTX induced decrease of MMP-2 and MMP-9 activity accentuated by CTX-NO

In order to measure the activity of MMP-2 and MMP-9, conditioned media from cell cultures exposed to CTX or CTX-NO was incubated with an MMP-2 and MMP-9 specific fluorogenic substrate. Conditioned media collected from T98G cells exposed to CTX, showed a modest decrease in enzyme activity, but exposure to CTX-NO resulted in

a more pronounced decrease in enzymatic activity (Fig. 4.12A). After a 48-hour incubation with 36 nM CTX, MMP-2 and MMP-9 activity was decreased to 92.5 ± 4.39% of the control. Incubation with 36 nM CTX-NO showed a greater decrease in enzyme activity, measured as 83.3 ± 1.4% of the control (Fig. 4.12A). Exposure to 72 nM of CTX-NO decreased enzymatic activity to 76.7 ± 1.4% of the control, whereas exposure to the same concentration of CTX only reduced the activity to 95.0 ± 0.4% (Fig. 4.12A). At the highest concentration of CTX-NO, 145 nM, enzymatic activity was reduced to 66.4 ± 2.2% of the control, whereas the same concentration of CTX reduced enzymatic activity to 93.5 ± 1.8%.

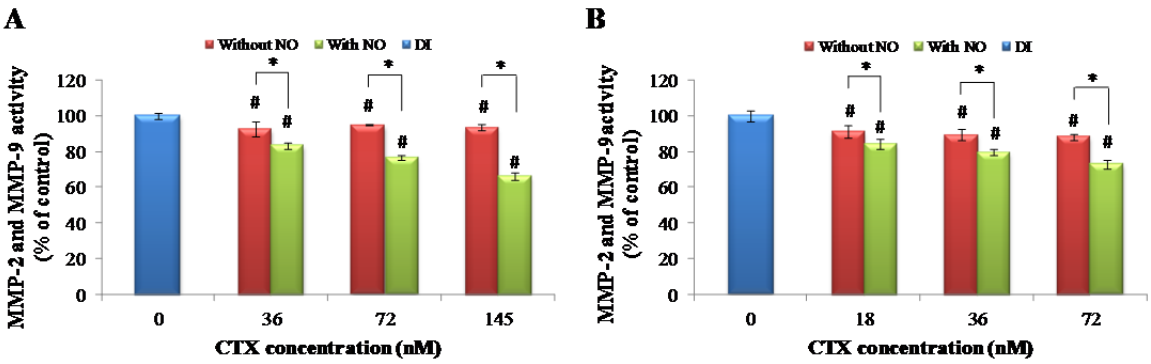

Figure 4.12: MMP2/MMP-9 activity of (A) T98Gs and (B) U-87MGs. CTX-NO enhances the inhibitory effect of CTX on the activity of MMP-2 and MMP-9 in a dose dependent manner. *p < 0.05, #p < 0.05 compared to DI water, n=3-6.

MMP-2 and MMP-9 enzymatic activity in U-87MG cells was decreased by both CTX and CTX-NO in a dose dependent manner. At the lowest concentration of CTX and CTX-NO, enzymatic activity in U-87MG cells was decreased to 91.3 ± 3.5% and 84.1 ± 2.6% of the control, respectively. At a higher concentration, 36 nM, CTX-NO decreased enzyme activity in U-87MG cells to 79.6 ± 1.9% of the control and CTX reduced activity to 89.2 ± 3.1% of the control. At the highest concentration of CTX and CTX-NO, 72 nM, the greatest decreases in enzymatic activity in U-87MG cells were observed. At this

concentration, CTX and CTX-NO decreased enzymatic activity to 88.3 ± 1.7% and 73.0 ± 2.6% of the control, respectively (Fig. 4.12A).

4.5.7 DQ-collagen assay

In order to visually assess the effect of CTX and CTX-NO treatment on the proteolytic activity of MMPs, cells grown on a mixture of matrigel and DQ-collagen were treated with CTX or CTX-NO. Activated collagenases, including MMP-2 and MMP-9, resulted in the release of fluorogenic degradation products from DQ-collagen, which were imaged using confocal microscopy. Images of T98G cells showed that the cells grew in clusters, and cells treated with DI, CTX and CTX-NO, all showed pericellular degradation of the DQ-collagen (Fig, 4.13). Nonetheless, a difference in the pattern of the fluorescence was observed in the cells treated with CTX-NO. After treatment with CTX-NO, the fluorescence was concentrated towards the center of the cluster whereas for the other conditions fluorescence was observed on the periphery of the clusters, i.e. the invading edge (Fig. 4.13).

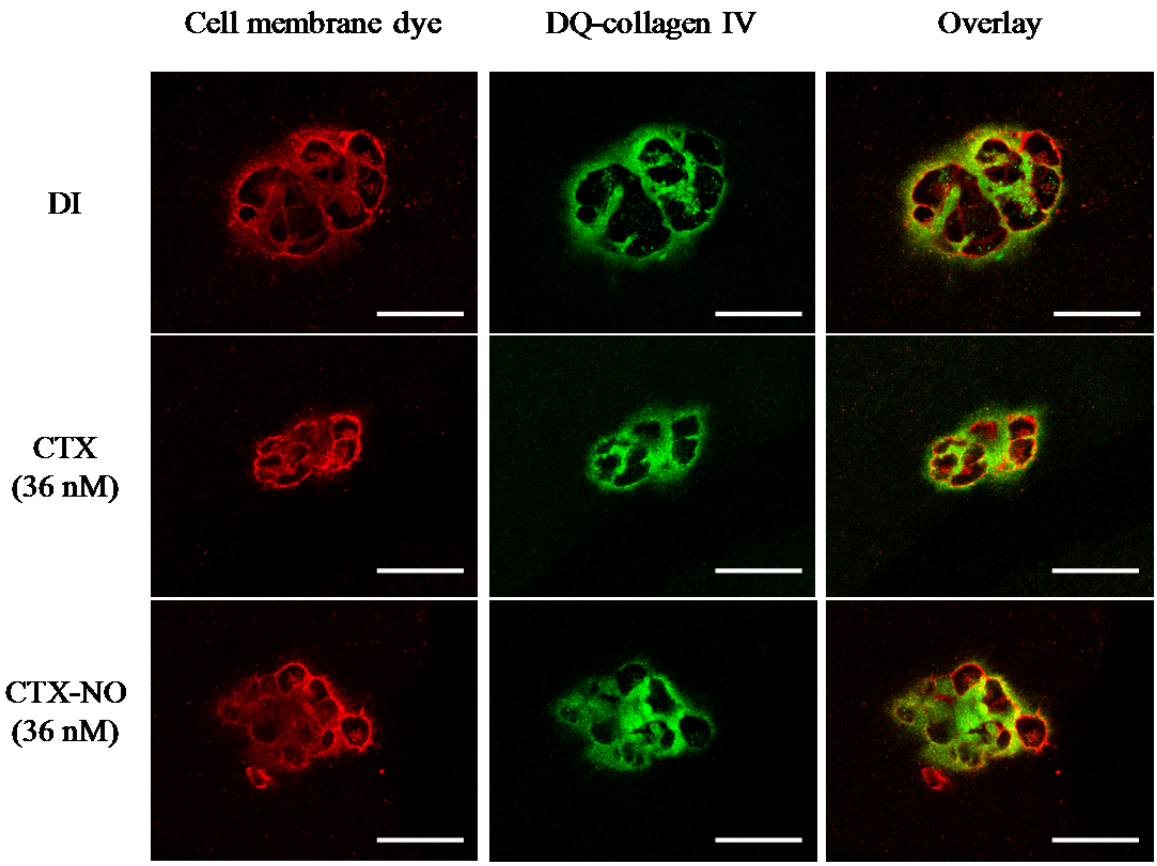

Figure 4.13. Confocal images of T98G cells gown on Matrigel/DQ-collagen mixture and exposed to DI water (top row), 36 nM of CTX (middle row) and 36 nM of CTX-NO (bottom row) for 48 hours. Secretion of MMPs from the cells results in the degradation of DQ-collagen and the subsequent release of fluorescence (middle column). Pictures show pericellular release of MMPs. Scale bar = 50 μm

Images of U-87 cells showed, that in contrast to the clusters observed in T98G cells, these cells grew in a more diffuse manner (Fig. 4.14). However, similar to the observations in T98G cells, pericellular degradation of DQ-collagen was observed. However, in contrast to the T98G cells, when U-87MG cells were incubated with CTX-NO, green fluorescence was also observed within the cell, indicating intracellular expression of MMPs. This suggests that CTX-NO maybe inhibiting the secretion of MMPs and consequently inhibiting invasion.

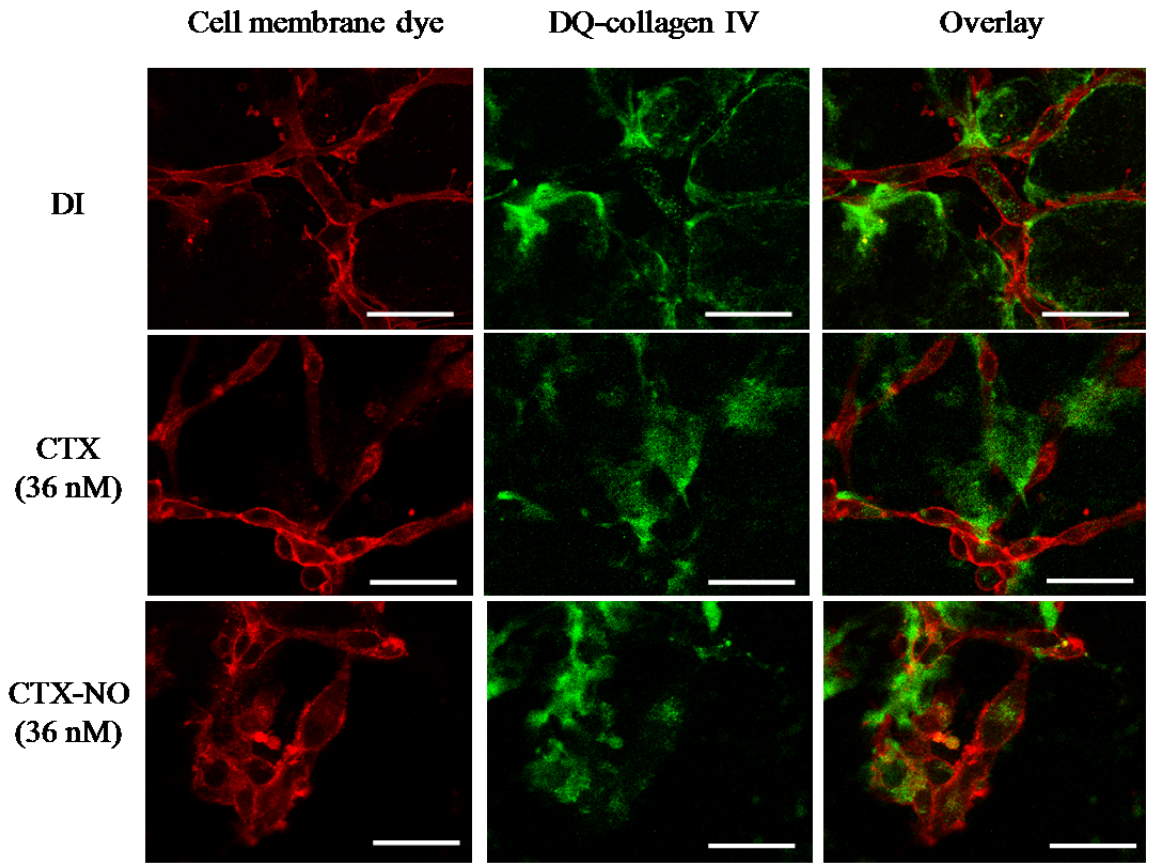

Figure 4.14. Confocal pictures of U-87MG cells gown on Matrigel/DQ-collagen mixture and exposed to DI water (top row), 36 nM of CTX (middle row) and 36 nM of CTX-NO (bottom row) for 48 hours. Secretion of MMPs from the cells results in the degradation of DQ-collagen and the subsequent release of fluorescence (middle column). Pictures show pericellular release of MMPs. Scale bar = 50 µm

4.6 Discussion

Glioma invasion is a significant challenge in successful treatment of the disease, even though gliomas are the only cancers to grow in a confined space [253]. Gliomas initially invade the fluid-filled space in the cranium, which corresponds to about 15% of the cranial space [253]. However, when this space becomes insufficient for further tumor growth, the glioma cells invade the peritumoral region by degrading the ECM of

surrounding brain tissue [31]. Increased expression of ECM degrading enzymes, including MMPs, has been observed in highly invasive gliomas.

CTX, a protein extracted from scorpion venom, has been extensively studied, not only because of its ability to target glioma cells but because of its anti-invasive properties [180, 187, 210, 265]. Although CTX has well-documented anti-invasive properties, the role of NO in tumor cell invasion is debated. Some studies have indicated that NO aids in tumor invasion [153, 156, 157, 266], whereas other work suggests the opposite [267, 268]. Hence, after the characterization of the glioma-targeting NO donor, CTX-NO, it was imperative to study the effect of the transformation of CTX into an NO donor on the anti-invasive properties of the former protein.

Boyden chamber invasion assays confirmed that CTX does indeed inhibit glioma invasion. It was also observed that CTX-NO enhanced the ability of CTX to decrease glioma cell invasion in both T98G and U-87MG cells to less than 70% of the control. Migration studies of T98G cells reflected the same pattern observed in the invasion studies. CTX inhibited T98G migration by approximately 20%, but CTX-NO decreased T98G migration by over 50%. The migration studies of U-87MG cells did not result in observations of significant inhibition of migration and only at the highest concentration of CTX-NO was U-87MG migration reduced by 10%. The lack of response of U-87MG is partially attributed to the inability of the cells to form a uniform monolayer in 2D culture, thus making quantifying migration challenging. As an alternative, CTX and CTX-NO incubation times were reduced to 24 hours for the U-87MG migration studies. This reduction prevented the U-87MG cells from completely covering the detection zone allowed better measurement of migration. In this shortened experiment, it was observed

that CTX-NO inhibited migration to under 55% of the control, whereas migration remained above 60% when U-87MG cells were incubated with CTX. These studies demonstrated that low doses of NO (up to 2 μM) released from CTX-NO have anti-invasive properties. These results are in agreement with previous studies, which have shown NO donors are able to inhibit tumor cell invasion [145, 268, 269].

Localization of MMP-2 and MMP-9, along with other proteinases, on the cell surface in response to various integrins is an important step in cell invasion and migration [270-272]. Thus, in order to elucidate the mechanism by which NO enhanced the ability of CTX to attenuate glioma invasion, the effects of these treatments on MMP-2 and MMP-9 cell surface expression were studied using immunocytochemistry. CTX is known to bind to MMP-2 and consequently results in the internalization of the complex; therefore, as expected, CTX was able to decrease MMP-2 expression to less that 55% of the control in both T98G and U-87MG cells. At lower concentrations of CTX-NO comparable decreases in MMP-2 expression were observed. However, a statistically greater decrease in MMP-2 expression was observed at the highest concentration of CTX-NO treatment compared to CTX treatment. Conversely, although CTX treatment did not decrease MMP-9 surface expression, CTX-NO treatment resulted in MMP-9 reductions in a dose dependant manner. This observation is in agreement with previous studies using endothelial cells, which have shown that NO activated transcription factor 3 (ATF3), which in turn inhibited MMP-2 mRNA expression [273]. Although significant differences in the surface expression of MMP-2 in cells treated with CTX and CTX-NO were not observed, differences in MMP-9 expression were observed and the activation of ATF3 may be a possible mechanism for this observation.

While localization of MMPs to the cell surface is a valuable indicator of the invasive properties of glioma cells, activation of MMPs is essential for the degradation of the ECM by these enzymes [29, 255, 257]. Therefore, in order to determine the effect of CTX and CTX-NO on the proteolytic activity of MMP-2 and MMP-9, conditioned media was incubated with a fluorogenic substrate for these enzymes. Results from this experiment showed that while CTX incubation resulted in a decrease of approximately 15% of the enzymatic activity, incubation with CTX-NO, at the highest concentration, resulted in over 25% reduction in enzymatic activity. Although the aforementioned substrate has been optimized for MMP-2 and MMP-9, it may also be cleaved by other classes of MMPs [262]. Nonetheless, it can be inferred that in comparison to CTX, MMP activity is indeed decreased to a greater extent by CTX-NO. The reduction in enzymatic activity may be a direct consequence of the reduction of MMP surface expression or the NO could be decreasing the enzymatic activity of each MMP molecule. MMPs are activated by a cysteine switch, which results in the active zinc site being exposed [274]. *S*-nitrosylation of cysteine thiols on proteins has been shown to result in decreased enzymatic activity [129, 274-276]. Thus, it is proposed that one of the reasons for the decreased MMP-2 and MMP-9 activity observed after CTX-NO treatment is *S*-nitrosylation of cysteine residues, which in turn prevents the exposure of the active site. Interestingly, *S*-nitrosylation of MMP-9 has also been implicated as a mechanism by which the enzyme is activated [277]. As discussed previously, the effect of NO varies depending on cell type, duration of exposure, and origin [126, 278], and it is proposed that whereas endogenous NO may lead to activation of MMPs, exogenous NO can potentially have inhibitory effects on MMP activation.

Although both CTX and CTX-NO, at the concentrations investigated, were unable to inhibit glioma cell invasion completely, NO did enhance the anti-invasive properties of CTX. This was partially due to decreased MMP-2 and MMP-9 surface expression and activity by the NO released from CTX-NO. Invasion of glioma cells involves a variety of other MMPs, integrins and chemokines. Accordingly, it is likely that other enzymes are also affected by NO treatment. Postovit et al. showed that NO treatment resulted in activation of soluble guanylyl cyclase (sGC) and the subsequent activation of protein kinase G (PKG), which in turn phoshorylates proteins [279]. This resulted in inhibition of tumor cell invasion via the inhibition of urokinase plasminogen activator receptor (UPAR) expression [279]. NO has previously been shown to downregulate hypoxia-inducible factor α (HIF-α), a protein that activates the transcription of numerous proteins involved in angiogenesis and tumor invasion [157]. Additionally, NO has been shown to impair the function of mitochondria, and Wang et al. speculate that impaired mitochondria may reduce the energy supply for cell invasion or alter the expression of proteins involved in invasion, leading to decreased tumor cell invasion [157]. Another mechanism by which NO has been shown to inhibit tumor invasion is by upregulating tissue inhibitor of matrix metalloproteinase 2 (TIMP-2) [266]. Nitric oxide plays a complex role in tumor invasion, and although further studies need to be carried out, work discussed herein suggests that NO aids CTX in glioma invasion inhibition by decreasing MMP-2 and MMP-9 expression and activity.

CHAPTER 5: CONCLUSIONS AND FUTURE WORK

GBM is the most aggressive and prevalent kind of tumor in the central nervous tumor. For a number of years cytotoxic chemotherapeutic drugs have been used to treat a variety of tumors, including GBM. However, the non-specific nature of these chemotherapeutics necessitates that most anti-cancer drugs be administered at the maximum tolerated dose, which in turn leads to a variety of side effects in the patient. Therefore, in order to increase the survival of patients suffering from various cancers and minimize the toxic side effects of chemotherapy, it is imperative that targeted therapeutics be developed. In this thesis, the synthesis and characterization of two targeted NO donors, VTW-NO and CTX-NO is presented. Additionally, studies investigating the chemosensitizing and invasion inhibiting effects of CTX-NO are discussed.

5.1 Results and Implications

Synthesis and characterization of glioma targeting NO Donors

NO therapy has long been considered a promising avenue for glioma therapy, but the complexity of NO signaling, as well as the difficulty in balancing the potential side effects of NO donors, has limited its success *in vivo*. Therefore, in order to fully harness the chemotherapeutic effects of NO while at the same time minimizing its toxic side effects, GBM-targeting NO donors were synthesized. Studies presented in Chapter 2, using two different glioma-targeting biomolecules, CTX and VTW, demonstrated that peptides and proteins can be converted into NO-releasing diazeniumdiolates in a simple

reaction with NO gas. Furthermore, fluorescent and confocal microscopy studies showed that the targeting abilities of CTX-NO and VTW-NO were retained after the reaction of the biomolecules with NO.

Additionally, incubation of the NO donors with HB, an extracellular NO-scavenger, showed minimal attenuation of the cytotoxic effects of the NO donors. This suggested that the NO donors are efficiently endocytosed by glioma cells and most of the NO is released within the cell. Most importantly, it was demonstrated that targeted NO donors can inhibit glioma cell viability without significant harm to human astrocytes and brain microvascular endothelium. The work presented in Chapter 2 provides evidence to show that targeted NO delivery is an attractive treatment option for GBM, particularly because of the method's minimal toxic effects on normal cells. The techniques used to synthesize targeted NO donors, discussed in Chapter 2, can easily be modified to develop NO donors that are specific to different tumors.

Effect of targeted NO delivery on the chemosensitivity of glioma cells

GBM, in addition to being characterized by aggressive and highly invasive growth, is among the least therapeutically responsive tumors. The complex nature of GBM physiology has shown that for an effective treatment, a multimodal approach must be employed for tumor treatment. Hence, it was necessary to study the effect of CTX-NO on the chemosensitivity of glioma cells. Viability studies showed that a two hour pretreatment with CTX-NO resulted in an enhanced chemosensitivity towards BCNU and TMZ in glioma cells, but no sensitizing effects were observed in astrocytes or endothelial cells. Further studies showed that NO pretreatment resulted in decreased MGMT

expression, suggesting that MGMT played a role in the reduction of chemoresistance in glioma cells elicited by NO. A possible mechanism for the NO-mediated reduction in MGMT levels is the *S*-nitrosylation of the cysteine residue in the active site of MGMT, which results in decreased enzymatic activity. Additionally, it was found that NO pretreatment decreased p53 levels in GBM cells. This is particularly interesting because GBM cells often have mutations in the p53 protein which result in diminished ability to trigger apoptosis. A decrease in wildtype p53 indicated that NO increased nuclear retention of the protein leading to increased apoptosis.

While all of the precise mechanisms by which NO induces chemosensitivity are yet to be elucidated, the work discussed in Chapter 3 demonstrates that targeted NO delivery can enhance the chemosensitivity of glioma cells by decreasing MGMT and p53 levels (Fig. 5.1). This work verifies that targeted NO delivery can be used to sensitize cells towards chemotherapeutics and this therapy holds great potential as an adjuvant in the multimodal treatment of the numerous tumors that are normally unresponsive to chemotherapy.

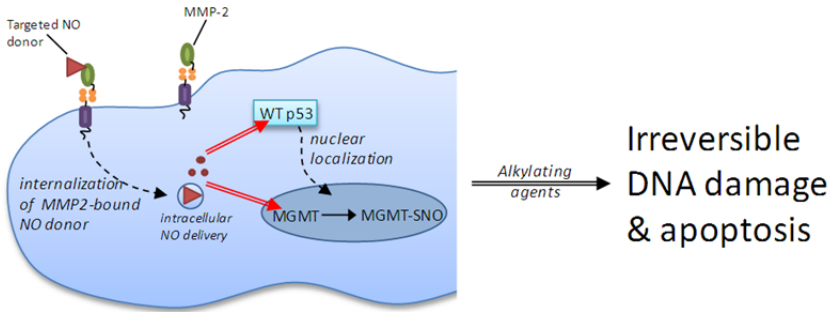

Figure 5.1. Proposed mechanism by which CTX-NO induces chemosensitivity in glioma cells. CTX-NO binds to the MMP-2 complex and is consequently internalized. NO is released in the intracellular space inhibiting the effect of DNA repair enzyme, MGMT and triggering the nulear localization of wildtype p53. These changes result in the glioma cells being more susceptible to the apoptotic inducing effects of alkylating agents

Effect of targeted NO delivery on the invasive properties of glioma cells

The highly invasive nature of GBM has proven to be a major obstacle to the successful treatment of GBM. The infiltrative nature of the tumor makes complete tumor resection without the loss of neurological function nearly impossible. Therefore, to successfully treat GBM, it is imperative to inhibit glioma cell invasion. While CTX has well documented anti-invasive properties, the role of NO is debated. In Chapter 4, the differences between the effect of CTX and CTX-NO treatments on glioma cell invasion and migration were investigated.

Boyden chamber studies showed that CTX-NO enhanced the ability of CTX to inhibit glioma cell invasion through Matrigel. Additionally, it was observed that CTX-NO also enhanced the ability of CTX to inhibit glioma cell migration. These studies suggest that NO has an inhibitory role in glioma cell invasion and to elucidate the mechanism by which this occurs, surface expression and activity of two important ECM degrading proteinases, MMP-2 and MMP-9, were quantified after treatment with CTX or CTX-NO. As CTX is known to bind to MMP-2, it is not surprising that CTX-NO was able to decrease MMP-2 surface expression. An added benefit of CTX-NO was its observed ability to decrease MMP-9, which CTX was unable to decrease. The reduction in enzymatic activity may be a consequence of reduced MMP expression or a result of NO exposure.

Hence, these studies suggest that even small doses of NO have anti-invasive properties, and this is due in part to the inhibitory effects of NO on MMP-2 and MMP-9. Invasion of glioma cells involves a variety of other MMPs and chemokines, therefore it is probable that other enzymes are also affected by the NO treatment. Though the work

discussed herein suggests that NO works synergistically with CTX to attenuate glioma cell invasion, it is recognized that tumor physiology is very complex and NO affects numerous pathways in the body; hence further studies are needed to validate the use of CTX-NO as a GBM therapeutic. Some avenues of further research are discussed in the following section.

5.2 Future work and Applications

Effect of CTX-NO on permeability of BBB

The BBB barrier is a major hindrance to drug delivery for the treatment of GBM. The transcellular tight junctions found in the endothelial cells that make up the BBB severely restrict the movement of soluble factors between the endothelial cells and the cerebrospinal fluid. While this barrier plays a critical role in preventing bacteria from reaching the brain, chemotherapeutics that have a molecular weight of greater than 400-500 Daltons are unable to passively cross the BBB. It is therefore of great interest to investigate the effect of targeted NO on the BBB.

It is hypothesized that the targeted NO delivery will affect the regions of the BBB that are in close proximity to the tumor. It is anticipated that CTX-NO treatment will increase the permeability of the BBB and result in greater tumor site accumulation of a systemically delivered drug. In order to test this hypothesis, it is suggested that brain endothelial and glioma cell co-culture models be used. An *in vitro* model that can be used to study the effects of CTX-NO on the BBB involves the use of collagen-coated Boyden chambers. Brain endothelial cells and astrocytes grown to monolayers on the upper and

lower sides of the inserts have been shown to be a reproducible model for studying the effects of drugs on the properties of the BBB [280-282].

Effect of CTX-NO on angiogenesis

Angiogenesis, the formation of new blood vessels, plays a pivotal role in GBM tumor growth, as it provides the tumor cells with oxygen and nutrient supply. NO, at certain concentrations, is able to inhibit not only the proliferation of endothelial and smooth muscle cells but also endothelial cell migration that ultimately results in an inhibition of tumor angiogenesis [126, 283-285]. Conversely, NO has also been implicated in promoting tumor angiogenesis [286, 287]. Therefore determining the effect of CTX-NO on angiogenesis is necessary before it can be considered as a viable anti-glioma drug.

One of the commonly used methods to investigate the effect of biomolecules on angiogenesis is the use of tube formation assays [62, 236, 238, 261]. The assay involves seeding endothelial cells on Matrigel- or collagen-coated well plates. Cells are then treated with the drug of interest and tube formation is visualized at various time points, using a microscope. NO has also been shown to affect the expression of VEGF, an important mediator of angiogenesis [287]. In addition, NO inhibits platelet aggregation, which store angiogenic factors and stimulate angiogenic vessel growth. It would therefore also be interesting to investigate the effect of CTX-NO on VEGF expression and platelet aggregation.

In vivo studies

In vitro studies are widely used to study the effects of novel chemotherapeutics since they provide a convenient model to screen drugs for cancer treatment. However, this model has severe limitations because it provides an isolated environment in which to study the effects of the investigational drug [288]. *In vitro* tumor cells have access to 20% oxygen, a full complement of nutrients, and plenty of space [5]. In contrast, *in vivo* oxygen levels can be lower than 1% and nutrient access is intermittent which often results enhanced chemoresistance in GBM cells [5]. Furthermore, it is expected that interactions with normal glial cells, neurons, immune cells, and the tumor microenvironment, which often has regions of low pH, will affect the kinetics of NO release as well as its efficacy as a chemotherapeutic. Therefore, in order to mimic the more complex nature of human physiology it is imperative to perform *in vivo* studies.

To test the efficacy of CTX-NO as a valid GBM treatment, it is recommended that animal studies be performed using intracranial rat glioma models or subcutaneous rat models. While the intracranial models mimic the microtumor environment to a greater degree and have been used extensively in recent studies [146, 289, 290], the subcutaneous models remain a popular choice due to the ease of use and accurate knowledge of the location of the tumor [61, 62, 291-295]. Performing animal studies with intratumoral injections of CTX-NO will provide a greater insight into the potential role of targeted NO as a therapeutic for GBM patients.

This work has demonstrated the efficacy of CTX-NO as a valuable cytotoxic, chemosensitizing and anti-invasion drug. Improving GBM treatment remains a challenge and in this thesis a novel approach for the treatment of this tumor is presented. Although

NO donors have previously been investigated as potential GBM treatments, this is the first study to develop a glioma-targeting NO donor. The material developed herein may be easily translated into a novel adjuvant to current cancer therapies.

References

1. Society, A.C., *Cancer Facts and Figures 2012*. 2012: Atlanta, Ga.

2. Minniti, G., et al., *Chemotherapy for Glioblastoma: Current Treatment and Future Perspectives for Cytotoxic and Targeted Agents.* Anticancer Research, 2009. **29**(12): p. 5171-5184.

3. Robins, H., et al., *Therapeutic advances for glioblastoma multiforme: Current status and future prospects.* Current Oncology Reports, 2007. **9**(1): p. 66-70.

4. Qiang, L., et al., *Inhibition of glioblastoma growth and angiogenesis by gambogic acid: An in vitro and in vivo study.* Biochemical Pharmacology, 2008. **75**(5): p. 1083-1092.

5. Herst, P.M., et al., *Pharmacological concentrations of ascorbate radiosensitize glioblastoma multiforme primary cells by increasing oxidative DNA damage and inhibiting G2/M arrest.* Free Radical Biology and Medicine, 2012. **52**(8): p. 1486-1493.

6. Beal, K., L. Abrey, and P. Gutin, *Antiangiogenic agents in the treatment of recurrent or newly diagnosed glioblastoma: Analysis of single-agent and combined modality approaches.* Radiation Oncology, 2011. **6**(1): p. 2.

7. Beier, D., et al., *Temozolomide preferentially depletes cancer stem cells in glioblastoma.* Cancer Research, 2008. **68**(14): p. 5706-5715.

8. Nakada, M., et al., *Molecular targets of glioma invasion.* Cellular and Molecular Life Sciences, 2007. **64**(4): p. 458-478.

9. Kenig, S., et al., *Glioblastoma and endothelial cells cross-talk, mediated by SDF-1, enhances tumour invasion and endothelial proliferation by increasing expression of cathepsins B, S, and MMP-9.* Cancer Letters, 2010. **289**(1): p. 53-61.

10. Rao, J.S., *Molecular mechanisms of glioma invasiveness: the role of proteases.* Nat Rev Cancer, 2003. **3**(7): p. 489-501.

11. Tervonen, O., et al., *Diffuse "fibrillary" astrocytomas: correlation of MRI features with histopathologic parameters and tumor grade.* Neuroradiology, 1992. **34**(3): p. 173-178.

12. Yamanaka, R., *Cell- and peptide-based immunotherapeutic approaches for glioma.* Trends in Molecular Medicine, 2008. **14**(5): p. 228-235.

13. Hartmann, C., et al., *Patients with <i>IDH1</i> wild type anaplastic astrocytomas exhibit worse prognosis than <i>IDH1-</i>mutated glioblastomas, and <i>IDH1</i> mutation status accounts for the*

unfavorable prognostic effect of higher age: implications for classification of gliomas. Acta Neuropathologica, 2010. **120**(6): p. 707-718.

14. Hou, L.C., et al., *Recurrent glioblastoma multiforme: a review of natural history and management options.* Neurosurgical Focus, 2006. **20**(4): p. E3.

15. Lefranc, F., et al., *Present and potential future issues in glioblastoma treatment.* Expert Review of Anticancer Therapy, 2006. **6**(5): p. 719-732.

16. Mitchell, P., D.W. Ellison, and A.D. Mendelow, *Surgery for malignant gliomas: mechanistic reasoning and slippery statistics.* The Lancet Neurology, 2005. **4**(7): p. 413-422.

17. Grobben, B., P. De Deyn, and H. Slegers, *Rat C6 glioma as experimental model system for the study of glioblastoma growth and invasion.* Cell and Tissue Research, 2002. **310**(3): p. 257-270.

18. Haj-Hosseini, N., et al., *Optical touch pointer for fluorescence guided glioblastoma resection using 5-aminolevulinic acid.* Lasers in Surgery and Medicine, 2010. **42**(1): p. 9-14.

19. Weyerbrock, A., B. Baumer, and A. Papazoglou, *Growth inhibition and chemosensitization of exogenous nitric oxide released from NONOates in glioma cells in vitro.* Journal of Neurosurgery, 2009. **110**(1): p. 128-136.

20. De Bonis, P., et al., *The influence of surgery on recurrence pattern of glioblastoma.* Clinical Neurology and Neurosurgery, (0).

21. Wang, M.-Y., et al., *Comparison of volumetric methods for tumor measurements on two and three dimensional MRI in adult glioblastoma.* Neuroradiology, 2011. **53**(8): p. 565-569.

22. Maier-Hauff, K., et al., *Efficacy and safety of intratumoral thermotherapy using magnetic iron-oxide nanoparticles combined with external beam radiotherapy on patients with recurrent glioblastoma multiforme.* Journal of Neuro-Oncology, 2011. **103**(2): p. 317-324.

23. Hu, B., et al., *Angiopoietin-2 induces human glioma invasion through the activation of matrix metalloprotease-2.* Proceedings of the National Academy of Sciences of the United States of America, 2003. **100**(15): p. 8904-8909.

24. Forsyth, P.A., et al., *Gelatinase-A (MMP-2), gelatinase-B (MMP-9) and membrane type matrix metalloproteinase-1 (MT1-MMP) are involved in different aspects of the pathophysiology of malignant gliomas.* British Journal of Cancer, 1999. **79**(11-12): p. 1828-1835.

25. Lakka, S.S., et al., *Adenovirus-mediated expression of antisense MMP-9 in glioma cells inhibits tumor growth and invasion.* Oncogene, 2002. **21**(52): p. 8011-8019.

26. Mohanam, S., et al., *Expression of tissue inhibitors of metalloproteinases: negative regulators of human glioblastoma invasion in vivo.* Clinical and Experimental Metastasis, 1995. **13**(1): p. 57-62.

27. Badiga, A.V., et al., *MMP-2 siRNA Inhibits Radiation-Enhanced Invasiveness in Glioma Cells.* PLoS ONE, 2011. **6**(6).

28. Deryugina, E.I., L. Soroceanu, and A.Y. Strongin, *Up-regulation of vascular endothelial growth factor by membrane-type 1 matrix metalloproteinase stimulates human glioma xenograft growth and angiogenesis.* Cancer Research, 2002. **62**(2): p. 580-588.

29. Nakada, M., Y. Okada, and J. Yamashita, *The role of matrix metalloproteinases in glioma invasion.* Frontiers in Bioscience, 2003. **8**: p. E261-E269.

30. Roomi, M.W., et al., *Patterns of MMP-2 and MMP-9 expression in human cancer cell lines.* Oncology Reports, 2009. **21**(5): p. 1323-1333.

31. VanMeter, T.E., et al., *The Role of Matrix Metalloproteinase Genes in Glioma Invasion: Co-dependent and Interactive Proteolysis.* Journal of Neuro-Oncology, 2001. **53**(2): p. 213-235.

32. Chamberlain, M.C., *Treatment options for glioblastoma.* Neurosurgical Focus, 2006. **20**(4): p. E19.

33. van Genugten, J., et al., *Effectiveness of temozolomide for primary glioblastoma multiforme in routine clinical practice.* Journal of Neuro-Oncology, 2010. **96**(2): p. 249-257.

34. Ananda, S., et al., *Phase 2 trial of temozolomide and pegylated liposomal doxorubicin in the treatment of patients with glioblastoma multiforme following concurrent radiotherapy and chemotherapy.* Journal of Clinical Neuroscience, 2011. **18**(11): p. 1444-1448.

35. Stummer, W., M. van den Bent, and M. Westphal, *Cytoreductive surgery of glioblastoma as the key to successful adjuvant therapies: new arguments in an old discussion.* Acta Neurochirurgica, 2011. **153**(6): p. 1211-1218.

36. Brandes, A.A., et al., *MGMT Promoter Methylation Status Can Predict the Incidence and Outcome of Pseudoprogression After Concomitant Radiochemotherapy in Newly Diagnosed Glioblastoma Patients.* Journal of Clinical Oncology, 2008. **26**(13): p. 2192-2197.

37. Denbo, J.W., et al., *Continuous local delivery of interferon-β stabilizes tumor vasculature in an orthotopic glioblastoma xenograft resection model.* Surgery, 2011. **150**(3): p. 497-504.

38. Johannessen, T.-C.A. and R. Bjerkvig, *Molecular mechanisms of temozolomide resistance in glioblastoma multiforme.* Expert Review of Anticancer Therapy, 2012. **12**(5): p. 635-642.

39. Walker, M.D., et al., *Evaluation of BCNU and/or radiotherapy in the treatment of anaplastic gliomas.* Journal of Neurosurgery, 1978. **49**(3): p. 333-343.

40. Sith Sathornsumetee, et al., *Molecularly targeted therapy for malignant glioma.* Cancer, 2007. **110**(1): p. 13-24.

41. Cohen, M.H., et al., *FDA Drug Approval Summary: Bevacizumab (Avastin®) as Treatment of Recurrent Glioblastoma Multiforme.* The Oncologist, 2009. **14**(11): p. 1131-1138.

42. Parney, I.F. and S.M. Chang, *Current Chemotherapy for Glioblastoma.* The Cancer Journal, 2003. **9**(3): p. 149-156.

43. Yang, D.-I., et al., *NO-Mediated Chemoresistance in C6 Glioma Cells.* Annals of the New York Academy of Sciences, 2002. **962**(1): p. 8-17.

44. Yang, J.-J., J.-H. Yin, and D.-I. Yang, *Nitric oxide donors attenuate clongenic potential in rat C6 glioma cells treated with alkylating chemotherapeutic agents.* Neuroscience Letters, 2007. **418**(1): p. 106-110.

45. Esther Gil-Alegre, M., et al., *Three weeks release BCNU loaded hydrophilic-PLGA microspheres for interstitial chemotherapy: Development and activity against human glioblastoma cells.* Journal of Microencapsulation, 2008. **25**(8): p. 561-568.

46. Ueda-Kawamitsu, H., T.A. Lawson, and P.R. Gwilt, *In vitro pharmacokinetics and pharmacodynamics of 1,3-bis(2-chloroethyl)-1-nitrosourea (BCNU).* Biochemical Pharmacology, 2002. **63**(7): p. 1209-1218.

47. Bock, H., et al., *First-line treatment of malignant glioma with carmustine implants followed by concomitant radiochemotherapy: a multicenter experience.* Neurosurgical Review, 2010. **33**(4): p. 441-449.

48. Nagpal, S., *The Role of BCNU Polymer Wafers (Gliadel) in the Treatment of Malignant Glioma.* Neurosurgery clinics of North America, 2012. **23**(2): p. 289-295.

49. Shapiro, J.R., et al., *Chromosome-number and carmustine sensitivity in human gliomas.* Cancer, 1993. **71**(12): p. 4007-4021.

50. Lesniak, M.S. and H. Brem, *Targeted therapy for brain tumours.* Nat Rev Drug Discov, 2004. **3**(6): p. 499-508.

51. Becker, K.P. and J. Yu, *Status Quo—Standard-of-Care Medical and Radiation Therapy for Glioblastoma.* The Cancer Journal, 2012. **18**(1): p. 12-19 10.1097/PPO.0b013e318244d7eb.

52. Houghton, P.J., et al., *Antitumor Activity of Temozolomide Combined with Irinotecan Is Partly Independent of O6-Methylguanine-DNA Methyltransferase and Mismatch Repair Phenotypes in Xenograft Models.* Clinical Cancer Research, 2000. **6**(10): p. 4110-4118.

53. Gunther, W., et al., *Temozolomide induces apoptosis and senescence in glioma cells cultured as multicellular spheroids.* British Journal of Cancer, 2003. **88**(3): p. 463-469.

54. Kanzawa, T., et al., *Role of autophagy in temozolomide-induced cytotoxicity for malignant glioma cells.* Cell Death and Differentiation, 2004. **11**(4): p. 448-457.

55. Chakravarti, A., et al., *Temozolomide-mediated radiation enhancement in glioblastoma: A report on underlying mechanisms.* Clinical Cancer Research, 2006. **12**(15): p. 4738-4746.

56. McPherson, C., et al., *Results of phase I study of a multi-modality treatment for newly diagnosed glioblastoma multiforme using local implantation of concurrent BCNU wafers and permanent I-125 seeds followed by fractionated radiation and temozolomide chemotherapy.* Journal of Neuro-Oncology, 2012. **108**(3): p. 521-525.

57. Yovino, S. and S. Grossman, *Treatment of Glioblastoma in "Elderly" Patients.* Current Treatment Options in Oncology, 2011. **12**(3): p. 253-262.

58. Rosenfeld, M.R., K. Albright, and A.A. Pruitt, *Treatment of recurrent high-grade gliomas.* Community Oncology, 2011. **8**(4): p. 171-177.

59. Wong, E.T. and N.H. Yamaguchi, *Treatment advances for glioblastoma.* Expert Review of Neurotherapeutics, 2011. **11**(10): p. 1343-1345.

60. Stupp, R., et al., *NovoTTF-100A versus physician's choice chemotherapy in recurrent glioblastoma: A randomised phase III trial of a novel treatment modality.* European Journal of Cancer, (0).

61. Chen, Q., et al., *Pharmacologic doses of ascorbate act as a prooxidant and decrease growth of aggressive tumor xenografts in mice.* Proceedings of the National Academy of Sciences, 2008. **105**(32): p. 11105-11109.

62. Perry, M.-C., et al., *Curcumin inhibits tumor growth and angiogenesis in glioblastoma xenografts.* Molecular Nutrition & Food Research, 2010. **54**(8): p. 1192-1201.

63. Zanotto-Filho, A., et al., *The curry spice curcumin selectively inhibits cancer cells growth in vitro and in preclinical model of glioblastoma.* The Journal of Nutritional Biochemistry, 2012. **23**(6): p. 591-601.

64. Su, C.C., M.J. Wang, and T.L. Chiu, *The anti-cancer efficacy of curcumin scrutinized through core signaling pathways in glioblastoma.* International Journal of Molecular Medicine, 2010. **26**(2): p. 217-224.

65. Kundu, P., C. Mohanty, and S.K. Sahoo, *Antiglioma activity of curcumin-loaded lipid nanoparticles and its enhanced bioavailability in brain tissue for effective glioblastoma therapy.* Acta Biomaterialia, 2012. **8**(7): p. 2670-2687.

66. Zhao, Y., et al., *Targeted suicide gene therapy for glioma using human embryonic stem cell-derived neural stem cells genetically modified by baculoviral vectors.* Gene Ther, 2012. **19**(2): p. 189-200.

67. Cottin, S., et al., *Gap junctions in human glioblastomas: implications for suicide gene therapy.* Cancer Gene Ther, 2011. **18**(9): p. 674-681.

68. Birks, S.M., et al., *Targeting the GD3 acetylation pathway selectively induces apoptosis in glioblastoma.* Neuro-Oncology, 2011. **13**(9): p. 950-960.

69. Zhan, C., et al., *Co-delivery of TRAIL gene enhances the anti-glioblastoma effect of paclitaxel in vitro and in vivo.* Journal of Controlled Release, 2012. **160**(3): p. 630-636.

70. Liu, S., et al., *Gene and doxorubicin co-delivery system for targeting therapy of glioma.* Biomaterials, 2012. **33**(19): p. 4907-4916.

71. Hamed, H.A., et al., *Inhibition of Multiple Protective Signaling Pathways and Ad.5/3 Delivery Enhances mda-7/IL-24 Therapy of Malignant Glioma.* Mol Ther, 2010. **18**(6): p. 1130-1142.

72. Reddy, E.M., et al., *Dlxin-1, a member of MAGE family, inhibits cell proliferation, invasion and tumorigenicity of glioma stem cells.* Cancer Gene Ther, 2011. **18**(3): p. 206-218.

73. Clarke J, B.N.C.S., *REcent advances in therapy for glioblastoma.* Archives of Neurology, 2010. **67**(3): p. 279-283.

74. Reardon, D., et al., *The Emerging Role of Anti-Angiogenic Therapy for Malignant Glioma[†].* Current Treatment Options in Oncology, 2008. **9**(1): p. 1-22.

75. Batchelor, T.T., et al., *Phase II Study of Cediranib, an Oral Pan–Vascular Endothelial Growth Factor Receptor Tyrosine Kinase Inhibitor, in Patients With Recurrent Glioblastoma.* Journal of Clinical Oncology, 2010. **28**(17): p. 2817-2823.

76. Nabors, L.B., et al., *Phase I trial of sorafenib in patients with recurrent or progressive malignant glioma.* Neuro-Oncology, 2011. **13**(12): p. 1324-1330.

77. Gilbert, M., et al., *Cilengitide in patients with recurrent glioblastoma: the results of NABTC 03-02, a phase II trial with measures of treatment delivery.* Journal of Neuro-Oncology, 2012. **106**(1): p. 147-153.

78. Iwamoto, F.M., et al., *Phase II trial of pazopanib (GW786034), an oral multi-targeted angiogenesis inhibitor, for adults with recurrent glioblastoma (North American Brain Tumor Consortium Study 06-02).* Neuro-Oncology, 2010. **12**(8): p. 855-861.

79. Chaskis, C., et al., *Phase II trial of sunitinib malate in patients with temozolomide refractory recurrent high-grade glioma.* Surgical neurology, 2009. **72**(5): p. 518.

80. Reardon, D.A., et al., *Randomized Phase II Study of Cilengitide, an Integrin-Targeting Arginine-Glycine-Aspartic Acid Peptide, in Recurrent Glioblastoma Multiforme.* Journal of Clinical Oncology, 2008. **26**(34): p. 5610-5617.

81. Groothuis, D.R., *The blood-brain and blood-tumor barriers: A review of strategies for increasing drug delivery.* Neuro-Oncology, 2000. **2**(1): p. 45-59.

82. Gutman, R.L., G. Peacock, and D.R. Lu, *Targeted drug delivery for brain cancer treatment.* Journal of Controlled Release, 2000. **65**(1-2): p. 31-41.

83. Lee, S.-W., et al., *Blood-brain barrier interfaces and brain tumors.* Archives of Pharmacal Research, 2006. **29**(4): p. 265-275.

84. Kratzer, I., et al., *Apolipoprotein A-I coating of protamine–oligonucleotide nanoparticles increases particle uptake and transcytosis in an in vitro model of the blood–brain barrier.* Journal of Controlled Release, 2007. **117**(3): p. 301-311.

85. Pardridge, W.M., *Blood–brain barrier delivery of protein and non-viral gene therapeutics with molecular Trojan horses.* Journal of Controlled Release, 2007. **122**(3): p. 345-348.

86. Zhang, Z., et al., *Synergistic effect of low-frequency ultrasound and low-dose bradykinin on increasing permeability of the blood–tumor barrier by opening tight junction.* Journal of Neuroscience Research, 2009. **87**(10): p. 2282-2289.

87. Yin, D., et al., *Increase in Brain Tumor Permeability in Glioma-Bearing Rats with Nitric Oxide Donors.* Clin Cancer Res, 2008. **14**(12): p. 4002-4009.

88. Schneider, S., et al., *Glioblastoma cells release factors that disrupt blood-brain barrier features.* Acta Neuropathologica, 2004. **107**(3): p. 272-276.

89. Wolburg, H., et al., *The disturbed blood–brain barrier in human glioblastoma.* Molecular Aspects of Medicine, (0).

90. Walter, K.A., et al., *Intratumoral Chemotherapy.* Neurosurgery, 1995. **37**(6): p. 1129-1145.

91. Buonerba, C., et al., *A comprehensive outlook on intracerebral therapy of malignant gliomas.* Critical Reviews in Oncology/Hematology, 2011. **80**(1): p. 54-68.

92. McGirt, M.J., et al., *Gliadel (BCNU) wafer plus concomitant temozolomide therapy after primary resection of glioblastoma multiforme.* Journal of Neurosurgery, 2009. **110**(3): p. 583-588.

93. Recinos, V.R., et al., *Combination of Intracranial Temozolomide With Intracranial Carmustine Improves Survival When Compared With Either Treatment Alone in a Rodent Glioma Model.* Neurosurgery, 2010. **66**(3): p. 530-537 10.1227/01.NEU.0000365263.14725.39.

94. Patchell, R.A., et al., *A Phase I Trial of Continuously Infused Intratumoral Bleomycin for the Treatment of Recurrent Glioblastoma Multiforme.* Journal of Neuro-Oncology, 2002. **60**(1): p. 37-42.

95. Voulgaris, S., et al., *Intratumoral Doxorubicin in Patients With Malignant Brain Gliomas.* American Journal of Clinical Oncology, 2002. **25**(1): p. 60-64.

96. Held, N., et al., *A safety and toxicity assessment of the administration of multiple intracerebral injections of irinotecan or doxorubicin drug-eluting beads.* Clinical and Translational Oncology, 2011. **13**(10): p. 742-746.

97. Barth, R.F., et al., *Comparison of intracerebral delivery of carboplatin and photon irradiation with an optimized regimen for boron neutron capture therapy of the F98 rat glioma.* Applied Radiation and Isotopes, 2011. **69**(12): p. 1813-1816.

98. Yang, W., et al., *Convection enhanced delivery of carboplatin in combination with radiotherapy for the treatment of brain tumors.* Journal of Neuro-Oncology, 2011. **101**(3): p. 379-390.

99. Sheleg, S.V., et al., *Local Chemotherapy with Cisplatin-depot for Glioblastoma Multiforme.* Journal of Neuro-Oncology, 2002. **60**(1): p. 53-59.

100. Han, L., et al., *Peptide-Conjugated PAMAM for Targeted Doxorubicin Delivery to Transferrin Receptor Overexpressed Tumors.* Molecular Pharmaceutics, 2010. **7**(6): p. 2156-2165.

101. Iyer, A.K., et al., *Exploiting the enhanced permeability and retention effect for tumor targeting.* Drug Discovery Today, 2006. **11**(17–18): p. 812-818.

102. Orringer, D.A., et al., *Small Solutions for Big Problems: The Application of Nanoparticles to Brain Tumor Diagnosis and Therapy.* Clin Pharmacol Ther, 2009. **85**(5): p. 531-534.

103. Maeda, H., *The enhanced permeability and retention (EPR) effect in tumor vasculature: the key role of tumor-selective macromolecular drug targeting.* Advances in Enzyme Regulation, 2001. **41**(1): p. 189-207.

104. Lammers, T., W.E. Hennink, and G. Storm, *Tumour-targeted nanomedicines: principles and practice.* Br J Cancer, 2008. **99**(3): p. 392-397.

105. Brigger, I., C. Dubernet, and P. Couvreur, *Nanoparticles in cancer therapy and diagnosis.* Advanced Drug Delivery Reviews, 2002. **54**(5): p. 631-651.

106. Brioschi, A., et al., *Solid lipid nanoparticles: could they help to improve the efficacy of pharmacologic treatments for brain tumors?* Neurological Research, 2007. **29**(3): p. 324-330.

107. Blasi, P., et al., *Solid Lipid Nanoparticles to Improve Brain Drug Delivery*, in *Nanotechnologies for the Life Sciences*. 2007, Wiley-VCH Verlag GmbH & Co. KGaA.

108. Kuo, Y.-C. and C.-T. Liang, *Catanionic solid lipid nanoparticles carrying doxorubicin for inhibiting the growth of U87MG cells.* Colloids and Surfaces B: Biointerfaces, 2011. **85**(2): p. 131-137.

109. Jin, J., et al., *In Vivo Specific Delivery of c-Met siRNA to Glioblastoma Using Cationic Solid Lipid Nanoparticles.* Bioconjugate Chemistry, 2011. **22**(12): p. 2568-2572.

110. Zhang, F., et al., *Noninvasive monitoring of orthotopic glioblastoma therapy response using RGD-conjugated iron oxide nanoparticles.* Biomaterials, 2012. **33**(21): p. 5414-5422.

111. Hadjipanayis, C.G., et al., *EGFRvIII Antibody–Conjugated Iron Oxide Nanoparticles for Magnetic Resonance Imaging–Guided Convection-Enhanced Delivery and Targeted Therapy of Glioblastoma.* Cancer Research, 2010. **70**(15): p. 6303-6312.

112. van Landeghem, F.K.H., et al., *Post-mortem studies in glioblastoma patients treated with thermotherapy using magnetic nanoparticles.* Biomaterials, 2009. **30**(1): p. 52-57.

113. Veiseh, O., et al., *Chlorotoxin bound magnetic nanovector tailored for cancer cell targeting, imaging, and siRNA delivery.* Biomaterials, 2010. **31**(31): p. 8032-8042.

114. Xu, Z., et al., *In vitro and in vivo evaluation of actively targetable nanoparticles for paclitaxel delivery.* International Journal of Pharmaceutics, 2005. **288**(2): p. 361-368.

115. Sun, C., et al., *In Vivo MRI Detection of Gliomas by Chlorotoxin-Conjugated Superparamagnetic Nanoprobes.* Small, 2008. **4**(3): p. 372-379.

116. Sandoval, M.A., et al., *EGFR-targeted stearoyl gemcitabine nanoparticles show enhanced anti-tumor activity.* Journal of Controlled Release, 2012. **157**(2): p. 287-296.

117. Yang, F.-Y., et al., *Focused ultrasound and interleukin-4 receptor-targeted liposomal doxorubicin for enhanced targeted drug delivery and antitumor effect in glioblastoma multiforme.* Journal of Controlled Release, 2012. **160**(3): p. 652-658.

118. Ren, J., et al., *The targeted delivery of anticancer drugs to brain glioma by PEGylated oxidized multi-walled carbon nanotubes modified with angiopep-2.* Biomaterials, 2012. **33**(11): p. 3324-3333.

119. Chari, R.V.J., *Targeted Cancer Therapy: Conferring Specificity to Cytotoxic Drugs.* Accounts of Chemical Research, 2007. **41**(1): p. 98-107.

120. Dean, M., T. Fojo, and S. Bates, *Tumour stem cells and drug resistance.* Nat Rev Cancer, 2005. **5**(4): p. 275-284.

121. Cho, J., et al., *Glioblastoma-Derived Epidermal Growth Factor Receptor Carboxyl-Terminal Deletion Mutants Are Transforming and Are Sensitive to EGFR-Directed Therapies.* Cancer Research, 2011. **71**(24): p. 7587-7596.

122. Raizer, J.J., et al., *A phase II trial of erlotinib in patients with recurrent malignant gliomas and nonprogressive glioblastoma multiforme postradiation therapy.* Neuro-Oncology, 2010. **12**(1): p. 95-103.

123. Nabors, L.B., et al., *A safety run-in and randomized phase 2 study of cilengitide combined with chemoradiation for newly diagnosed glioblastoma (NABTT 0306).* Cancer, 2012: p. n/a-n/a.

124. Shinoda, J. and I.R. Whittle, *Nitric oxide and glioma: a target for novel therapy?* British Journal Of Neurosurgery, 2001. **15**(3): p. 213-220.

125. Miller, M.R. and I.L. Megson, *Recent developments in nitric oxide donor drugs.* British Journal of Pharmacology, 2007. **151**(3): p. 305-321.

126. Fukumura, D., S. Kashiwagi, and R.K. Jain, *The role of nitric oxide in tumour progression.* Nature Reviews. Cancer, 2006. **6**(7): p. 521-534.

127. Matsumoto, A., et al., *Screening for nitric oxide-dependent protein-protein interactions.* Science, 2003. **301**(5633): p. 657-661.

128. Mocellin, S., *Nitric oxide: cancer target or anticancer agent?* Current Cancer Drug Targets, 2009. **9**(2): p. 214-236.

129. Cordes, C.M., et al., *Nitric oxide inhibits insulin-degrading enzyme activity and function through S-nitrosylation.* Biochemical Pharmacology, 2009. **77**(6): p. 1064-1073.

130. Janero, D.R., *Nitric oxide (NO)-related pharmaceuticals: contemporary approaches to therapeutic no modulation.* Free Radical Biology and Medicine, 2000. **28**(10): p. 1495-1506.

131. Graziewicz, M., D.A. Wink, and F. Laval, *Nitric oxide inhibits DNA ligase activity: potential mechanisms for NO-mediated DNA damage.* Carcinogenesis, 1996. **17**(11): p. 2501-2505.

132. Eiserich, J.P., R.P. Patel, and V.B. O'Donnell, *Pathophysiology of nitric oxide and related species: free radical reactions and modification of biomolecules.* Molecular Aspects of Medicine, 1998. **19**(4-5): p. 221-357.

133. Denninger, J.W. and M.A. Marletta, *Guanylate cyclase and the [dot operator]NO/cGMP signaling pathway.* Biochimica et Biophysica Acta (BBA) - Bioenergetics, 1999. **1411**(2-3): p. 334-350.

134. Alderton, W.K., C.E. Cooper, and R.G. Knowles, *Nitric oxide synthases: structure, function and inhibition.* Biochemical Journal, 2001. **357**: p. 593-615.

135. Wink, D.A., et al., *The multifaceted roles of nitric oxide in cancer.* Carcinogenesis, 1998. **19**(5): p. 711-721.

136. Nathan, C.X., Q.-W. , *Nitric Oxide Synthases: Roles, Tolls, and Controls.* Cellular And Molecular Life Sciences: CMLS, 1994. **78**(6): p. 4.

137. Michel, T. and O. Feron, *Nitric oxide synthases: Which, where, how, and why?* Journal of Clinical Investigation, 1997. **100**(9): p. 2146-2152.

138. Kleinert, H., P.M. Schwarz, and U. Forstermann, *Regulation of the expression of inducible nitric oxide synthase.* Biological Chemistry, 2003. **384**(10-11): p. 1343-1364.

139. Bonavida, B., et al., *Novel therapeutic applications of nitric oxide donors in cancer: Roles in chemo- and immunosensitization to apoptosis and inhibition of metastases.* Nitric Oxide, 2008. **19**(2): p. 152-157.

140. Al-Sa'doni, H. and A. Ferro, *S-Nitrosothiols: a class of nitric oxide-donor drugs.* Clinical Science, 2000. **98**(5): p. 507-520.

141. Badn, W. and P. Siesjo, *The Dual Role of Nitric Oxide in Glioma.* Current Pharmaceutical Design, 2010. **16**(4): p. 428-430.

142. Blackburn, R.V., et al., *Differential induction of cell death in human glioma cell lines by sodium nitroprusside.* Cancer, 1998. **82**(6): p. 1137-1145.

143. Kurimoto, M., et al., *Growth Inhibition and Radiosensitization of Cultured Glioma Cells by Nitric Oxide Generating Agents.* Journal of Neuro-Oncology, 1999. **42**(1): p. 35-44.

144. Viani, P., et al., *Ceramide in Nitric Oxide Inhibition of Glioma Cell Growth.* Journal of Biological Chemistry, 2003. **278**(11): p. 9592-9601.

145. Weyerbrock, A., et al., *JS-K, a Glutathione S-Transferase–Activated Nitric Oxide Donor With Antineoplastic Activity in Malignant Gliomas.* Neurosurgery, 2012. **70**(2): p. 497-510

146. Kogias, E., et al., *Growth-inhibitory and chemosensitizing effects of the glutathione-S-transferase-π-activated nitric oxide donor PABA/NO in malignant gliomas.* International Journal of Cancer, 2012. **130**(5): p. 1184-1194.

147. Kim, K.M., et al., *Regulation of apoptosis by nitrosative stress.* Journal of biochemistry and molecular biology, 2002. **35**(1): p. 127-33.

148. Lala, P.K. and C. Chakraborty, *Role of nitric oxide in carcinogenesis and tumour progression.* The Lancet Oncology, 2001. **2**(3): p. 149-156.

149. Cobbs, C.S., et al., *Expression of Nitric Oxide Synthase in Human Central Nervous System Tumors.* Cancer Res, 1995. **55**(4): p. 727-730.

150. Ellie, E., et al., *Differential expression of inducible nitric oxide synthase mRNA in human brain tumours.* NeuroReport, 1995. **7**(1): p. 294-296.

151. Jadeski, L.C., C. Chakraborty, and P.K. Lala, *Role of nitric oxide in tumour progression with special reference to a murine breast cancer model.* Canadian Journal of Physiology and Pharmacology, 2002. **80**(2): p. 125-135.

152. Eyler, Christine E., et al., *Glioma Stem Cell Proliferation and Tumor Growth Are Promoted by Nitric Oxide Synthase-2.* Cell, 2011. **146**(1): p. 53-66.

153. Pullen, N. and H. Fillmore, *Induction of matrix metalloproteinase-1 and glioma cell motility by nitric oxide.* Journal of Neuro-Oncology, 2010. **96**(2): p. 201-209.

154. Lin, Y.-M., et al., *Dexamethasone reduced invasiveness of human malignant glioblastoma cells through a MAPK phosphatase-1 (MKP-1) dependent mechanism.* European Journal of Pharmacology, 2008. **593**(1–3): p. 1-9.

155. McCarthy, S.M., et al., *Nitric oxide regulation of MMP-9 activation and its relationship to modifications of the cysteine switch.* Biochemistry, 2008. **47**(21): p. 5832-5840.

156. Jadeski, L.C., et al., *Nitric oxide promotes murine mammary tumour growth and metastasis by stimulating tumour cell migration, invasiveness and angiogenesis.* International Journal of Cancer, 2000. **86**(1): p. 30-39.

157. Wang, F., et al., *Inhibitory effects of nitric oxide on invasion of human cancer cells.* Cancer Letters, 2007. **257**(2): p. 274-282.

158. Kim, J.-H., et al., *Pro-apoptotic role of integrin β3 in glioma cells.* Journal of Neurochemistry, 2011. **117**(3): p. 494-503.

159. Findlay, V.J., et al., *Tumor Cell Responses to a Novel Glutathione S-Transferase–Activated Nitric Oxide-Releasing Prodrug.* Molecular Pharmacology, 2004. **65**(5): p. 1070-1079.

160. Zak, P., K. Kleibl, and F. Laval, *Repair of O6-methylguanine and O4-methylthymine by the human and rat O6- methylguanine-DNA methyltransferases.* J. Biol. Chem., 1994. **269**(1): p. 730-733.

161. Yang, D.I., et al., *Nitric oxide and BCNU chemoresistance in C6 glioma cells: Role of S-nitrosoglutathione.* Free Radical Biology and Medicine, 2004. **36**(10): p. 1317-1328.

162. Hiroshi Maeda, et al., *Enhanced Vascular Permeability in Solid Tumor Is Mediated by Nitric Oxide and Inhibited by Both New Nitric Oxide Scavenger and Nitric Oxide Synthase Inhibitor.* Cancer Science, 1994. **85**(4): p. 331-334.

163. Iadecola, C., F. Zhang, and X. Xu, *SIN-1 reverses attenuation of hypercapnic cerebrovasodilation by nitric oxide synthase inhibitors.* Am J Physiol Regul Integr Comp Physiol, 1994. **267**(1): p. R228-235.

164. Yamaguchi, S., et al., *Glioma tumourgenicity is decreased by iNOS knockout: experimental studies using the C6 striatal implantation glioma model.* British Journal Of Neurosurgery, 2002. **16**(6): p. 567-572.

165. Morbidelli, L., S. Donnini, and M. Ziche, *Role of Nitric Oxide in Tumor Angiogenesis in Brain Tumors*, M. Kirsch and P.M. Black, Editors. 2004, Springer US. p. 155-167.

166. Lejeune, P., et al., *Nitric oxide involvement in tumor-induced immunosuppression.* J Immunol, 1994. **152**(10): p. 5077-5083.

167. Badn, W., et al., *Inhibition of Inducible Nitric Oxide Synthase Enhances Anti-tumour Immune Responses in Rats Immunized with IFN-γ-Secreting Glioma Cells.* Scandinavian Journal of Immunology, 2007. **65**(3): p. 289-297.

168. Carpenter, A.W. and M.H. Schoenfisch, *Nitric oxide release: Part II. Therapeutic applications.* Chemical Society Reviews, 2012. **41**(10): p. 3742-3752.

169. Saraiva, J., et al., *Nanocarriers for nitric oxide delivery.* Journal of Drug Delivery, 2011. **2011**: p. 936438.

170. Katsumi, H., M. Nishikawa, and M. Hashida, *Development of Nitric Oxide Donors for the Treatment of Cardiovascular Diseases*, in *Cardiovascular & Hematological Agents in Medicinal Chemistry*. 2007, Bentham Science Publishers Ltd. p. 204-208.

171. Taylor, D.K., et al., *Toward the Generation of NO in Biological Systems Theoretical Studies of the N2O2 Grouping.* The Journal of Organic Chemistry, 1995. **60**(2): p. 435-444.

172. Davies, K.M., et al., *Chemistry of the Diazeniumdiolates. 2. Kinetics and Mechanism of Dissociation to Nitric Oxide in Aqueous Solution.* Journal of the American Chemical Society, 2001. **123**(23): p. 5473-5481.

173. Taite, L. and J. West, *Sustained Delivery of Nitric Oxide from Poly(ethylene glycol) Hydrogels Enhances Endothelialization in a Rat Carotid Balloon Injury Model.* Cardiovascular Engineering and Technology, 2011. **2**(2): p. 113-123.

174. Miranda, K.M., et al., *Comparison of the NO and HNO Donating Properties of Diazeniumdiolates: Primary Amine Adducts Release HNO in Vivo.* Journal of Medicinal Chemistry, 2005. **48**(26): p. 8220-8228.

175. Maksimovic-Ivanic, D., et al., *Anticancer properties of the novel nitric oxide-donating compound (S,R)-3-phenyl-4,5-dihydro-5-isoxazole acetic acid-nitric oxide in vitro and in vivo.* Molecular Cancer Therapeutics, 2008. **7**(3): p. 510-520.

176. Chen, C., et al., *A Glycosylated Nitric Oxide Donor, β-Gal-NONOate, and its Site-specific Antitumor Activity.* Archiv der Pharmazie, 2006. **339**(7): p. 366-371.

177. DeBin, J.A., J.E. Maggio, and G.R. Strichartz, *Purification and characterization of chlorotoxin, a chloride channel ligand from the venom of the scorpion.* Am J Physiol Cell Physiol, 1993. **264**(2): p. C361-369.

178. Lippens, G., et al., *NMR Sequential Assignments and Solution Structure of Chlorotoxin, a Small Scorpion Toxin That Blocks Chloride Channels.* Biochemistry, 1995. **34**(1): p. 13-21.

179. Soroceanu, L., et al., *Use of Chlorotoxin for Targeting of Primary Brain Tumors.* Cancer Res, 1998. **58**(21): p. 4871-4879.

180. Deshane, J., C.C. Garner, and H. Sontheimer, *Chlorotoxin Inhibits Glioma Cell Invasion via Matrix Metalloproteinase-2.* Journal of Biological Chemistry, 2003. **278**(6): p. 4135-4144.

181. Lyons, S.A., J. O'Neal, and H. Sontheimer, *Chlorotoxin, a scorpion-derived peptide, specifically binds to gliomas and tumors of neuroectodermal origin.* Glia, 2002. **39**(2): p. 162-173.

182. Veiseh, M., et al., *Tumor Paint: A Chlorotoxin:Cy5.5 Bioconjugate for Intraoperative Visualization of Cancer Foci.* Cancer Research, 2007. **67**(14): p. 6882-6888.

183. Kesanakurti, D., et al., *Role of MMP-2 in the regulation of IL-6/Stat3 survival signaling via interaction with [alpha]5[beta]1 integrin in glioma.* Oncogene, 2012.

184. Puli, S., J. Lai, and A. Bhushan, *Inhibition of matrix degrading enzymes and invasion in human glioblastoma (U87MG) Cells by isoflavones.* Journal of Neuro-Oncology, 2006. **79**(2): p. 135-142.

185. Demuth, T. and M.E. Berens, *Molecular mechanisms of glioma cell migration and invasion.* Journal of Neuro-Oncology, 2004. **70**(2): p. 217-228.

186. Conroy, S., et al., *In Vivo MRI Detection of Gliomas by Chlorotoxin-Conjugated Superparamagnetic Nanoprobes.* Small, 2008. **4**(3): p. 372-379.

187. Akcan, M., et al., *Chemical Re-engineering of Chlorotoxin Improves Bioconjugation Properties for Tumor Imaging and Targeted Therapy.* Journal of Medicinal Chemistry, 2011. **54**(3): p. 782-787.

188. Kievit, F.M., et al., *Chlorotoxin Labeled Magnetic Nanovectors for Targeted Gene Delivery to Glioma.* Acs Nano, 2010. **4**(8): p. 4587-4594.

189. Mok, H., et al., *pH-Sensitive siRNA Nanovector for Targeted Gene Silencing and Cytotoxic Effect in Cancer Cells.* Molecular Pharmaceutics, 2010. **7**(6): p. 1930-1939.

190. Huang, R., et al., *Targeted delivery of chlorotoxin-modified DNA-loaded nanoparticles to glioma via intravenous administration.* Biomaterials, 2011. **32**(9): p. 2399-2406.

191. Wu, C., et al., *A peptide-based carrier for intracellular delivery of proteins into malignant glial cells in vitro.* Journal of Controlled Release, 2008. **130**(2): p. 140-145.

192. Weissig, V. and G.G. D'Souza, *Organelle-Specific Pharmaceutical Nanotechnology*. 2010, Hoboken, NJ, USA: Wiley.

193. Bohl, K.S. and J.L. West, *Nitric oxide-generating polymers reduce platelet adhesion and smooth muscle cell proliferation.* Biomaterials, 2000. **21**(22): p. 2273-2278.

194. Jun, H.-W., L.J. Taite, and J.L. West, *Nitric Oxide-Producing Polyurethanes.* Biomacromolecules, 2005. **6**(2): p. 838-844.

195. Taite, L.J., et al., *Nitric oxide-releasing polyurethane–PEG copolymer containing the YIGSR peptide promotes endothelialization with decreased platelet adhesion.* Journal of Biomedical Materials Research Part B: Applied Biomaterials, 2008. **84B**(1): p. 108-116.

196. Moore, S., *Amino Acid Analysis: Aqueous Dimethyl Sulfoxide As Solvent for the Ninhydrin Reaction.* Journal of Biological Chemistry, 1968. **243**(23): p. 6281-6283.

197. Chertok, B., A.E. David, and V.C. Yang, *Polyethyleneimine-modified iron oxide nanoparticles for brain tumor drug delivery using magnetic targeting and intra-carotid administration.* Biomaterials, 2010. **31**(24): p. 6317-6324.

198. Zhang, X., *Real time and in vivo monitoring of nitric oxide by electrochemical sensors-from dream to reality* Frontiers in Bioscience, 2004. **9**: p. 3434-3446.

199. Soloviev, A., et al., *Nitric oxide relaxes rat tail artery smooth muscle by cyclic GMP-independent decrease in calcium sensitivity of myofilaments.* Cell Calcium, 2004. **36**(2): p. 165-173.

200. Samy, A. and O. Igwe, *Regulation of IL-1β-Induced Cyclooxygenase-2 Expression by Interactions of Aβ Peptide, Apolipoprotein E and Nitric Oxide in Human Neuroglioma.* Journal of Molecular Neuroscience, 2012. **47**(3): p. 533-545.

201. Adami, A., et al., *Biotransformation and cytotoxic properties of NO-donors on MCF7 and U251 cell lines.* Life Sciences, 1998. **63**(23): p. 2097-2105.

202. Jin, H.-O., et al., *Up-regulation of Bak and Bim via JNK downstream pathway in the response to nitric oxide in human glioblastoma cells.* Journal of Cellular Physiology, 2006. **206**(2): p. 477-486.

203. Terwel, D., et al., *S-nitroso-N-acetylpenicillamine and nitroprusside induce apoptosis in a neuronal cell line by the production of different reactive molecules.* European Journal of Pharmacology, 2000. **400**(1): p. 19-33.

204. Ignarro, L.J., et al., *Mechanism of vascular smooth muscle relaxation by organic nitrates, nitrites, nitroprusside and nitric oxide: evidence for the involvement of S-nitrosothiols as active intermediates.* Journal of Pharmacology and Experimental Therapeutics, 1981. **218**(3): p. 739-749.

205. Papadopoulos, N.G., et al., *An improved fluorescence assay for the determination of lymphocyte-mediated cytotoxicity using flow cytometry.* Journal of Immunological Methods, 1994. **177**(1-2): p. 101-111.

206. Park, B.C., et al., *Chloroquine-induced nitric oxide increase and cell death is dependent on cellular GSH depletion in A172 human glioblastoma cells.* Toxicology Letters, 2008. **178**(1): p. 52-60.

207. Janjetovic, K., et al., *Synergistic antiglioma action of hyperthermia and nitric oxide.* European Journal of Pharmacology, 2008. **583**(1): p. 1-10.

208. Kawahara, K., et al., *Increased resistance to nitric oxide cytotoxicity associated with differentiation of neuroblastoma-glioma hybrid (NG108-15) cells.* Free Radical Research, 2002. **36**(5): p. 545-554.

209. Zhang, N. and A.F. Palmer, *Liposomes surface conjugated with human hemoglobin target delivery to macrophages.* Biotechnology and Bioengineering, 2012. **109**(3): p. 823-829.

210. Veiseh, O., et al., *Inhibition of Tumor-Cell Invasion with Chlorotoxin-Bound Superparamagnetic Nanoparticles.* Small, 2009. **5**(2): p. 256-264.

211. Krex, D., et al., *Long-term survival with glioblastoma multiforme.* Brain, 2007. **130**: p. 2596-2606.

212. Hussain, S.F., et al., *A Novel Small Molecule Inhibitor of Signal Transducers and Activators of Transcription 3 Reverses Immune Tolerance in Malignant Glioma Patients.* Cancer Research, 2007. **67**(20): p. 9630-9636.

213. Miglierini, P., et al., *Impact of the per-operatory application of GLIADEL wafers (BCNU, carmustine) in combination with temozolomide and radiotherapy in patients with glioblastoma multiforme: Efficacy and toxicity.* Clinical Neurology and Neurosurgery, (In press).

214. Johnson, D. and B. O'Neill, *Glioblastoma survival in the United States before and during the temozolomide era.* Journal of Neuro-Oncology, 2012. **107**(2): p. 359-364.

215. Darefsky, A.S., J.T. King, and R. Dubrow, *Adult glioblastoma multiforme survival in the temozolomide era: A population-based analysis of Surveillance, Epidemiology, and End Results registries.* Cancer, 2012. **118**(8): p. 2163-2172.

216. Hegi, M.E., et al., *Correlation of O6-Methylguanine Methyltransferase (MGMT) Promoter Methylation With Clinical Outcomes in Glioblastoma and Clinical Strategies to Modulate MGMT Activity.* Journal of Clinical Oncology, 2008. **26**(25): p. 4189-4199.

217. Hansen, R.J., et al., *Role of O6-Alkylguanine-DNA Alkyltransferase in Protecting against 1,3-Bis(2-chloroethyl)-1-nitrosourea (BCNU)-Induced Long-Term Toxicities.* Journal of Pharmacology and Experimental Therapeutics, 2005. **315**(3): p. 1247-1255.

218. Yuan, L., et al., *Tissue transglutaminase 2 inhibition promotes cell death and chemosensitivity in glioblastomas.* Molecular Cancer Therapeutics, 2005. **4**(9): p. 1293-1302.

219. Minniti, G., et al., *Correlation between O6-methylguanine-DNA methyltransferase and survival in elderly patients with glioblastoma treated with radiotherapy plus concomitant and adjuvant temozolomide.* Journal of Neuro-Oncology, 2011. **102**(2): p. 311-316.

220. Baer, J.C., et al., *Depletion of O6-Alkylguanine-DNA alkyl transferase correlates with potentiation of temozolomide and CCNU toxicity in human tumor-cells.* British Journal of Cancer, 1993. **67**(6): p. 1299-1302.

221. Denny, B.J., et al., *NMR and Molecular Modeling Investigation of the Mechanism of Activation of the Antitumor Drug Temozolomide and Its Interaction with DNA.* Biochemistry, 1994. **33**(31): p. 9045-9051.

222. Kokkinakis, D.M., et al., *Sensitization of Pancreatic Tumor Xenografts to Carmustine and Temozolomide by Inactivation of Their O6-Methylguanine-DNA Methyltransferase with O6-Benzylguanine or O6-Benzyl-2'-Deoxyguanosine.* Clinical Cancer Research, 2003. **9**(10): p. 3801-3807.

223. Liu, Y. and M. Kulesz-Martin, *p53 protein at the hub of cellular DNA damage response pathways through sequence-specific and non-sequence-specific DNA binding.* Carcinogenesis, 2001. **22**(6): p. 851-860.

224. Yount, G.L., et al., *Cell Cycle Synchrony Unmasks the Influence of p53 Function on Radiosensitivity of Human Glioblastoma Cells.* Cancer Research, 1996. **56**(3): p. 500-506.

225. Badie, B., et al., *Combined radiation and p53 gene therapy of malignant glioma cells.* Cancer gene therapy, 1999. **6**(2): p. 155-62.

226. Iwadati, Y., et al., *Association of p53 gene mutation with decreased chemosensitivity in human malignant gliomas.* International Journal of Cancer, 1996. **69**(3): p. 236-240.

227. Lu, D.-Y., et al., *Glial cell line-derived neurotrophic factor induces cell migration and matrix metalloproteinase-13 expression in glioma cells.* Biochemical Pharmacology, 2010. **80**(8): p. 1201-1209.

228. Tsuji, T., et al., *Regulation of melanoma cell migration and invasion by laminin-5 and α3β1 integrin (VLA-3).* Clinical and Experimental Metastasis, 2002. **19**(2): p. 127-134.

229. Esteller, M., et al., *Inactivation of the DNA-Repair Gene MGMT and the Clinical Response of Gliomas to Alkylating Agents.* New England Journal of Medicine, 2000. **343**(19): p. 1350-1354.

230. Hermisson, M., et al., *O-6-methylguanine DNA methyltransferase and p53 status predict temozolomide sensitivity in human malignant glioma cells.* Journal of Neurochemistry, 2006. **96**(3): p. 766-776.

231. Policastro, L., et al., *Selective radiosensitization by nitric oxide in tumor cell lines.* Cancer Letters, 2007. **248**(1): p. 123-130.

232. Roos, W.P., et al., *Apoptosis in malignant glioma cells triggered by the temozolomide-induced DNA lesion O-6-methylguanine.* Oncogene, 2007. **26**(2): p. 186-197.

233. Stupp, R., et al., *Effects of radiotherapy with concomitant and adjuvant temozolomide versus radiotherapy alone on survival in glioblastoma in a randomised phase III study: 5-year analysis of the EORTC-NCIC trial.* The Lancet Oncology, 2009. **10**(5): p. 459-466.

234. Dunn, J., et al., *Extent of MGMT promoter methylation correlates with outcome in glioblastomas given temozolomide and radiotherapy.* Br J Cancer, 2009. **101**(1): p. 124-131.

235. Nutt, C.L., et al., *O6-Methylguanine-DNA methyltransferase activity, p53 gene status and BCNU resistance in mouse astrocytes.* Carcinogenesis, 1999. **20**(12): p. 2361-2365.

236. Zhang, M.X., et al., *Trimodal Glioblastoma Treatment Consisting of Concurrent Radiotherapy, Temozolomide, and the Novel TGF-beta Receptor I Kinase Inhibitor LY2109761.* Neoplasia, 2011. **13**(6): p. 537-U61.

237. Remington, M., et al., *The L84F polymorphic variant of human O6-methylguanine-DNA methyltransferase alters stability in U87MG glioma cells but not temozolomide sensitivity.* Neuro-Oncology, 2009. **11**(1): p. 22-32.

238. Chahal, M., et al., *MGMT modulates glioblastoma angiogenesis and response to the tyrosine kinase inhibitor sunitinib.* Neuro-Oncology, 2010. **12**(8): p. 822-833.

239. Liu, L., et al., *Inactivation and Degradation of O6-Alkylguanine-DNA Alkyltransferase after Reaction with Nitric Oxide.* Cancer Research, 2002. **62**(11): p. 3037-3043.

240. Korkolopoulou P., et al., *MDM2 and p53 expression in gliomas: a multivariate survival analysis including proliferation markers and epidermal growth factor receptor.* Br J Cancer, 1997. **75**(9): p. 1269-78.

241. Srivenugopal, K.S., et al., *Enforced Expression of Wild-Type p53 Curtails the Transcription of the O6-Methylguanine-DNA Methyltransferase Gene in Human Tumor Cells and Enhances Their Sensitivity to Alkylating Agents.* Clinical Cancer Research, 2001. **7**(5): p. 1398-1409.

242. Gomez-Manzano, C., et al., *Adenovirus-mediated Transfer of the p53 Gene Produces Rapid and Generalized Death of Human Glioma Cells via Apoptosis.* Cancer Research, 1996. **56**(4): p. 694-699.

243. Van Meir, E.G., et al., *Analysis of the p53 Gene and Its Expression in Human Glioblastoma Cells.* Cancer Research, 1994. **54**(3): p. 649-652.

244. Wang, C.-C., et al., *HDJ-2 as a Target for Radiosensitization of Glioblastoma Multiforme Cells by the Farnesyltransferase Inhibitor R115777 and the Role of the p53/p21 Pathway.* Cancer Research, 2006. **66**(13): p. 6756-6762.

245. Wang, P.G., et al., *Nitric Oxide Donors: Chemical Activities and Biological Applications.* Chemical Reviews, 2002. **102**(4): p. 1091-1134.

246. Calmels, S., P. Hainaut, and H. Ohshima, *Nitric Oxide Induces Conformational and Functional Modifications of Wild-Type p53 Tumor Suppressor Protein.* Cancer Research, 1997. **57**(16): p. 3365-3369.

247. Yamamoto, M., et al., *The role of proteolysis in tumor invasiveness in glioblastoma and metastatic brain tumors.* Anticancer Research, 2002. **22**(6C): p. 4265-4268.

248. Miller, C.R. and A. Perry, *Glioblastoma.* Archives of Pathology & Laboratory Medicine, 2007. **131**(3): p. 397-406.

249. Giese, A., et al., *Cost of Migration: Invasion of Malignant Gliomas and Implications for Treatment.* Journal of Clinical Oncology, 2003. **21**(8): p. 1624-1636.

250. Tamaki, M., et al., *Implantation of C6 astrocytoma spheroid into collagen type I gels: invasive, proliferative, and enzymatic characterizations.* Journal of Neurosurgery, 1997. **87**(4): p. 602-609.

251. Tonn, J.C., et al., *Invasive behaviour of human gliomas is mediated by interindividually different integrin patterns.* Anticancer Research, 1998. **18**(4A): p. 2599-2605.

252. Talvensaari-Mattila, A., et al., *Matrix metalloproteinase-2 immunoreactive protein.* Cancer, 1998. **83**(6): p. 1153-1162.

253. Sontheimer, H., *An unexpected role for ion channels in brain tumor metastasis.* Experimental Biology and Medicine, 2008. **233**(7): p. 779-791.

254. Soroceanu, L., T.J. Manning, and H. Sontheimer, *Modulation of glioma cell migration and invasion using Cl- and K+ ion channel blockers.* Journal of Neuroscience, 1999. **19**(14): p. 5942-5954.

255. ROOMI, et al., *Patterns of MMP-2 and MMP-9 expression in human cancer cell lines*. Vol. 21. 2009, Athens, GRECE: Spandidos. 11.

256. Raithatha, S.A., et al., *Localization of gelatinase-A and gelatinase-B mRNA and protein in human gliomas.* Neuro-Oncology, 2000. **2**(3): p. 145-150.

257. Forsyth, P.A., et al., *Gelatinase-A (MMP-2), gelatinase-B (MMP-9) and membrane type matrix metalloproteinase-1 (MT1-MMP) are involved in different aspects of the pathophysiology of malignant gliomas*, Nature Publishing Group.

258. Kachra, Z., et al., *Expression of matrix metalloproteinases and their inhibitors in human brain tumors.* Clinical and Experimental Metastasis, 1999. **17**(7): p. 555-566.

259. Lakka, S.S., et al., *Inhibition of cathepsin B and MMP-9 gene expression in glioblastoma cell line via RNA interference reduces tumor cell invasion, tumor growth and angiogenesis.* Oncogene, 2004. **23**(27): p. 4681-4689.

260. Kondraganti, S., et al., *Selective Suppression of Matrix Metalloproteinase-9 in Human Glioblastoma Cells by Antisense Gene Transfer Impairs Glioblastoma Cell Invasion.* Cancer Research, 2000. **60**(24): p. 6851-6855.

261. Ezhilarasan, R., et al., *The hemopexin domain of MMP-9 inhibits angiogenesis and retards the growth of intracranial glioblastoma xenograft in nude mice.* International Journal of Cancer, 2009. **124**(2): p. 306-315.

262. Nilsson, U., S. Garvin, and C. Dabrosin, *MMP-2 and MMP-9 activity is regulated by estradiol and tamoxifen in cultured human breast cancer cells.* Breast Cancer Research and Treatment, 2007. **102**(3): p. 253-261.

263. Sameni, M., J. Dosescu, and B.F. Sloane, *Imaging proteolysis by living human glioma cells.* Biological Chemistry, 2001. **382**(5): p. 785-788.

264. Premzl, A., V. Turk, and J. Kos, *Intracellular proteolytic activity of cathepsin B is associated with capillary-like tube formation by endothelial cells in vitro.* Journal of Cellular Biochemistry, 2006. **97**(6): p. 1230-1240.

265. Fu, Y., et al., *Chlorotoxin-conjugated nanoparticles as potential glioma-targeted drugs.* Journal of Neuro-Oncology, 2012. **107**(3): p. 457-462.

266. Simeone, A.-M., et al., *TIMP-2 mediates the anti-invasive effects of the nitric oxide-releasing prodrug JS-K in breast cancer cells.* Breast Cancer Research, 2008. **10**(3): p. 1-10.

267. Jespersen, C., et al., *Molecular mechanisms of nitric oxide-dependent inhibition of TPA-induced matrix metalloproteinase-9 (MMP-9) in MCF-7 cells.* Journal of Cellular Physiology, 2009. **219**(2): p. 276-287.

268. Sugita, H., et al., *Nitric Oxide Inhibits the Proliferation and Invasion of Pancreatic Cancer Cells through Degradation of Insulin Receptor Substrate-1 Protein.* Molecular Cancer Research, 2010. **8**(8): p. 1152-1163.

269. Bonavida, B., et al., *Nitric Oxide Donors Are a New Class of Anti-cancer Therapeutics for the Reversal of Resistance and Inhibition of Metastasis*

Nitric Oxide (NO) and Cancer, B. Bonavida, Editor. 2010, Springer New York. p. 459-477.

270. Brooks, P.C., et al., *Localization of matrix metalloproteinase MMP-2 to the surface of invasive cells by interaction with integrin alpha v beta 3.* Cell, 1996. **85**(5): p. 683-693.

271. Emonard, H.P., et al., *Tumor cell surface-associated binding site for the M(R)72,000 type-IV collagenase.* Cancer Research, 1992. **52**(20): p. 5845-5848.

272. Yu, Q. and I. Stamenkovic, *Cell surface-localized matrix metalloproteinase-9 proteolytically activates TGF-beta and promotes tumor invasion and angiogenesis.* Genes & Development, 2000. **14**(2): p. 163-176.

273. Chen, H.-H. and D.L. Wang, *Nitric Oxide Inhibits Matrix Metalloproteinase-2 Expression via the Induction of Activating Transcription Factor 3 in Endothelial Cells.* Molecular Pharmacology, 2004. **65**(5): p. 1130-1140.

274. Phillips, P.G. and L.M. Birnby, *Nitric oxide modulates caveolin-1 and matrix metalloproteinase-9 expression and distribution at the endothelial cell/tumor cell interface.* American Journal of Physiology - Lung Cellular and Molecular Physiology, 2004. **286**(5): p. L1055-L1065.

275. Stamler, J.S., S. Lamas, and F.C. Fang, *Nitrosylation: The Prototypic Redox-Based Signaling Mechanism.* Cell, 2001. **106**(6): p. 675-683.

276. Ascenzi, P., et al., *Inhibition of Cysteine Protease Activity by NO-donors.* Current Protein and Peptide Science, 2001. **2**(2): p. 137-153.

277. Gu, Z., et al., *S-Nitrosylation of Matrix Metalloproteinases: Signaling Pathway to Neuronal Cell Death.* Science, 2002. **297**(5584): p. 1186-1190.

278. Gooch, K.J., C.A. Dangler, and J.A. Frangos, *Exogenous, basal, and flow-induced nitric oxide production and endothelial cell proliferation.* Journal of Cellular Physiology, 1997. **171**(3): p. 252-258.

279. Postovit, L.-M., et al., *Oxygen-mediated Regulation of Tumor Cell Invasiveness.* Journal of Biological Chemistry, 2002. **277**(38): p. 35730-35737.

280. Gaillard, P.J., et al., *Establishment and functional characterization of an in vitro model of the blood–brain barrier, comprising a co-culture of brain capillary endothelial cells and astrocytes.* European Journal of Pharmaceutical Sciences, 2001. **12**(3): p. 215-222.

281. Garberg, P., et al., *In vitro models for the blood-brain barrier.* Toxicology in Vitro, 2005. **19**(3): p. 299-334.

282. Hatherell, K., et al., *Development of a three-dimensional, all-human in vitro model of the blood-brain barrier using mono-, co-, and tri-cultivation Transwell models.* Journal of Neuroscience Methods, 2011. **199**(2): p. 223-229.

283. Lau, Y.-T. and W.-C. Ma, *Nitric Oxide Inhibits Migration of Cultured Endothelial Cells.* Biochemical and Biophysical Research Communications, 1996. **221**(3): p. 670-674.

284. Yang, W.D., et al., *Exogenous Nitric Oxide Inhibits Proliferation of Cultured Vascular Endothelial Cells.* Biochemical and Biophysical Research Communications, 1994. **203**(2): p. 1160-1167.

285. Cornwell, T.L., et al., *Inhibition of smooth muscle cell growth by nitric oxide and activation of cAMP-dependent protein kinase by cGMP.* American Journal of Physiology - Cell Physiology, 1994. **267**(5): p. C1405-C1413.

286. Kostourou, V., et al., *The role of tumour-derived iNOS in tumour progression and angiogenesis.* Br J Cancer, 2011. **104**(1): p. 83-90.

287. Flitney, F.W., et al., *Antitumor Actions of Ruthenium(III)-Based Nitric Oxide Scavengers and Nitric Oxide Synthase Inhibitors.* Molecular Cancer Therapeutics, 2011. **10**(9): p. 1571-1580.

288. Aggarwal, B.B., et al., *Models for prevention and treatment of cancer: Problems vs promises.* Biochemical Pharmacology, 2009. **78**(9): p. 1083-1094.

289. Huszthy, P.C., et al., *Oncolytic Herpes Simplex Virus Type-1 Therapy in a Highly Infiltrative Animal Model of Human Glioblastoma.* Clinical Cancer Research, 2008. **14**(5): p. 1571-1580.

290. Prasad, G., et al., *Inhibition of PI3K/mTOR pathways in glioblastoma and implications for combination therapy with temozolomide.* Neuro-Oncology, 2011. **13**(4): p. 384-392.

291. Koul, D., et al., *Cellular and in vivo activity of a novel PI3K inhibitor, PX-866, against human glioblastoma.* Neuro-Oncology, 2010. **12**(6): p. 559-569.

292. Yuan, L., et al., *Novel chemo-sensitizing agent, ERW1227B, impairs cellular motility and enhances cell death in glioblastomas.* Journal of Neuro-Oncology, 2011. **103**(2): p. 207-219.

293. Day, E., et al., *Nanoshell-mediated photothermal therapy improves survival in a murine glioma model.* Journal of Neuro-Oncology, 2011. **104**(1): p. 55-63.

294. Stedt, H., et al., *Specific Inhibition of SRC Kinase Impairs Malignant Glioma Growth In Vitro and In Vivo.* Mol Ther Nucleic Acids, 2012. **1**: p. e19.

295. Burke, C.W., et al., *Inhibition of glioma growth by microbubble activation in a subcutaneous model using low duty cycle ultrasound without significant heating.* Journal of Neurosurgery, 2011. **114**(6): p. 1654-1661.